NASA/TP—2014–218198

Statistical Aspects of North Atlantic Basin Tropical Cyclones During the Weather Satellite Era, 1960–2013: Part 2

Robert M. Wilson
Marshall Space Flight Center, Huntsville, Alabama

July 2014

The NASA STI Program…in Profile

Since its founding, NASA has been dedicated to the advancement of aeronautics and space science. The NASA Scientific and Technical Information (STI) Program Office plays a key part in helping NASA maintain this important role.

The NASA STI Program Office is operated by Langley Research Center, the lead center for NASA's scientific and technical information. The NASA STI Program Office provides access to the NASA STI Database, the largest collection of aeronautical and space science STI in the world. The Program Office is also NASA's institutional mechanism for disseminating the results of its research and development activities. These results are published by NASA in the NASA STI Report Series, which includes the following report types:

- TECHNICAL PUBLICATION. Reports of completed research or a major significant phase of research that present the results of NASA programs and include extensive data or theoretical analysis. Includes compilations of significant scientific and technical data and information deemed to be of continuing reference value. NASA's counterpart of peer-reviewed formal professional papers but has less stringent limitations on manuscript length and extent of graphic presentations.

- TECHNICAL MEMORANDUM. Scientific and technical findings that are preliminary or of specialized interest, e.g., quick release reports, working papers, and bibliographies that contain minimal annotation. Does not contain extensive analysis.

- CONTRACTOR REPORT. Scientific and technical findings by NASA-sponsored contractors and grantees.

- CONFERENCE PUBLICATION. Collected papers from scientific and technical conferences, symposia, seminars, or other meetings sponsored or cosponsored by NASA.

- SPECIAL PUBLICATION. Scientific, technical, or historical information from NASA programs, projects, and mission, often concerned with subjects having substantial public interest.

- TECHNICAL TRANSLATION. English-language translations of foreign scientific and technical material pertinent to NASA's mission.

Specialized services that complement the STI Program Office's diverse offerings include creating custom thesauri, building customized databases, organizing and publishing research results…even providing videos.

For more information about the NASA STI Program Office, see the following:

- Access the NASA STI program home page at <http://www.sti.nasa.gov>

- E-mail your question via the Internet to <help@sti.nasa.gov>

- Phone the NASA STI Help Desk at 757–864–9658

- Write to:
  NASA STI Information Desk
  Mail Stop 148
  NASA Langley Research Center
  Hampton, VA 23681–2199, USA

NASA/TP—2014–218198

Statistical Aspects of North Atlantic Basin Tropical Cyclones During the Weather Satellite Era, 1960–2013: Part 2

Robert M. Wilson
Marshall Space Flight Center, Huntsville, Alabama

National Aeronautics and
Space Administration

Marshall Space Flight Center • Huntsville, Alabama 35812

July 2014

Available from:

NASA STI Information Desk
Mail Stop 148
NASA Langley Research Center
Hampton, VA 23681–2199, USA
757–864–9658

This report is also available in electronic form at
<http://www.sti.nasa.gov>

TABLE OF CONTENTS

LIST OF FIGURES

LIST OF FIGURES (Continued)

LIST OF FIGURES (Continued)

LIST OF TABLES

LIST OF ABBREVIATIONS, ACRONYMS, DESIGNATORS, AND SYMBOLS

ACE	accumulated cyclone energy
<ACE>	mean seasonal ACE
AMO	Atlantic Multidecadal Oscillation (index)
<AMO>	mean seasonal AMO
ASAT	Armagh surface air temperature
<ASAT>	mean seasonal ASAT
CO_2	carbon dioxide
CPC	Climate Prediction Center
CRU	Climate Research Unit
DOY	day of year
ENL	El Niño-like
ENY	El Niño year
FSD	first storm day
GLOTI	Global Land-Ocean Temperature Index
<GLOTI>	mean seasonal GLOTI
HISACE	highest individual storm ACE
HISPDI	highest individual storm PDI
<LAT>	mean seasonal latitude
LISNSD	longest individual storm NSD
LNL	La Niña-like

LNY	La Niña year
<LONG>	mean seasonal longitude
LOS	length of season
LP	lowest pressure
<LP>	mean seasonal LP
LSD	last storm day
MLCO2	Mauna Loa CO_2 (index)
<MLCO2>	mean seasonal MLCO2
NAO	North Atlantic Oscillation (index)
<NAO>	mean seasonal NAO
NENM	number of ENL months
NENY	non-El Niño year
NH	number of hurricanes
NHD	number of hurricane days
NLNM	number of LNL months
NMH	number of major hurricanes
NMHD	number of major hurricane days
NNM	number of neutral months
NSD	number of storm days
<NSD>	mean seasonal NSD
NTC	number of tropical cyclones

LIST OF ABBREVIATIONS, ACRONYMS, DESIGNATORS, AND SYMBOLS (Continued)

NTCA	Net Tropical Cyclone Activity
NUSLFH	number of United States land-falling hurricanes
<NUSLFH>	mean seasonal NUSLFH
ONI	Oceanic Niño Index
<ONI>	mean yearly ONI
PDI	Power Dissipation Index
<PDI>	mean seasonal PDI
PWS	peak wind speed
<PWS>	mean seasonal PWS
QBO	Quasi-Biennial Oscillation (index)
<QBO>	mean seasonal QBO
SOI	Southern Oscillation Index
<SOI>	mean yearly SOI
SST	sea surface temperature
THC	thermohaline circulation
TP	Technical Publication

NOMENCLATURE

a	y-intercept
b	slope
cl	confidence level
na	number above median
nb	number below median
nra	number of positive runs
P	probability
R_{y12}	sample coefficient of multiple correlation
r	coefficient of correlation
r^2	coefficient of determination
S_{y12}	sample coefficient of multiple standard error of estimate
sd	standard deviation
se	standard error of estimate
t	t-statistic for independent samples
x	independent variable
y	dependent variable
z	normal deviate for the sample results

TECHNICAL PUBLICATION

STATISTICAL ASPECTS OF NORTH ATLANTIC BASIN TROPICAL CYCLONES DURING THE WEATHER SATELLITE ERA, 1960–2013: PART 2

1. INTRODUCTION

This Technical Publication (TP) is part 2 of a two-part study of the North Atlantic basin tropical cyclones that occurred during the weather satellite era, 1960–2013. In particular, this TP examines the inferred statistical relationships between 25 tropical cyclone parameters and 9 specific climate-related factors, including the (1) Oceanic Niño Index (ONI), (2) Southern Oscillation Index (SOI), (3) Atlantic Multidecadal Oscillation (AMO) index, (4) Quasi-Biennial Oscillation (QBO) index, (5) North Atlantic Oscillation (NAO) index of the Climate Prediction Center (CPC), (6) NAO index of the Climate Research Unit (CRU), (7) Armagh surface air temperature (ASAT), (8) Global Land-Ocean Temperature Index (GLOTI), and (9) Mauna Loa carbon dioxide (CO_2) (MLCO2) index. Part 1 of this two-part study examined the statistical aspects of the 25 tropical cyclone parameters (e.g., frequencies, peak wind speed (PWS), accumulated cyclone energy (ACE), etc.) and provided the results of statistical testing (i.e., runs-testing, the *t*-statistic for independent samples, and Poisson distributions). Also, the study gave predictions for the frequencies of the number of tropical cyclones (NTC), number of hurricanes (NH), number of major hurricanes (NMH), and number of United States land-falling hurricanes (NUSLFH) expected for the 2014 season, based on the statistics of the overall interval 1960–2013, the subinterval 1995–2013, and whether the year 2014 would be either an El Niño year (ENY) or a non-El Niño year (NENY).[1]

2. RESULTS AND DISCUSSION

Table 1 provides a detailed listing of the yearly values for each of the climate-related factors that will be discussed in the following subsections. Also given in the table are the extreme monthly values per year (highs and lows) for ONI and SOI, as well as the statistics for the overall interval 1960–2013, the two subintervals 1960–1994 and 1995–2013, and the results of statistical testing.

Table 1. Summary of selected climate-related parametric values, 1960–2013.

Year	NENM	NNM	NLNM	<ONI>	ONI (High/Low)	<SOI>	SOI (High/Low)	<AMO>	<QBO>	<NAO> CPC	<NAO> CRU	<ASAT>	<GLOTI>	<MLCO2>
1960	–	12	–	0.00	0.32/–0.36	3.8	7.8/–2.3	0.237	–7.76	–0.56	–0.30	9.44	–0.04	316.91
1961	1	11	–	0.01	0.54/–0.38	0.8	13.8/–20.9	0.101	4.42	0.01	1.05	9.58	0.06	317.64
1962	–	11	1	–0.24	0.01/–0.52	5.4	17.0/–1.4	0.074	–7.73	–0.38	–0.13	8.76	0.05	318.45
1963	6	5	1	0.64	1.43/–0.50	–2.0	9.4/–12.9	0.006	–8.75	–0.56	–0.39	8.57	0.07	318.99
1964	2	2	8	–0.38	1.05/–0.86	6.3	14.3/–4.0	–0.094	2.38	–0.18	0.24	9.49	–0.20	319.62
1965	8	3	1	0.91	2.04/–0.58	–16.8	2.9/–22.6	–0.158	–11.93	–0.22	–0.23	8.82	–0.11	320.04
1966	4	8	–	0.37	1.29/–0.25	–4.2	4.0/–13.9	0.006	1.29	–0.49	–0.22	9.38	–0.05	321.38
1967	–	11	1	–0.23	0.12/–0.58	3.2	14.6/–5.5	–0.096	0.93	0.34	0.56	9.40	–0.01	322.16
1968	3	6	3	0.07	0.97/–0.87	3.0	14.7/–3.4	–0.165	–14.41	–1.04	–0.62	9.32	–0.05	323.04
1969	11	1	–	0.83	1.29/0.26	–5.4	3.7/–13.5	0.011	4.81	–0.19	–0.44	8.93	0.07	324.62
1970	1	5	6	–0.23	0.61/–0.98	3.9	19.7/–10.7	–0.102	–13.76	–0.35	0.18	9.29	0.03	325.68
1971	–	–	12	–0.90	–0.63/–1.42	11.0	22.6/2.1	–0.311	4.80	–0.04	–0.55	9.72	–0.06	326.32
1972	8	3	1	0.94	2.27/–0.67	–7.4	8.2/–18.6	–0.353	–8.10	0.49	–0.04	8.74	0.01	327.45
1973	3	1	8	–0.57	1.91/–2.08	7.3	31.6/–13.5	–0.215	4.40	–0.16	–0.09	9.33	0.15	329.68
1974	–	2	10	–0.84	–0.30/–1.99	9.9	20.8/–1.4	–0.420	–13.42	0.11	0.59	8.94	–0.07	330.18
1975	–	2	10	–1.04	–0.33/–1.76	13.6	22.5/–4.9	–0.298	1.25	–0.16	0.05	9.70	–0.01	331.08
1976	3	5	4	–0.08	0.88/–1.78	1.1	13.2/–13.0	–0.363	0.85	0.18	–0.07	9.34	–0.12	332.05
1977	6	6	–	0.52	0.83/0.08	–9.9	7.7/–17.7	–0.189	–11.27	–0.42	–0.21	8.92	0.15	333.78
1978	1	11	–	–0.08	0.81/–0.47	–1.7	16.3/–24.4	–0.179	6.81	0.28	0.21	9.21	0.06	335.41
1979	3	9	–	0.23	0.56/–0.10	–1.9	6.7/–8.2	–0.110	–13.16	0.05	0.19	8.35	0.12	336.78
1980	2	10	–	0.21	0.59/–0.09	–3.1	3.2/–12.9	–0.018	5.27	–0.55	–0.37	9.11	0.22	338.68
1981	–	9	3	–0.35	–0.12/–0.69	1.8	11.5/–16.6	–0.075	–1.91	–0.27	–0.09	9.09	0.28	340.10
1982	8	4	–	0.91	2.31/–0.11	–13.1	9.4/–31.1	–0.211	–5.74	0.36	0.67	9.44	0.09	341.44
1983	6	2	4	0.42	2.25/–1.09	–8.3	9.9/–33.3	–0.069	1.15	0.30	0.34	9.77	0.27	343.03
1984	–	7	5	–0.48	–0.08/–1.23	–0.1	5.8/–8.7	–0.206	–17.02	0.23	0.26	9.29	0.12	344.58
1985	–	5	7	–0.61	–0.26/–1.09	0.9	14.4/–9.6	–0.265	9.63	–0.28	–0.47	8.70	0.08	346.04
1986	4	7	1	0.26	1.17/–0.52	–10.7	10.7/–13.9	–0.273	–0.98	0.43	0.56	8.57	0.15	347.39
1987	12	–	–	1.29	1.72/0.93	–13.1	–1.4/–24.4	0.069	–6.25	–0.22	–0.51	9.07	0.28	349.16
1988	1	3	8	–0.82	0.94/–1.89	7.8	21.0/–5.0	–0.002	1.56	–0.08	–0.32	9.66	0.34	351.56
1989	–	7	5	–0.63	0.01/–1.85	6.8	21.0/–6.3	–0.080	–10.70	0.68	0.57	10.07	0.24	353.07
1990	–	12	–	0.27	0.41/0.07	–2.2	13.1/–17.3	–0.035	7.38	0.61	1.23	9.94	0.39	354.35
1991	7	5	–	0.65	1.55/0.02	–8.8	5.1/–19.3	–0.129	–3.24	0.25	0.34	9.42	0.38	355.57

Table 1. Summary of selected climate-related parametric values, 1960–2013 (Continued).

Year	NENM	NNM	NLNM	<ONI>	ONI (High/Low)	<SOI>	SOI (High/Low)	<AMO>	<QBO>	<NAO> CPC	<NAO> CRU	<ASAT>	<GLOTI>	<MLCO2>
1992	6	6	–	0.58	1.65/–0.45	–10.4	1.4/–25.4	–0.216	–7.61	0.54	1.11	9.45	0.19	356.38
1993	2	10	–	0.31	0.81/0.04	–9.5	1.6/–21.1	–0.207	3.90	0.16	0.12	9.27	0.20	357.07
1994	3	9	–	0.48	1.26/0.05	–11.9	0.6/–22.8	–0.173	–13.67	0.54	0.51	9.38	0.28	358.82
1995	3	4	5	–0.08	1.04/–0.96	–1.8	4.2/–16.2	0.139	7.82	–0.09	–0.61	10.23	0.43	360.80
1996	–	8	4	–0.43	–0.18/–0.85	14.0	13.9/–0.1	–0.054	–16.06	–0.25	–1.01	9.23	0.33	362.59
1997	8	3	1	1.11	2.38/–0.58	–11.7	13.3/–24.1	0.056	7.86	–0.20	–0.18	10.32	0.45	363.71
1998	5	1	6	–0.03	2.30/–1.57	–1.1	14.6/–28.5	0.377	–12.83	–0.54	0.26	10.09	0.61	366.65
1999	–	–	12	–1.19	–0.87/–1.72	16.3	18.5/–0.4	0.123	10.17	0.33	0.05	10.18	0.40	368.33
2000	–	1	11	–0.88	–0.46/–1.78	7.8	22.4/–5.5	0.034	–6.49	0.16	0.04	9.93	0.40	369.52
2001	–	10	2	–0.26	0.10/–0.74	0.5	11.9/–9.1	0.118	–15.24	–0.24	–0.45	9.57	0.52	371.13
2002	8	4	–	0.65	1.39/–0.18	–6.1	7.7/–14.6	0.071	8.72	0.00	–0.04	10.20	0.61	373.22
2003	4	8	–	0.34	1.01/–0.49	–3.1	9.8/–12.0	0.237	–13.81	0.03	–0.16	10.03	0.60	375.77
2004	6	6	–	0.44	0.76/0.08	–4.8	13.1/–15.4	0.213	6.60	0.16	0.01	10.21	0.52	377.49
2005	1	9	2	0.08	0.64/–0.88	–3.6	10.9/–14.5	0.298	–17.13	–0.31	–0.25	10.25	0.65	379.80
2006	4	5	3	0.13	1.18/–1.01	–1.9	15.2/–15.9	0.273	4.47	–0.31	–0.20	10.42	0.59	381.90
2007	1	6	5	–0.45	0.72/–1.30	–0.6	14.4/–7.3	0.148	–15.91	0.11	–0.38	10.60	0.62	383.76
2008	–	5	7	–0.69	–0.12/–1.58	10.2	21.3/–4.3	0.146	6.98	–0.45	–0.73	9.76	0.49	385.59
2009	6	3	3	0.37	1.78/–0.94	–0.2	14.8/–14.7	0.047	–3.49	–0.32	–0.42	9.84	0.59	387.37
2010	4	2	6	–0.33	1.57/–1.53	9.8	27.1/–14.5	0.358	–7.95	–1.29	–2.19	8.72	0.66	389.85
2011	–	4	8	–0.73	–0.05/–1.59	13.3	25.1/0.2	0.110	1.96	0.20	0.64	10.28	0.55	391.63
2012	2	8	2	–0.06	0.75/–0.84	–0.8	9.4/–10.4	0.222	–20.79	–0.53	–0.63	9.70	0.57	393.82
2013	–	10	2	–0.34	0.00/–0.78	4.0	13.9/–3.6	0.176	9.06	0.15	0.59	9.84	0.60	396.48
1960–2013 (*n* = 54)														
sum			178											
mean	3	6	3	–	0.81/–0.80	–0.3	12.6/–12.8	–0.026	–3.38	–0.07	–0.04	9.50	0.25	350.52
sd	3	3	4	0.59	0.84/0.68	7.9	7.2/8.5	0.193	8.88	0.40	0.57	0.54	0.25	23.90
high	–	–	–	1.29	2.38/0.93	16.3	31.6/2.1	0.377	10.17	0.68	1.11	10.60	0.66	396.48
low	–	–	–	–1.19	–0.87/–2.08	–16.8	–1.4/–33.3	–0.420	–20.79	–1.29	–2.19	8.35	–0.20	316.91
med	–	–	–	–0.02	0.81/–0.74	–0.7	13.2/–13.0	–0.027	–1.91	–0.08	–0.07	9.44	0.24	349.16
na	–	–	–	30	–	28	–		27	27	27	28	27	27
nb	–	–	–	24	–	26	–		27	27	27	26	27	27
nra	–	–	–	11	–	12	–	7	23	14	15	10	4	1
z	–	–	–	–1.57	–	–1.08	–		4.86	–	0.54	2.16	–5.40	–7.02
1960–1994 (*n* = 35)														
sum	111		99											
mean	3	6	3	0.07	0.85/–0.68	–1.5	11.4/–13.7	–0.129	–3.33	–0.02	0.11	9.24	0.10	335.67
sd	3	4	4	0.60	0.81/0.73	7.8	7.6/8.8	0.144	7.60	0.40	0.48	0.40	0.15	13.42
1995–2013 (*n* = 19)														
sum	52	97	79											
mean	3	5	4	–0.12	0.73/–1.01	2.1	14.8/–11.1	0.163	–3.48	–0.18	–0.30	9.97	0.54	377.86
sd	3	3	4	0.56	0.91/0.53	7.7	5.9/7.8	0.113	11.09	0.38	0.62	0.44	0.09	11.11
***t* test (1960–1994) and (1995–2013)**														
t	–	1.0		1.14	0.5/1.7	–1.6	–1.7/–1.1	–7.642	0.06	1.43	2.70	–6.18	–11.67	–11.69

2.1 Oceanic Niño Index and Southern Oscillation Index

Figure 1 displays the variation of (a) the mean yearly ONI (<ONI>) and (b) the number of months during the year when El Niño-like (ENL) and La Niña-like (LNL) conditions prevailed, based on the ONI monthly values for the overall interval 1960–2013. The <ONI> is simply the average of the 12 monthly values (January–December) contained in the listing of ONI values.[2,3] The monthly values of the ONI are the anomalous deviations from the climate-adjusted monthly averages of the sea surface temperature (SST) in the Niño 3.4 region of the Pacific Ocean (i.e., the region bounded by ±5° latitude about the equator and ±25° longitude about long. 145° W.) based on centered 30-year base periods every 5 years and calculated by the National Oceanic and Atmospheric Administration/National Weather Service/CPC. The number of ENL (thick line) and LNL (thin line) months, as used in this study, is simply the number of months during the year when ONI ≥ 0.5 °C and ≤ –0.5 °C, respectively. As an example, for the year 2013, <ONI> = –0.34 °C and the number of ENL months (NENM) was 0, the number of neutral months (NNM) was 10, and the number of LNL months (NLNM) was 2 (January and February).

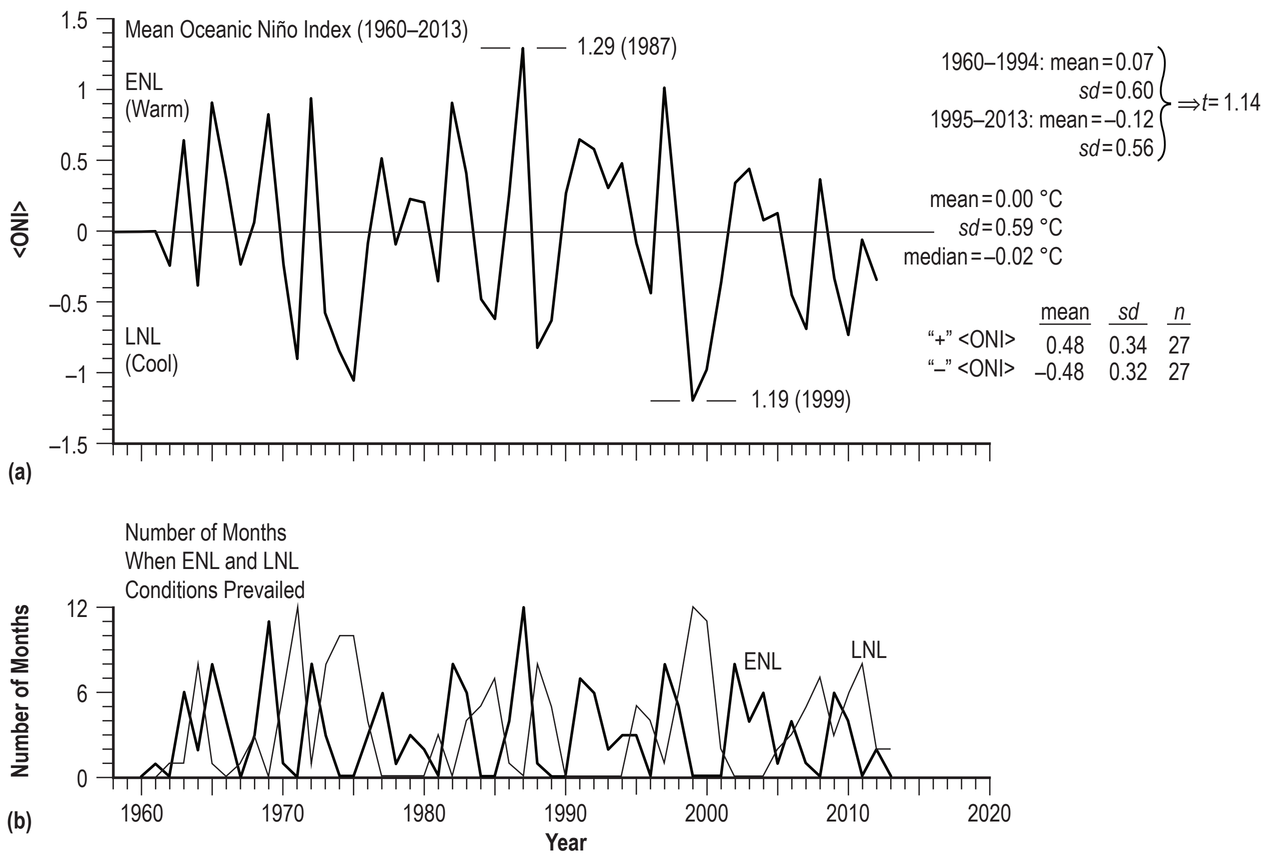

Figure 1. Variation of (a) <ONI> and (b) number of months when ENL and LNL conditions prevailed for the interval 1960–2013.

The mean <ONI> for the overall interval 1960–2013 is 0.00 °C, having a standard deviation $sd = 0.59$ °C, median = –0.02 °C, and extremes of 1.29 °C in 1987 (an ENY) and –1.19 °C in 1999 (a NENY, best described as a La Niña year (LNY)). Positive-valued <ONI> occurred in 27 years and negative-valued <ONI> also occurred in 27 years. Runs-testing suggests that <ONI> varies randomly, having a normal deviate for the sample results $z = -1.57$. Likewise, a comparison of the means for the two subintervals 1960–1994 and 1995–2013 suggests that the t-statistic for independent samples measures 1.14, inferring that the difference in the means for the two subintervals is not statistically important (even though the mean for the more recent subinterval is about 0.19 °C cooler than the mean for the earlier subinterval). The large positive spikes reflect ENL warm conditions synonymous with the occurrence of traditional El Niño events, and the large negative dips reflect LNL cool conditions synonymous with the occurrence of traditional La Niña events (i.e., at least 5 consecutive months with monthly ONI values meeting the conventional El Niño or La Niña definitions).

Figure 2 shows the variation of the mean yearly SOI (<SOI>). Like the ONI, the SOI gives an indication as to the development and intensity of El Niño and La Niña events. It is calculated by the Australian Bureau of Meteorology as the pressure difference between Tahiti, French Polynesia and Darwin, Australia, based on means and standard deviations calculated over the period 1933 to 1992 inclusive.[4,5] Sustained negative monthly values of the SOI below about –8 often indicate the occurrence of an El Niño event, while sustained positive monthly values of the SOI above 8 often indicate the occurrence of a La Niña event; hence, the SOI and ONI vary inversely, with positive (negative) SOI being associated with negative (positive) ONI.

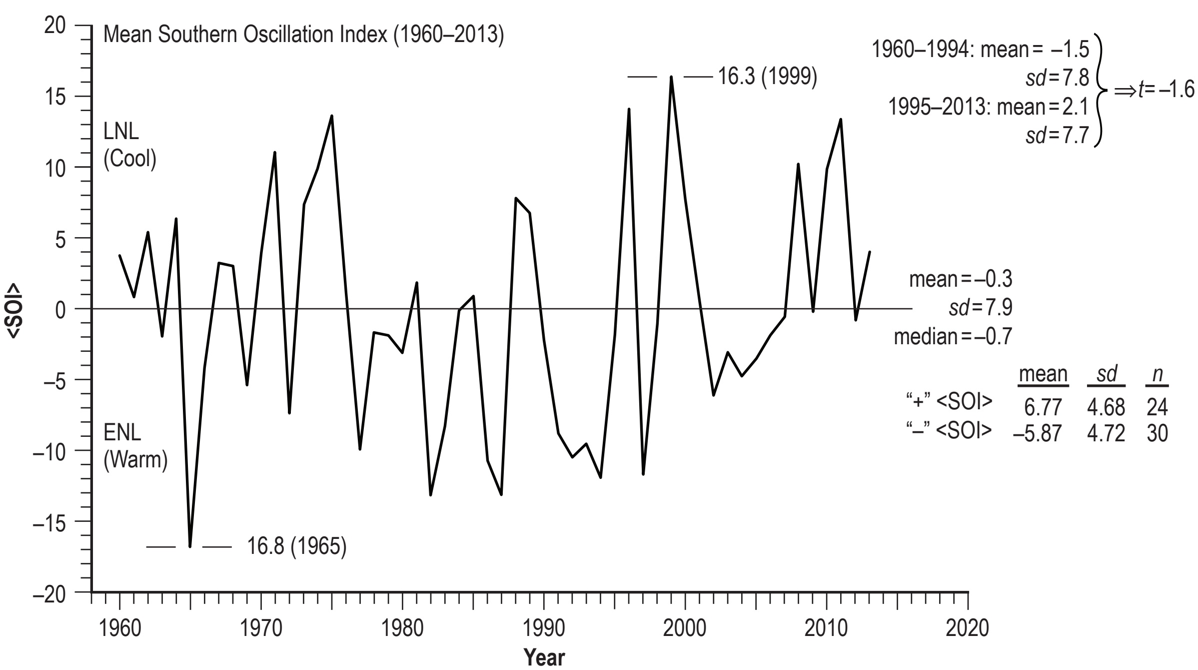

Figure 2. Variation of <SOI> for the interval 1960–2013.

The mean <SOI> for the overall interval 1960–2013 is –0.3, having $sd = 7.9$, a median = –0.7, and extremes of 16.3 in 1999 (an LNY) and –16.8 in 1965 (an ENY). For the year 2013, <SOI> measured 4.0. Positive-valued <SOI> occurred in 24 years, and negative-valued <SOI> occurred in 30 years. Runs-testing suggests that <SOI> varies randomly having $z = –1.08$, and a comparison of the means for the two subintervals 1960–1994 and 1995–2013 yields $t = –1.6$, inferring that the difference in the means is not statistically important (though to the eye, the observed variation hints of being cyclic, with warm ENL conditions prevailing in the late 1970s to the late 2000s and cooler LNL conditions prevailing in the early 1960s and now after about 2007).

Figure 3 depicts the scatterplot of <SOI> versus <ONI>. Plainly, the two parameters vary inversely (the diagonal line) as $y = –0.238 – 12.004x$, where y is <SOI> and x is <ONI>, having a coefficient of correlation $r = –0.896$, a coefficient of determination $r^2 = 0.802$ (meaning that about 80% of the variance in <SOI> can be explained by the variation in <ONI> alone, and vice versa), a standard error of estimate $se = 3.530$, and a confidence level cl » 99.9%. Identified in the scatterplot are the years of parametric extremes for <SOI> (1965 and 1999) and <ONI> (1987 and 1999). Also shown in the scatterplot is the result of Fisher's exact test for 2×2 contingency tables (the vertical and horizontal lines are the parametric medians), which indicates that the probability of obtaining the observed result, or one more suggestive of a departure from independence (chance), is $P = 1.6 \times 10^{-5}\%$. Hence, if the year 2014 happens to be an ENY, one clearly should expect the <ONI> and <SOI> values to lie in the lower-right quadrant of the scatterplot; on the other hand, if the year 2014 happens to be a NENY, one should expect the <ONI> and <SOI> values to lie in the upper-left quadrant of the scatterplot.

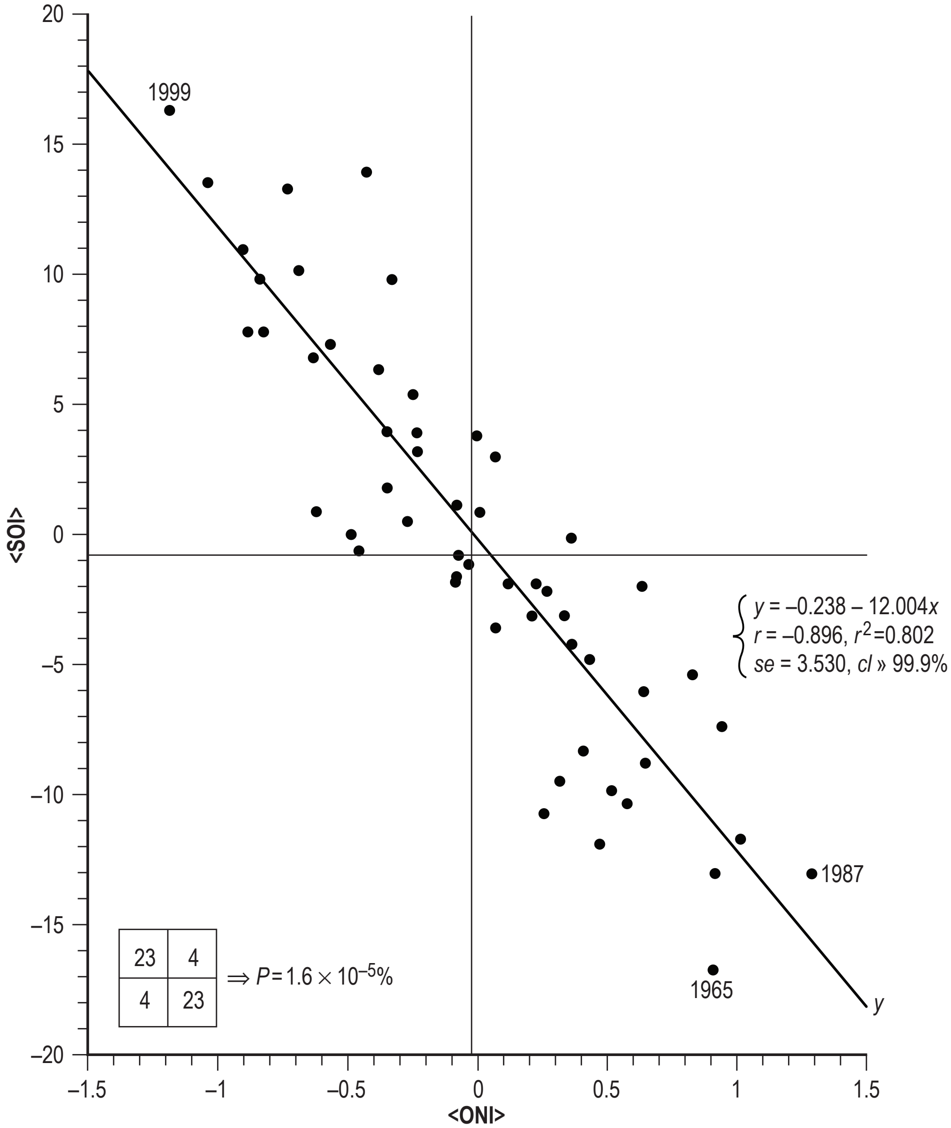

Figure 3. Scatterplot of <SOI> versus <ONI>.

2.2 Atlantic Multidecadal Oscillation Index

Figure 4 displays the yearly variation of the mean seasonal AMO (<AMO>) for the overall interval 1960–2013. The AMO is defined as a fluctuation in the SST in the North Atlantic Ocean between the equator and lat. 70° N.[6–11] It appears to have a cycle length or period of about 70 years, fluctuating between warm (positive) and cool (negative) phases, with this pattern possibly being associated with variations in the strength of the Atlantic thermohaline circulation (THC), a density-driven, global circulation pattern that involves the movement of warm salty equatorial surface waters to higher latitudes and the subsequent cooling and sinking of these waters into the deep ocean (also called the Atlantic Meridional Overturning Circulation). As such, the warm phase of the AMO seems to represent faster THC, while the cool phase seems to represent slower THC.

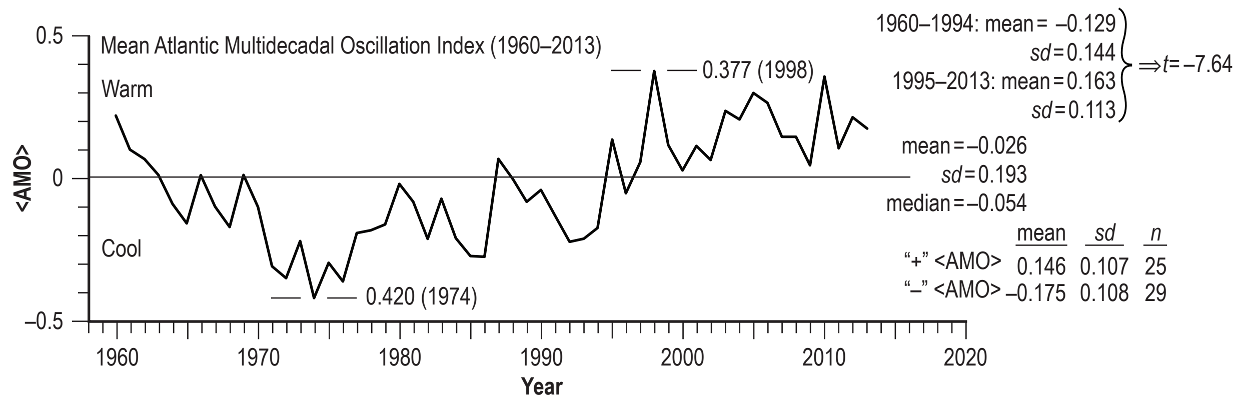

Figure 4. Variation of <AMO> for the interval 1960–2013.

The mean <AMO> measures –0.026 °C for the overall interval 1960–2013, having *sd* = 0.193 °C and a median = –0.054 °C. Runs-testing suggests that the variation of <AMO> is nonrandom, having *z* = –3.78 and *cl* > 99.9%. Comparison of the means for the two subintervals shows that the mean for the more recent subinterval is nearly 0.3 °C warmer than the mean for the earlier subinterval, with *t* = –7.64 and *cl* > 99.9%. During the overall interval 1960–2013, there have been 25 warm years and 29 cool years. Inspection of figure 4 indicates that the <AMO> switched from the warm phase to the cool phase about the mid-1960s, remaining in the cool phase until about the mid-1990s, when it switched back again to the warm phase where it has remained for the about the last 20 years. The peak yearly <AMO> occurred in 1998 (0.377 °C), although another peak occurred in 2010 (0.358 °C). One anticipates that the warm phase will continue for at least several years or more. (For the year 2013, <AMO> measured 0.176 °C.)

2.3 Quasi-Biennial Oscillation Index

The QBO refers to the quasi-periodic oscillation of the equatorial zonal winds (in ms^{-1}) in the tropical stratosphere having a mean period of about 28 months (range of 20 to 36 months) that was first discovered in the 1950s.[12–17] The winds alternate between the stronger easterlies (negative values) and the somewhat weaker westerlies (positive values), first developing at the top of the lower stratosphere and then slowly propagating downwards at the rate of about 1 km per month until dissipating in the tropical tropopause.

Figure 5 depicts the yearly variation of the mean seasonal QBO (<QBO>) for the overall interval 1960–2013. Its mean measures about –3.38, having *sd* = 8.88 and a median = –1.91. Runs-testing reveals, as expected, that the variation of <QBO> values is nonrandom (*z* = 4.86, *cl* > 99.9%), although the comparison of the means for the two subintervals suggests that the difference in the means is not statistically important (*t* = 0.06). Clearly, the easterlies (mean = –10.59) are about twice as strong as the westerlies (mean = 4.98). The strongest easterly occurred in 2012 (–20.79), while the strongest westerly occurred in 1999 (10.17). (For the year 2013, <QBO> measured 9.06. Because back-to-back positive-valued <QBO> has only occurred twice (1966–1967 and 1975–1976) during the overall interval 1960–2013, one strongly suspects that the year 2014 will be of negative value. For the 10 negative-valued years in the subinterval 1995–2013, it has averaged about –13, having *sd* = 5.4 and extremes of –3.49 and –20.79.

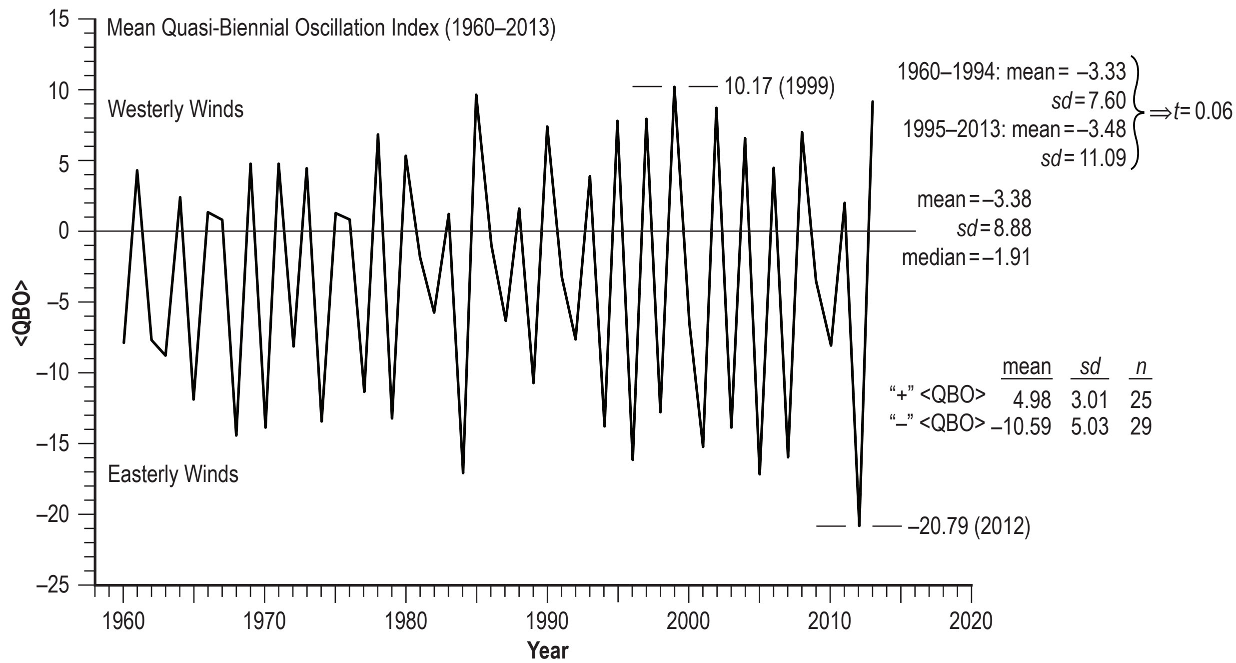

Figure 5. Variation of <QBO> for the interval 1960–2013.

2.4 North Atlantic Oscillation Index

Like the SOI, the NAO is one based on changes in surface air pressure between two widely separated locations (typically, Iceland and a location in the subtropical Atlantic basin: the Azores, Portugal or Gibraltar). Also, like the SOI, the NAO fluctuates between positive and negative values, where the positive phase is associated with a stronger-than-usual subtropical high pressure center and a deeper-than-usual Icelandic low, and the negative phase is associated with the opposite behavior.[18–21]

Figure 6 shows the yearly variation of the mean seasonal NAO (<NAO>) as computed by the CPC for the overall interval 1960–2013. Its mean measures –0.07, having $sd = 0.04$ and a median = –0.08. Runs-testing reveals that the variation of <NAO> CPC is random ($z = 0.00$), and comparison of the means for the two subintervals suggests that the difference in the means is not statistically important ($t = 1.43$). The strongest positive yearly value occurred in 1989 (0.68), and the strongest negative yearly value occurred in 2010 (–1.29), although the year 1968 also had a strong negative value as well (–1.04). (For the year 2013, <NAO> CPC measured 0.15.)

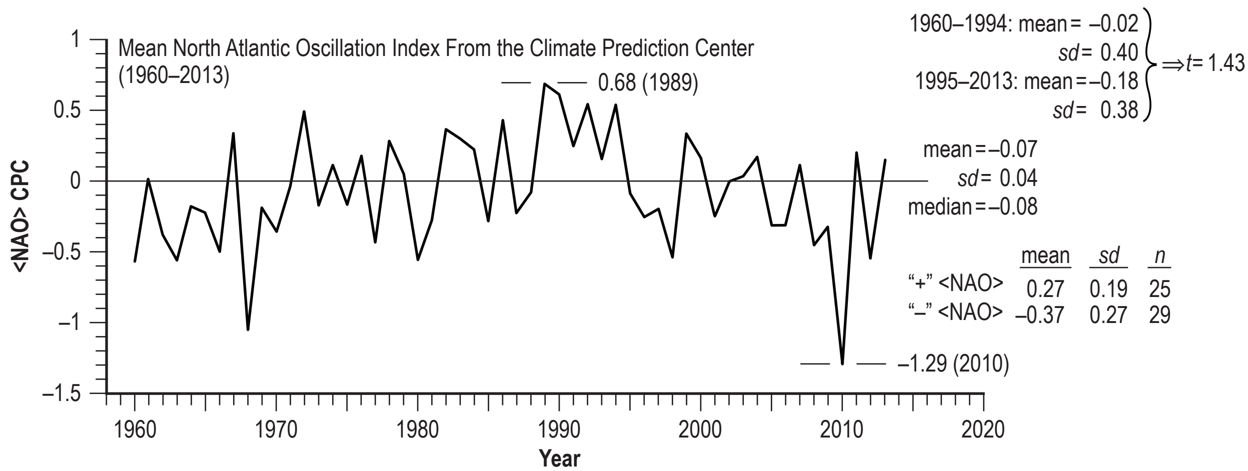

Figure 6. Variation of <NAO> CPC for the interval 1960–2013.

Figure 7 depicts the yearly variation of the <NAO> as computed by the CRU for the overall interval 1960–2013. Its mean measures –0.04, having $sd = 0.57$ and a median = –0.07. Like <NAO> CPC, runs-testing of the <NAO> CRU values suggests that its variation appears random ($z = 0.54$), but unlike <NAO> CPC, comparison of the means for the two subintervals suggests that the difference in the means is statistically important ($t = 2.70$, $cl > 99\%$). The strongest positive yearly value occurred in 1990 (1.23), although there have been at least two other strong positive peaks (1.05 in 1961 and 1.11 in 1992), and the strongest negative value occurred in 2010 (–2.19), which is also the strongest negative value ever recorded in the nearly 190-year record. (For the year 2013, <NAO> CRU measured 0.59.)

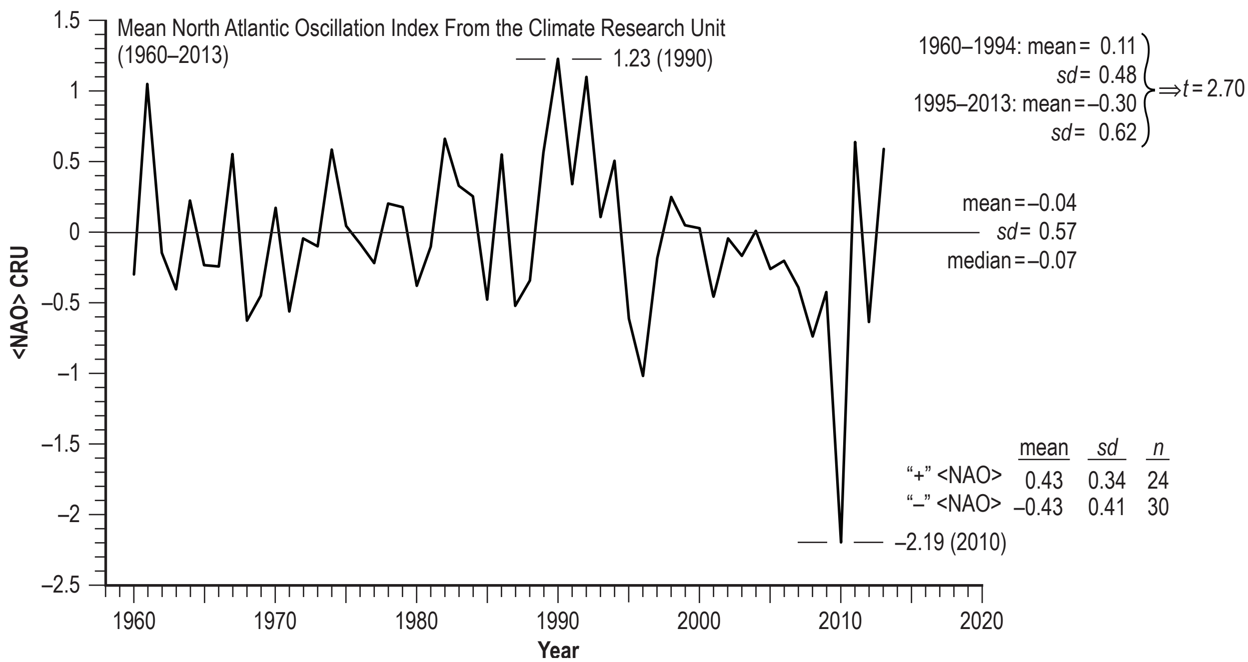

Figure 7. Variation of <NAO> CRU for the interval 1960–2013.

Figure 8 displays the scatterplot of <NAO> CRU versus <NAO> CPC. The inferred linear regression is $y = 0.044 + 1.079x$, having $r = 0.758$, $r^2 = 0.574$, $se = 0.372$, and $cl > 99.9\%$, where y is <NAO> CRU and x is <NAO> CPC. Based on Fisher's exact test for 2×2 contingency tables, the probability of obtaining the observed result, or one more suggestive a of a departure from independence (chance), is $P = 1.6 \times 10^{-5}\%$

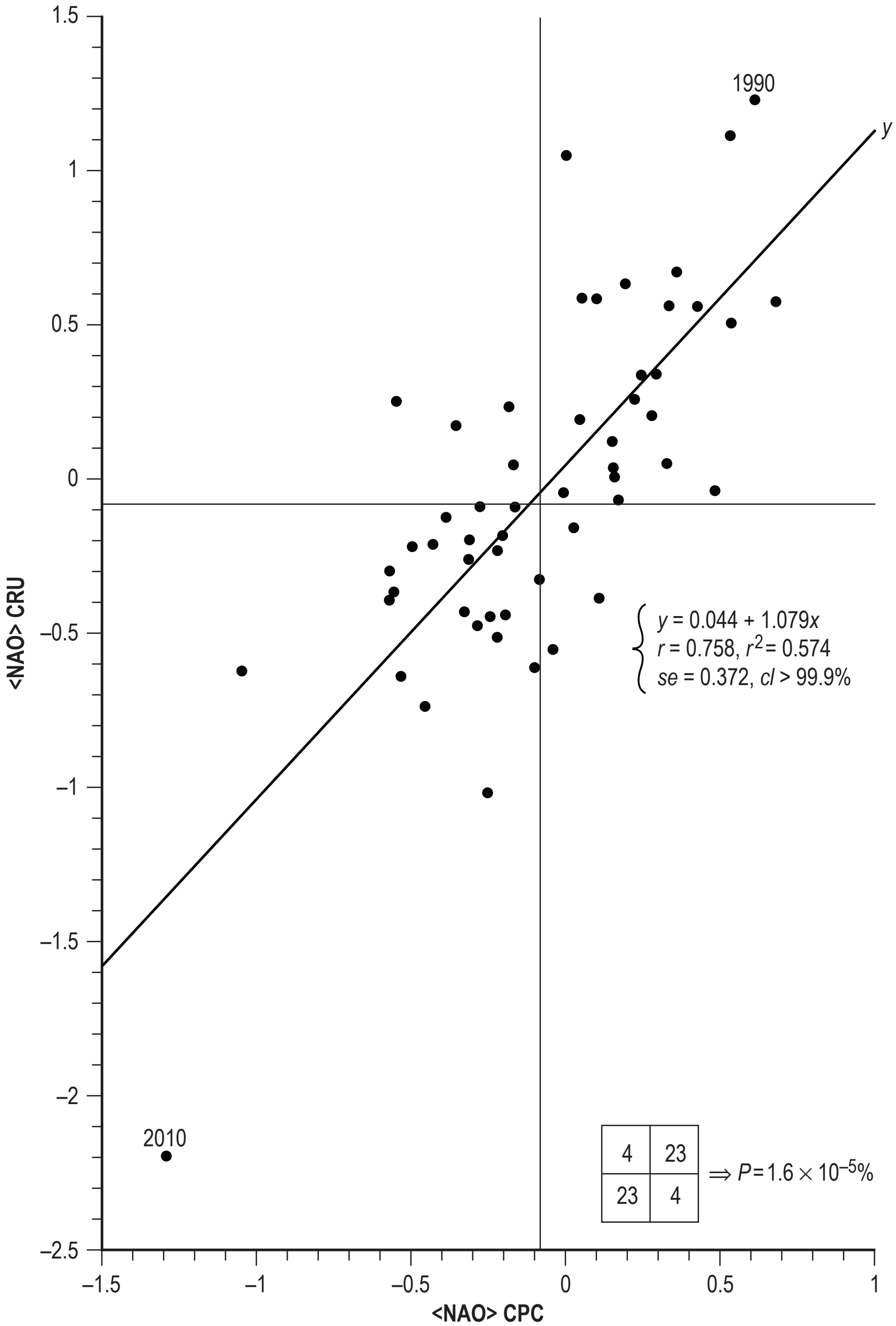

Figure 8. Scatterplot of <NAO> CRU versus <NAO> CPC.

2.5 Armagh Surface Air Temperature

The Armagh Observatory in Northern Ireland (lat. 54°21.2' N., long. 6°38.9' W.) is situated about 64 m above mean sea level at the top of a small hill in an estate of natural woodland and parkland that measures about 7 ha. Mean surface air temperature has been continuously measured there since 1844 using maximum and minimum thermometers.[22–30]

Figure 9 depicts the yearly variation of mean seasonal ASAT (<ASAT>) for the overall interval 1960–2013. Its mean measures 9.50 °C, having $sd = 0.54$ °C and a median = 9.44 °C. Runs-testing suggests that the variation of the <ASAT> values appears nonrandom ($z = 2.16$, $cl > 95\%$), and a comparison of the means for the two subintervals suggests that the difference in the means is statistically important ($t = –6.18$, $cl > 99.9\%$). The highest (warmest) yearly value of <ASAT> occurred in 2007 (10.60 °C), and the lowest (coolest) yearly value of <ASAT> occurred in 1979 (8.35 °C). For the more recent subinterval 1995–2013, only the years 1996 and 2010 had <ASAT> lower than the median (9.23 and 8.72 °C, respectively). (For the year 2013, <ASAT> measured 9.84 °C.)

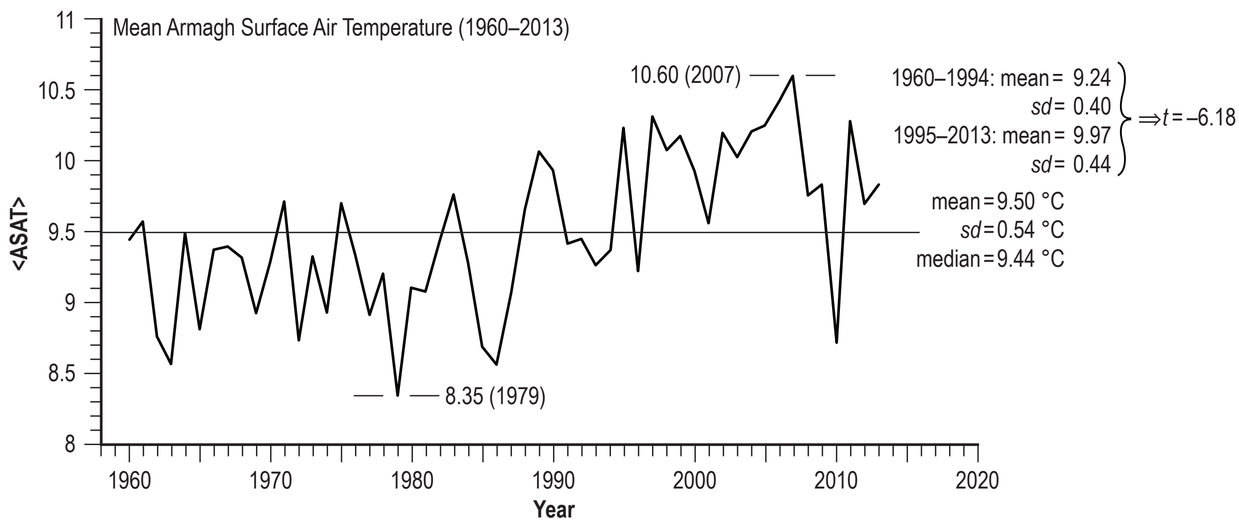

Figure 9. Variation of <ASAT> for the interval 1960–2013.

2.6 Global Land-Ocean Temperature Index and Mauna Loa Carbon Dioxide Index

Figure 10 shows the yearly variation of (a) mean seasonal GLOTI (<GLOTI>) and (b) mean seasonal MLCO2 (<MLCO2>) for the overall interval 1960–2013. The GLOTI is a measure of the anomaly in global land-ocean temperatures relative to the interval 1951–1980, where the data are taken from the Global Historical Climate Network, version 3, using elimination of outliers and homogeneity adjustment.[27,31–34] The MLCO2 index is a measure of the amount of atmospheric concentration of CO_2 as measured from the Mauna Loa Observatory in Hawaii, located in a barren lava field of an active volcano at lat. 19°32' N. and long. 155°35' W. and at an altitude of 3,397 m above mean sea level.[35–41]

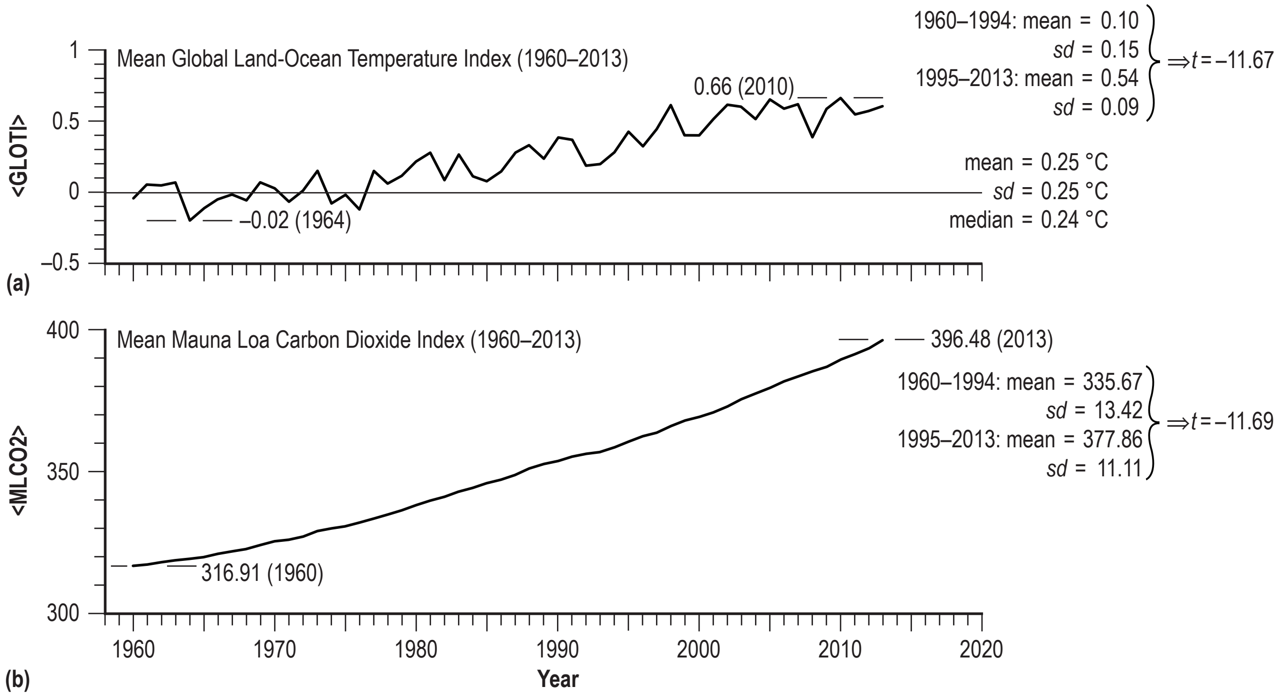

Figure 10. Variation of (a) <GLOTI> and (b) <MLCO2> for the interval 1960–2013.

For <GLOTI>, its mean measures 0.25 °C, having $sd = 0.25$ °C and a median = 0.24 °C. Runs-testing suggests that the variation of <GLOTI> is nonrandom ($z = -5.40$, $cl > 99.9\%$). In fact, every year post-1976 has been of positive value, and every year post-1994 has had a value larger than the mean or median. Furthermore, a comparison of the means for the two subintervals suggests that the difference in the means is statistically very important ($t = -11.67$, $cl \gg 99.9\%$). The warmest anomaly to date occurred in 2010, measuring 0.66 °C, and the coolest anomaly occurred in 1964, measuring –0.02 °C. (For the year 2013, <GLOTI> measured 0.60 °C.)

The <MLCO2> has been continuously rising from one year to the next, with the lowest value occurring in 1960 (316.91 ppm) and the highest value occurring in 2013 (396.48 ppm), rising at an average rate of about 1.47 ppm yr^{-1}. However, the rate of rise actually is rising faster than a simple linear increase, as a straight-edge along the figure plainly shows. Clearly, runs-testing reveals that the distribution of <MLCO2> is nonrandom ($z = -7.02$, $cl > 99.9\%$), as is also demonstrated from the comparison of the means for the two subintervals ($t = -11.69$, $cl \gg 99.9\%$). (In May 2014, the monthly value of MLCO2 reached 401.88 ppm.[42] However, the yearly average probably will not exceed 400 ppm until the year 2015, due to seasonal effects.)

Figure 11 shows the scatterplot of <GLOTI> versus <MLCO2>, identifying the years of parametric extremes (1960, 1964, 2010, and 2013). The inferred linear regression is $y = -3.1258 + 0.0096x$, having $r = 0.932$, $r^2 = 0.869$, $se = 0.1120$, and $cl > 99.9\%$. Based on Fisher's exact test for 2×2 contingency tables, the probability of obtaining the observed result, or one more suggestive of a departure from independence, is $P = 6.4 \times 10^{-9}\%$. Hence, one expects <GLOTI> to continue to increase with the passage of time due to the continuing increase in the greenhouse gas of CO_2 (with the 2014 yearly values lying in the upper-right quadrant of the scatterplot).

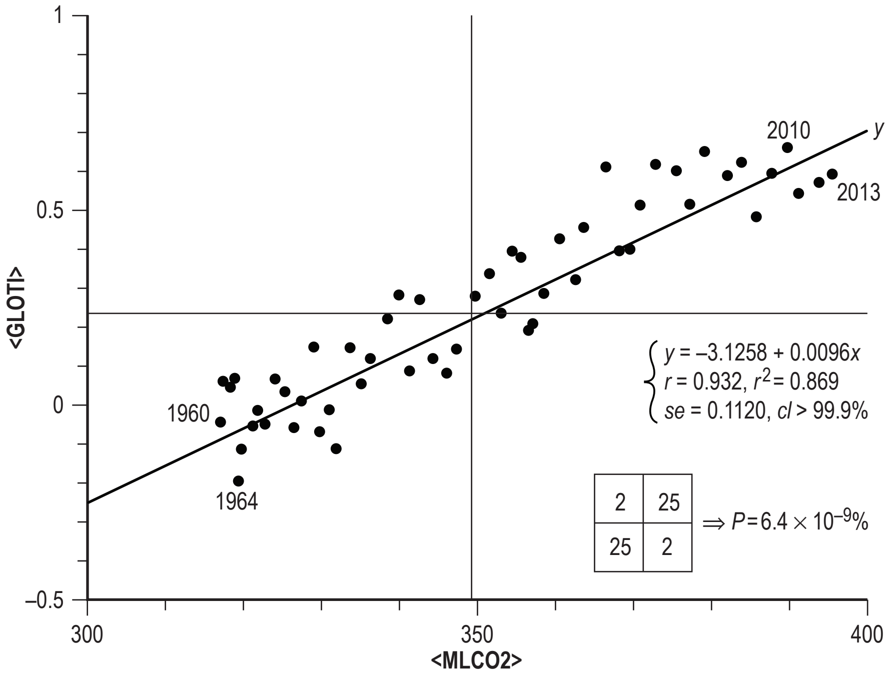

Figure 11. Scatterplot of <GLOTI> versus <MLCO2>.

2.7 Correlative Behavior of the Climate-Related Factors

Table 2 provides a listing of the inferred correlative statistics between the various climate-related factors. As an example, one finds that the only inferred correlation found to be statistically important ($cl > 98\%$) is the one between <ONI> and <SOI>. All other inferred correlations between either <ONI> or <SOI> and the other climate-related factors are found not to be statistically important ($cl < 90\%$). Also, one finds that <QBO> is not strongly correlated with any of the other climate-related factors, whereas <NAO> CPC and <NAO> CRU are inferred to strongly correlate not only with each other, but also with <AMO>. <ASAT> is inferred to correlate strongly with <AMO>, <GLOTI>, and <MLCO2>; <GLOTI> with <AMO>, <ASAT>, and <MLCO2>; and <MLCO2> with <AMO>, <ASAT>, and <GLOTI>.

Table 2. Summary of climate interrelational statistics, 1960–2013.

Parameter	*a*	*b*	*r*	r^2	*se*	*cl*
<ONI> vs. <SOI>	–0.016	–0.067	–0.896	0.802	0.262	>99.9%*
<ONI> vs. <AMO>	0.002	0.030	0.010	0.000	0.593	<90%
<ONI> vs. <QBO>	–0.015	–0.005	–0.071	0.005	0.591	<90%
<ONI> vs. <NAO> CPC	0.005	0.045	0.031	0.001	0.592	<90%
<ONI> vs. <NAO> CRU	0.004	0.073	0.071	0.005	0.591	<90%
<ONI> vs. <ASAT>	2.051	–0.216	–0.199	0.040	0.581	<90%
<ONI> vs. <GLOTI>	0.010	–0.034	–0.014	0.000	0.593	<90%
<ONI> vs. <MLCO2>	1.007	–0.003	–0.117	0.014	0.588	<90%
<SOI> vs. <ONI>	–0.238	–12.004	–0.896	0.802	3.530	>99.9%*
<SOI> vs. <AMO>	–0.141	4.296	0.106	0.011	7.898	<90%
<SOI> vs. <QBO>	0.020	0.081	0.091	0.008	7.909	<90%
<SOI> vs. <NAO> CPC	–0.536	–3.833	–0.193	0.037	7.792	<90%
<SOI> vs. <NAO> CRU	–0.357	–2.895	–0.208	0.043	7.768	<90%
<SOI> vs. <ASAT>	–22.991	2.394	0.165	0.027	7.833	<90%
<SOI> vs. <GLOTI>	–0.413	0.624	0.020	0.000	7.940	<90%
<SOI> vs. <MLCO2>	–10.149	0.028	0.086	0.007	7.912	<90%
<AMO> vs. <ONI>	–0.026	0.003	0.010	0.000	0.195	<90%
<AMO> vs. <SOI>	–0.026	0.003	0.106	0.011	0.194	<90%
<AMO> vs. <QBO>	–0.029	–0.001	–0.033	0.001	0.195	<90%
<AMO> vs. <NAO> CPC	–0.041	–0.199	–0.408	0.167	0.178	>99.5%*
<AMO> vs. <NAO> CRU	–0.030	–0.111	–0.325	0.105	0.185	>98%*
<AMO> vs. <ASAT>	–1.740	0.180	0.505	0.255	0.168	>99.9%*
<AMO> vs. <GLOTI>	–0.172	0.574	0.733	0.537	0.133	>99.9%*
<AMO> vs. <MLCO2>	–1.704	0.005	0.591	0.349	0.162	>99.9%*
<QBO> vs. <ONI>	–3.381	–1.080	–0.071	0.005	8.941	<90%
<QBO> vs. <SOI>	–3.356	0.103	0.091	0.008	8.927	<90%
<QBO> vs. <AMO>	–3.421	–1.495	–0.033	0.001	8.959	<90%
<QBO> vs. <NAO> CPC	–3.089	3.978	0.178	0.032	8.821	<90%
<QBO> vs. <NAO> CRU	–3.304	2.178	0.139	0.019	8.877	<90%
<QBO> vs. <ASAT>	–35.536	3.386	0.207	0.043	8.771	<90%
<QBO> vs. <GLOTI>	–3.250	–0.521	–0.015	0.000	8.963	<90%
<QBO> vs. <MLCO2>	–2.748	–0.002	–0.005	0.000	8.951	<90%
<NAO> CPC vs. <ONI>	–0.074	0.021	0.031	0.001	0.401	<90%
<NAO> CPC vs. <SOI>	–0.076	–0.010	–0.193	0.037	0.393	<90%
<NAO> CPC vs. <AMO>	–0.096	–0.838	–0.408	0.167	0.366	>99.5%*
<NAO> CPC vs. <QBO>	–0.047	0.008	0.178	0.032	0.394	<90%
<NAO> CPC vs. <NAO> CRU	–0.055	0.532	0.758	0.574	0.262	>99.9%*
<NAO> CPC vs. <ASAT>	–1.391	0.139	0.189	0.036	0.394	<90%
<NAO> CPC vs. <GLOTI>	–0.045	–0.112	–0.070	0.005	0.400	<90%
<NAO> CPC vs. <MLCO2>	–0.180	0.000	0.018	0.000	0.391	<90%

*Inferred correlations having *cl* > 98%.

Table 2. Summary of climate interrelational statistics, 1960–2013 (Continued).

Parameter	*a*	*b*	*r*	r^2	*se*	*cl*
<NAO> CRU vs. <ONI>	–0.036	0.068	0.071	0.005	0.568	<90%
<NAO> CRU vs. <SOI>	–0.040	–0.015	–0.208	0.043	0.558	<90%
<NAO> CRU vs. <AMO>	–0.061	–0.949	–0.325	0.105	0.540	>98%*
<NAO> CRU vs. <QBO>	–0.006	0.009	0.139	0.019	0.565	<90%
<NAO> CRU vs. <NAO> CPC	0.044	1.079	0.758	0.574	0.372	>99.9%*
<NAO> CRU vs. <ASAT>	–1.418	0.146	0.140	0.019	0.565	<90%
<NAO> CRU vs. <GLOTI>	0.086	–0.477	–0.209	0.044	0.558	<90%
<NAO> CRU vs. <MLCO2>	1.501	–0.004	–0.185	0.034	0.566	<90%
<ASAT> vs. <ONI>	9.498	–0.184	–0.199	0.040	0.533	<90%
<ASAT> vs. <SOI>	9.500	0.011	0.165	0.027	0.542	<90%
<ASAT> vs. <AMO>	9.535	1.416	0.505	0.255	0.467	>99.9%*
<ASAT> vs. <QBO>	9.540	0.013	0.207	0.043	0.547	<90%
<ASAT> vs. <NAO> CPC	9.516	0.258	0.189	0.036	0.541	<90%
<ASAT> vs. <NAO> CRU	9.502	0.134	0.140	0.019	0.544	<90%
<ASAT> vs. <GLOTI>	9.157	1.338	0.611	0.373	0.430	>99.9%*
<ASAT> vs. <MLCO2>	4.7949	0.0134	0.592	0.350	0.4998	>99.9%*
<GLOTI> vs. <ONI>	0.255	–0.006	–0.014	0.000	0.249	<90%
<GLOTI> vs. <SOI>	0.255	0.001	0.020	0.000	0.250	<90%
<GLOTI> vs. <AMO>	0.279	0.937	0.733	0.537	0.170	>99.9%*
<GLOTI> vs. <QBO>	0.253	0.000	–0.015	0.000	0.251	<90%
<GLOTI> vs. <NAO> CPC	0.251	–0.044	–0.070	0.005	0.249	<90%
<GLOTI> vs. <NAO> CRU	0.251	–0.091	–0.209	0.044	0.244	<90%
<GLOTI> vs. <ASAT>	–2.391	0.279	0.611	0.373	0.195	>99.9%*
<GLOTI> vs. <MLCO2>	–3.1258	0.0096	0.932	0.869	0.1120	>99.9%*
<MLCO2> vs. <ONI>	350.523	–4.756	–0.117	0.014	23.963	<90%
<MLCO2> vs. <SOI>	350.583	0.261	0.086	0.007	24.039	<90%
<MLCO2> vs. <AMO>	352.431	73.015	0.591	0.349	19.465	>99.9%*
<MLCO2> vs. <QBO>	350.472	–0.013	–0.005	0.000	24.134	<90%
<MLCO2> vs. <NAO> CPC	350.597	1.093	0.018	0.000	24.127	<90%
<MLCO2> vs. <NAO> CRU	350.237	–7.836	–0.185	0.034	23.708	<90%
<MLCO2> vs. <ASAT>	102.7349	26.0894	0.592	0.350	19.455	>99.9%*
<MLCO2> vs. <GLOTI>	327.5853	90.0584	0.932	0.8685	8.7483	>99.9%*

*Inferred correlations having *cl* > 98%.

Figures 12 and 13 display the scatterplots of <NAO> CPC and <NAO> CRU versus <AMO>, respectively, and identifies the years of extreme values. Both measures of <NAO> are inferred to correlate inversely against <AMO>, such that negative (positive) values of <NAO> usually are associated with positive (negative) values of <AMO>, and vice versa. Because <AMO> is expected to continue to be of positive value for the year 2014, one expects <NAO>, whether the CPC or CRU values, to probably be of negative value (about twice as likely as being that of positive value).

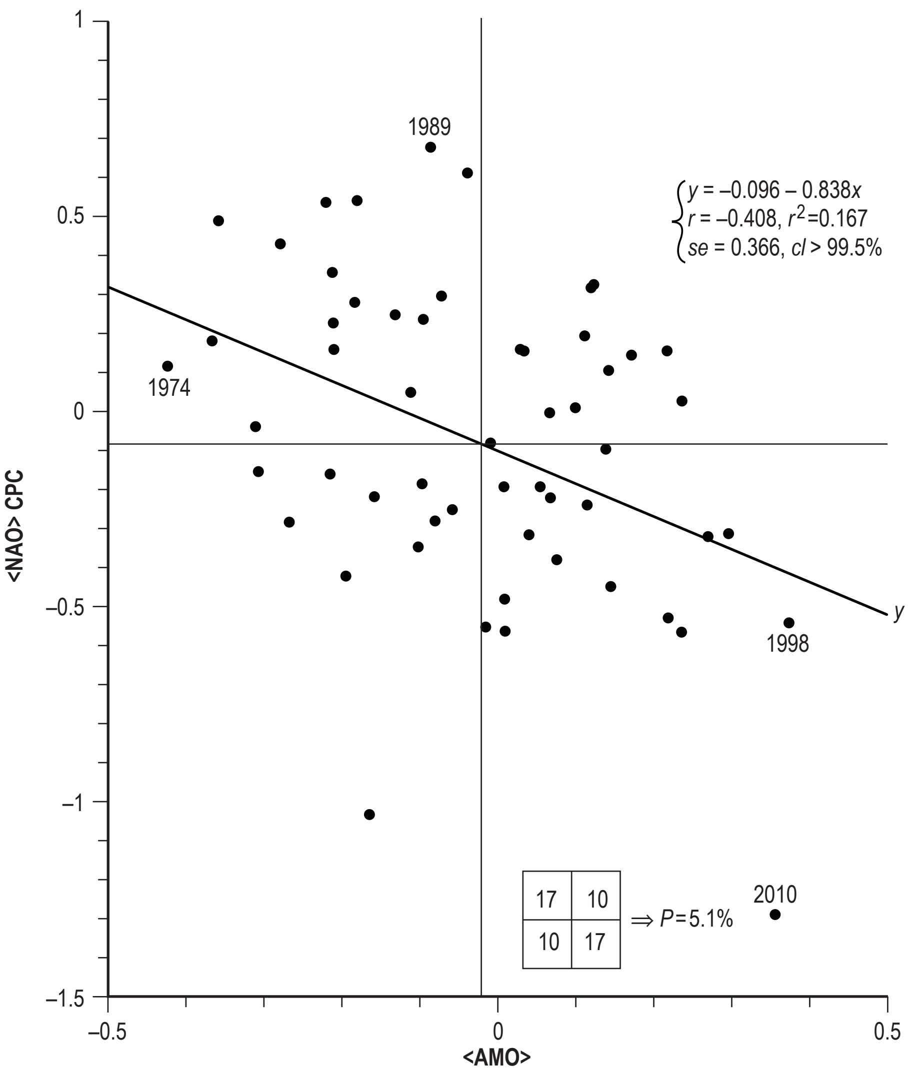

Figure 12. Scatterplot of <NAO> CPC versus <AMO>.

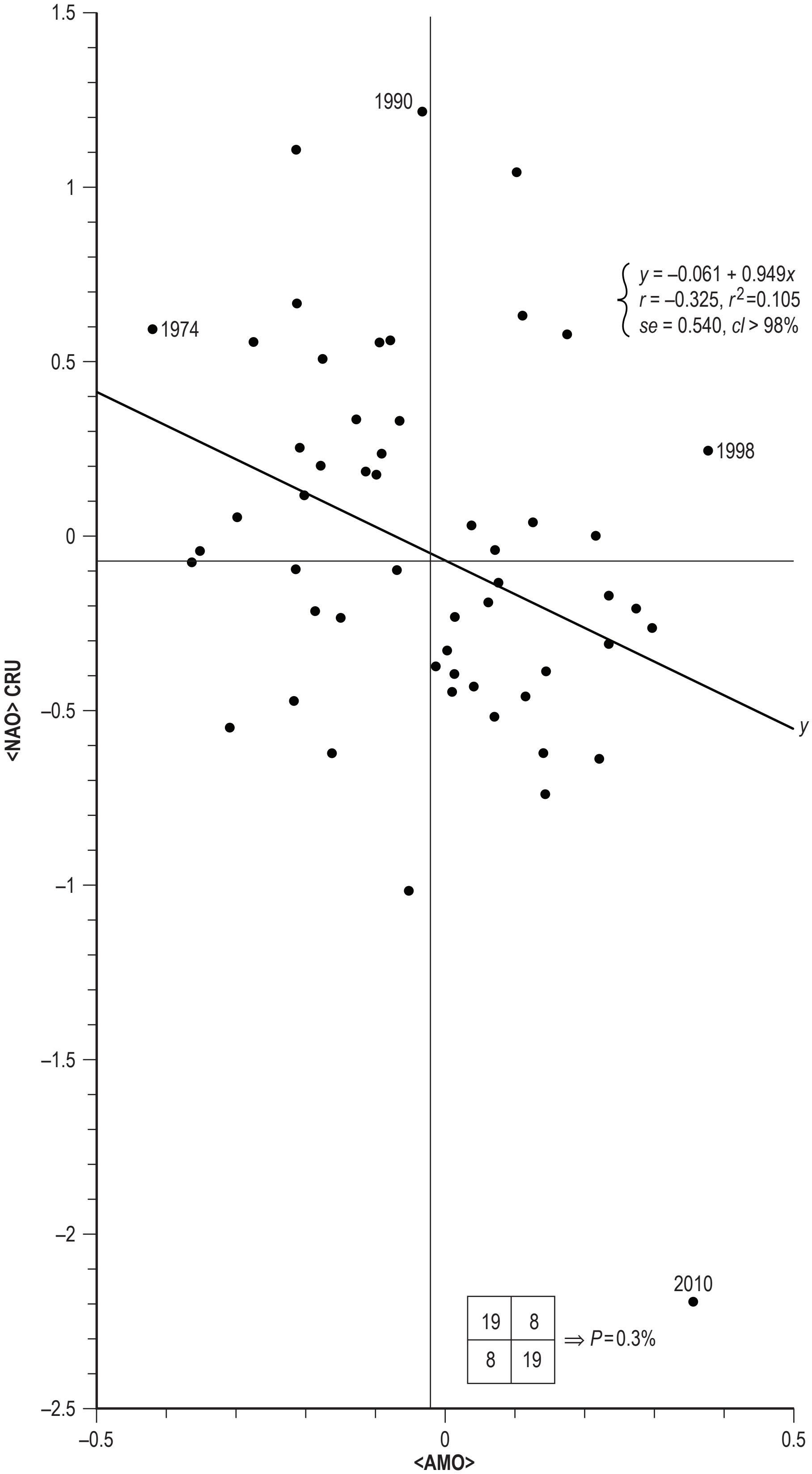

Figure 13. Scatterplot of <NAO> CRU versus <AMO>.

Figure 14 shows the scatterplot of <ASAT> versus <AMO>, identifying the years of extreme values. Clearly, <ASAT> tends to vary directly with <AMO>, having $r = 0.505$, $r^2 = 0.255$, $se = 0.467$ °C, and $cl > 99.9\%$. Based on Fisher's exact test for 2×2 contingency tables, the probability of obtaining the observed result, or one more suggestive of a departure from independence, is $P = 0.12\%$. Hence, a positive-valued <AMO> for the year 2014 suggests that <ASAT> probably will be ≥9.44 °C, possibly considerably greater.

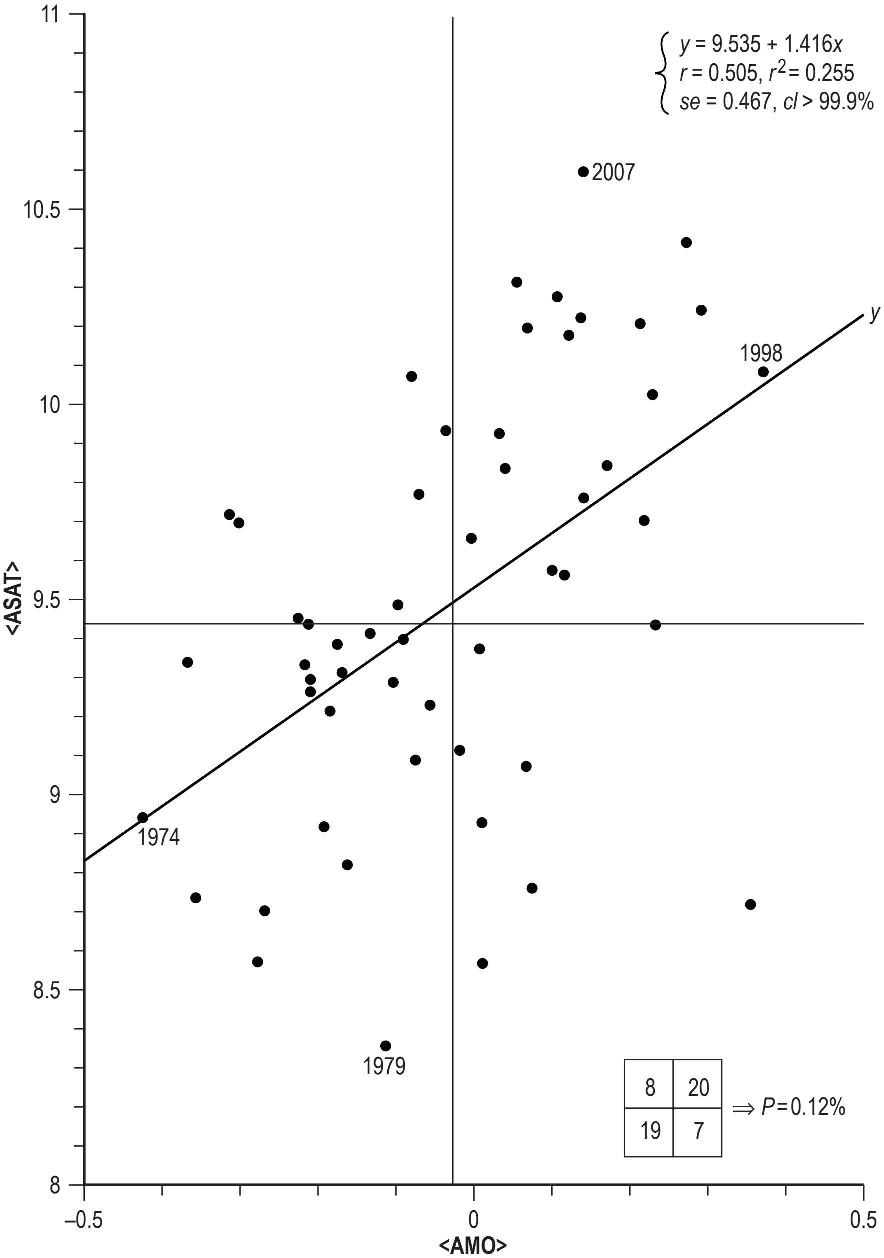

Figure 14. Scatterplot of <ASAT> versus <AMO>.

Figure 15 depicts the scatterplot of <GLOTI> versus <AMO>, identifying the years of extreme values. The inferred regression has $r=0.733$ and $r^2=0.537$, suggesting that about 54% of the variance in <GLOTI> can be explained by the variation in <AMO>, at least during the interval 1960–2013. Based on Fisher's exact test for 2×2 contingency tables, the probability of obtaining the observed result, or one more suggestive of a departure from independence, is $P=0.045\%$. Clearly, since <AMO> is expected to be of positive value in the year 2014, <GLOTI> likewise is expected to be of positive value (≥0.24 °C, in the upper-right quadrant).

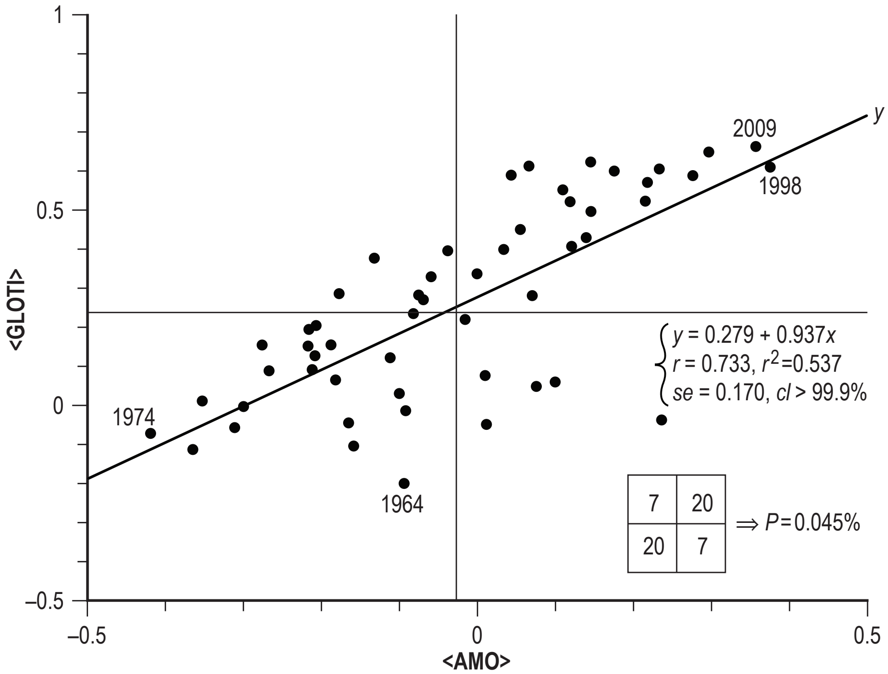

Figure 15. Scatterplot of <GLOTI> versus <AMO>.

Figure 16 displays the scatterplot of <ASAT> versus <GLOTI>, identifying the years of extreme values. The inferred regression has $r = 0.611$ and $r^2 = 0.323$, suggesting that about one-third of the variance in <ASAT> can be explained by the variation in <GLOTI>. Fisher's exact test for 2×2 contingency tables suggests that the probability of obtaining the observed result, or one more suggestive of a departure from independence, is $P = 0.015\%$. Because <GLOTI> undoubtedly will be of positive value in the year 2014, probably ≥0.6 °C, <ASAT> is expected to be ≥9.44 °C, probably ≥9.53 °C (in the upper-right quadrant).

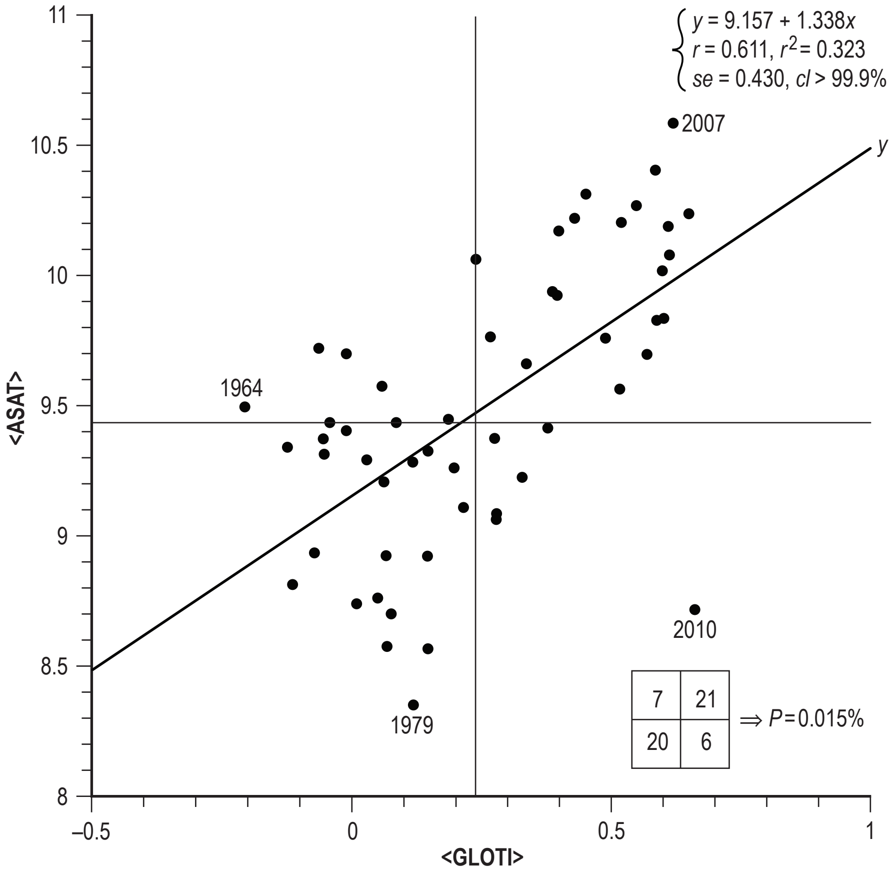

Figure 16. Scatterplot of <ASAT> versus <GLOTI>.

Figure 17 shows the scatterplot of <AMO> versus <MLCO2>, identifying the years of extreme values. The inferred regression has $r = 0.591$ and $r^2 = 0.349$, suggesting that about one-third of the variance in <AMO> can be explained by the variation in <MLCO2>, at least during the interval 1960–2013. Fisher's exact test for 2×2 contingency tables suggests that the probability of obtaining the observed result, or one more suggestive of a departure from independence, is $P = 0.12\%$. Because <MLCO2> continues to grow year-by-year, undoubtedly, its value for the year 2014 will be greater than its value for the year 2013 (=396.48 ppm) suggesting that <AMO> will be of positive value for the year 2014, having a yearly value in the upper-right quadrant.

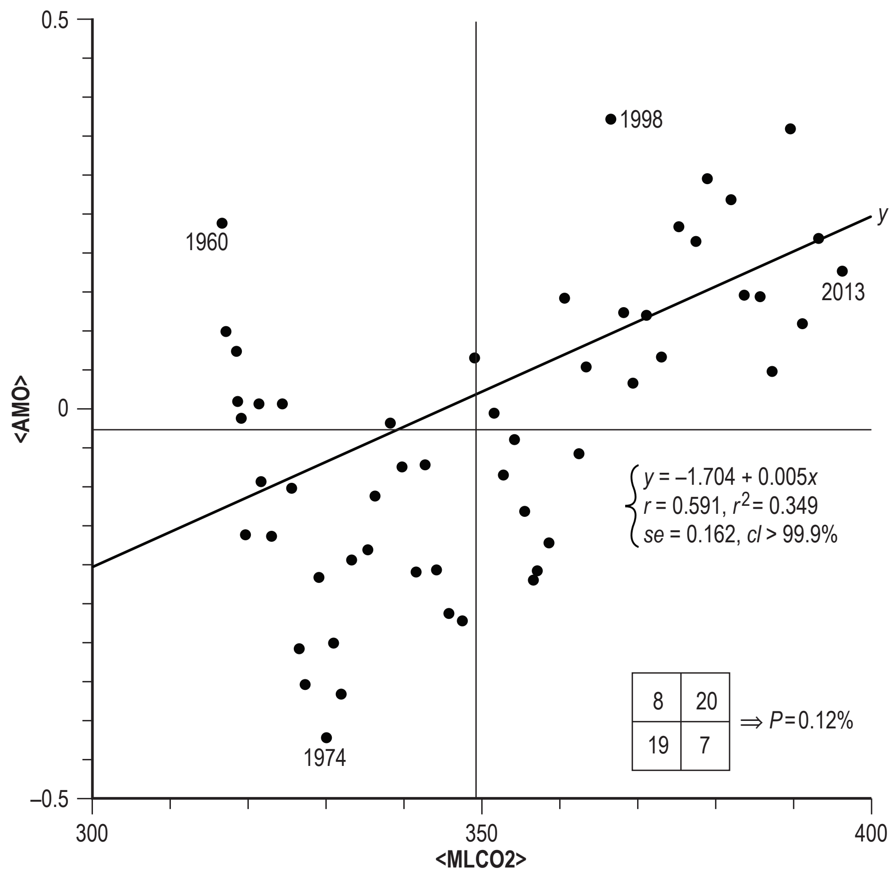

Figure 17. Scatterplot of <AMO> versus <MLCO2>.

Figure 18 depicts the scatterplot of <ASAT> versus <MLCO2>, identifying the years of extreme values. The inferred regression has $r = 0.592$ and $r^2 = 0.350$, suggesting that about one-third of the variance in <ASAT> can be explained by the variation in <MLCO2>, at least during the interval 1960–2013. Fisher's exact test for 2×2 contingency tables suggests that the probability of obtaining the observed result, or one more suggestive of a departure from independence, is $P = 0.015\%$. Because <MLCO2> continues to grow year-by-year, undoubtedly, its value for the year 2014 will be greater than its value for the year 2013 (=396.48 ppm) suggesting that <ASAT> will have a yearly value in the upper-right quadrant (≥9.44 °C).

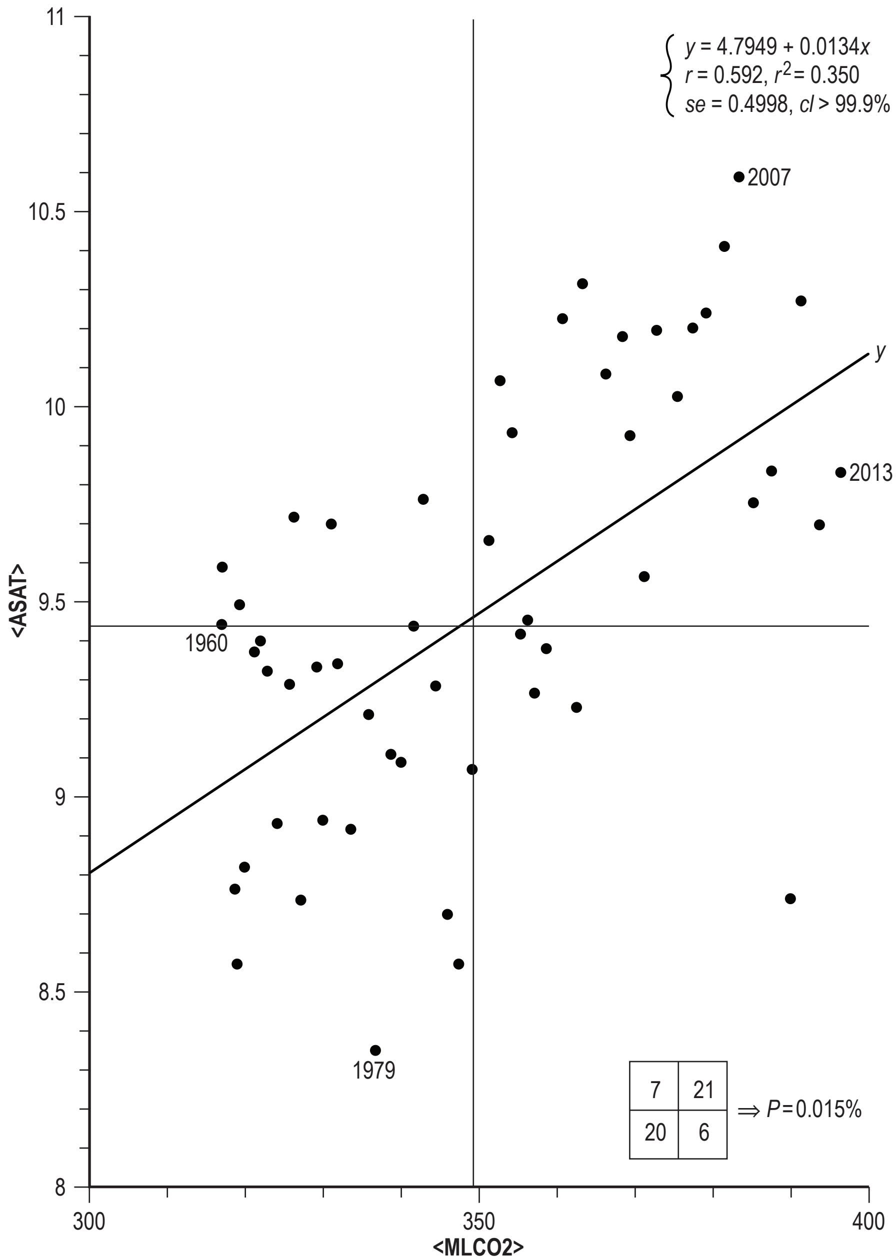

Figure 18. Scatterplot of <ASAT> versus <MLCO2>.

2.8 Inferred Statistical Relationships Between Tropical Cyclone Parametric Values and Selected Climate-Related Factors

Table 3 provides a summary of the statistics of the 25 tropical cyclone parameters identified in reference 1 against the 9 specific climate-related factors investigated in this TP. The 25 tropical cyclone parameters include:

- First storm day (FSD).
- Last storm day (LSD).
- Length of season (LOS).
- NTC.
- NH.
- NMH.
- NUSLFH.
- Mean seasonal latitude (<LAT>).
- Mean seasonal longitude (<LONG>).
- PWS.
- Mean seasonal PWS (<PWS>).
- Lowest pressure (LP).
- Mean seasonal LP (<LP>).
- Mean seasonal ACE (<ACE>).
- Total ACE.
- Highest individual storm ACE (HISACE).
- Mean seasonal Power Dissipation Index (PDI) (<PDI>).
- Total PDI.
- Highest individual storm PDI (HISPDI).
- Mean seasonal number of storm days (NSD) (<NSD>).
- Longest individual storm NSD (LISNSD).
- Total NSD.
- Total number of hurricane days (NHD).
- Total number of major hurricane days (NMHD).
- Net Tropical Cyclone Activity (NTCA).

From the table, one finds that none of the tropical cyclone parameters correlates strongly against <QBO>. The best climate-related factor that correlates with the most tropical cyclone parameters is <AMO>, having 15 correlations with $cl > 98\%$ and an additional 5 correlations with $cl > 95\%$. The second best climate-related factor is <SOI>, having 8 correlations with $cl > 98\%$ and an additional 5 correlations with $cl > 95\%$. In the following subsections, each of the scatterplots having $cl > 98\%$ is displayed, first those against <AMO>, then those against <SOI>, <MLCO2>, <GLOTI>, <ONI>, <NAO> CRU, <NAO> CPC, and <ASAT>. Furthermore, estimates are made for the selected tropical cyclone parameters based on the mean values of the specific climate-related factors for the more recent subinterval 1995–2013. When $cl > 98\%$ (from the linear regression analysis) and $P < 5\%$ (from Fisher's exact test), only then is the estimate considered reliable, presuming of course the accuracy for the projected value of the specific climate-related factor.

Table 3. Summary of tropical cyclone statistics against climate factors (single-variate fits), 1960–2013.

	<ONI>						<SOI>						<AMO>					
Parameter	***a***	***b***	***r***	***r^2***	***se***	***cl***	***a***	***b***	***r***	***r^2***	***se***	***cl***	***a***	***b***	***r***	***r^2***	***se***	***cl***
FSD	179.666	0.747	0.013	0.000	33.593	<90%	179.682	0.062	0.015	0.000	33.595	<90%	179.573	–3.579	–0.021	0.000	33.589	<90%
LSD	311.204	–14.770	–0.365	0.133	22.343	>99%**	311.398	0.838	0.277	0.077	23.052	>95%*	311.739	21.137	0.172	0.030	23.640	<90%
LOS	132.539	–15.517	–0.215	0.046	41.690	<90%	132.715	0.775	0.144	0.021	42.246	<90%	133.167	24.717	0.113	0.013	42.418	<90%
NTC	11.392	–2.562	–0.333	0.111	4.304	>98%**	11.440	0.200	0.348	0.121	4.278	>99%**	11.728	12.929	0.553	0.306	3.800	>99.9%**
NH	6.168	–1.177	–0.249	0.062	2.718	>90%	6.193	0.103	0.292	0.085	2.684	>95%*	6.352	7.082	0.493	0.243	2.442	>99.9%**
NMH	2.446	–0.936	–0.296	0.087	1.794	>95%*	2.468	0.094	0.397	0.157	1.724	>99.5%**	2.560	4.411	0.459	0.211	1.668	>99.9%**
NUSLFH	1.445	–0.321	–0.127	0.016	1.490	<90%	1.449	0.017	0.092	0.008	1.496	<90%	1.471	0.997	0.130	0.017	1.489	<90%
<LAT>	22.537	1.314	0.233	0.054	3.250	>90%	22.507	–0.127	–0.301	0.091	3.184	>95%*	22.298	–9.176	–0.536	0.288	2.821	>99.9%**
<LONG>	63.459	0.166	0.017	0.000	5.818	<90%	63.442	–0.067	–0.091	0.008	5.795	<90%	63.185	–10.456	–0.351	0.123	5.448	>99%**
PWS	124.264	–3.318	–0.089	0.008	21.912	<90%	124.320	0.241	0.087	0.008	21.910	<90%	125.080	31.305	0.278	0.077	21.134	>95%*
<PWS>	72.936	–3.470	–0.236	0.056	8.461	>90%	73.010	0.311	0.284	0.081	8.351	>95%*	73.125	7.389	0.166	0.027	7.863	<90%
LP	937.158	6.774	0.181	0.033	21.825	<90%	937.047	–0.472	–0.169	0.029	21.873	<90%	935.992	–44.795	–0.394	0.155	20.397	>99.5%**
<LP>	980.753	3.433	0.262	0.069	7.478	>90%	980.677	–0.317	–0.325	0.106	7.331	>98%**	980.446	–11.863	–0.299	0.089	7.421	>95%*
<ACE>	8.605	–0.788	–0.125	0.016	3.703	<90%	8.629	0.098	0.208	0.043	3.650	<90%	8.741	5.243	0.274	0.075	3.590	>95%*
Total ACE	100.507	–25.304	–0.251	0.063	57.816	>90%	101.087	2.416	0.321	0.103	56.564	>98%**	104.820	165.740	0.542	0.294	50.193	>99.9%**
HISACE	32.746	–2.978	–0.087	0.008	20.125	<90%	30.989	0.386	0.188	0.035	15.967	<90%	31.754	32.914	0.395	0.156	14.933	>99.5%**
<PDI>	6.949	–0.803	–0.122	0.015	3.884	<90%	6.973	0.099	0.201	0.040	3.833	<90%	7.110	6.181	0.309	0.095	3.722	>95%*
Total PDI	81.871	–20.496	–0.216	0.047	54.938	<90%	82.358	2.024	0.286	0.082	53.919	>95%*	85.900	154.648	0.537	0.288	47.466	>99.9%**
HISPDI	30.799	–1.963	–0.057	0.003	20.338	<90%	30.890	0.371	0.145	0.021	20.243	<90%	31.922	42.935	0.412	0.170	18.565	>99.8%**
<NSD>	4.942	–0.310	–0.135	0.018	1.347	<90%	4.952	0.045	0.261	0.068	1.314	>90%	5.007	2.528	0.363	0.132	1.269	>99%**
LISNSD	11.751	–0.456	–0.072	0.005	3.768	<90%	11.785	0.103	0.217	0.047	3.635	>99.8%**	11.907	5.638	0.292	0.085	3.631	>95%*
Total NSD	58.154	–15.196	–0.275	0.076	31.490	>95%*	58.495	1.495	0.363	0.131	30.519	>99%**	60.702	98.628	0.588	0.346	26.480	>99.9%**
Total NHD	23.712	–6.135	–0.246	0.061	14.304	<90%	23.854	0.593	0.319	0.102	13.987	>98%**	24.553	32.390	0.429	0.184	13.334	>99.8%**
Total NMHD	5.576	–1.355	–0.136	0.019	5.838	<90%	5.615	0.162	0.218	0.048	5.751	<90%	5.964	14.861	0.493	0.243	5.128	>99.9%**
NTCA	109.639	–28.679	–0.278	0.077	58.840	>95%*	110.310	2.791	0.362	0.131	57.094	>99%**	114.271	178.073	0.568	0.323	50.409	>99.9%**

*Inferred correlation is statistically significant at *cl* > 95%.
**Inferred correlation is statistically significant at *cl* > 98%.

Table 3. Summary of tropical cyclone statistics against climate factors (single-variate fits), 1960–2013 (Continued).

	<QBO>						<NAO> CPC						<NAO> CRU					
Parameter	***a***	***b***	***r***	r^2	***se***	***cl***	***a***	***b***	***r***	r^2	***se***	***cl***	***a***	***b***	***r***	r^2	***se***	***cl***
FSD	181.838	0.642	0.171	0.029	33.101	<90%	179.546	–1.631	–0.019	0.000	33.592	<90%	179.751	2.362	0.040	0.002	33.570	<90%
LSD	309.893	–0.382	–0.143	0.020	23.750	<90%	311.408	3.022	0.050	0.003	23.963	<90%	311.052	–3.716	–0.088	0.008	23.903	<90%
LOS	129.055	–1.024	–0.215	0.046	41.694	<90%	132.861	4.653	0.044	0.002	42.652	<90%	132.301	–6.077	–0.081	0.007	42.552	<90%
NTC	11.312	–0.023	–0.044	0.002	4.558	<90%	11.223	–2.246	–0.197	0.039	4.474	<90%	11.303	–2.396	–0.300	0.090	4.354	>95%*
NH	6.088	–0.023	–0.074	0.005	2.800	<90%	5.992	–2.372	–0.339	0.115	2.640	>98%**	6.100	–1.872	–0.381	0.145	2.595	<99.5%**
NMH	2.542	0.029	0.138	0.019	1.860	<90%	2.364	–1.089	–0.232	0.054	1.826	>90%	2.414	–0.840	–0.255	0.065	1.816	>90%
NUSLFH	1.493	0.014	0.085	0.007	1.496	<90%	1.435	–0.133	–0.035	0.001	1.501	<90%	1.435	–0.251	–0.095	0.009	1.496	<90%
<LAT>	22.556	0.005	0.014	0.000	3.340	<90%	22.615	1.033	0.124	0.015	3.316	<90%	22.577	1.077	0.184	0.034	3.285	<90%
<LONG>	63.271	–0.056	–0.086	0.007	5.790	<90%	63.440	–0.262	–0.018	0.000	5.818	<90%	63.447	–0.346	–0.034	0.001	5.814	<90%
PWS	123.948	–0.092	–0.038	0.001	21.986	<90%	123.772	–6.609	–0.120	0.015	21.841	<90%	124.113	–4.091	–0.106	0.011	21.877	<90%
<PWS>	73.068	0.040	0.042	0.002	8.696	<90%	72.632	–4.064	–0.187	0.035	8.555	<90%	72.909	–0.637	–0.042	0.002	8.699	<90%
LP	937.733	0.167	0.068	0.005	22.110	<90%	938.038	11.827	0.214	0.046	21.689	<90%	937.460	7.946	0.204	0.042	21.722	<90%
<LP>	980.611	–0.043	–0.050	0.003	7.807	<90%	981.055	4.040	0.209	0.044	7.605	<90%	980.799	1.174	0.086	0.007	7.748	<90%
<ACE>	8.734	0.039	0.093	0.009	3.718	<90%	8.522	–1.109	–0.119	0.014	3.706	<90%	8.602	–0.061	–0.009	0.000	3.732	<90%
Total ACE	101.624	0.340	0.051	0.003	59.652	<90%	98.251	–30.157	–0.202	0.041	58.493	<90%	99.661	–22.762	–0.217	0.047	58.299	<90%
HISACE	31.177	0.085	0.047	0.002	16.242	<90%	30.404	–6.600	–0.163	0.026	16.042	<90%	30.679	–5.938	–0.208	0.043	15.901	<90%
<PDI>	7.053	0.031	0.071	0.005	3.903	<90%	6.857	–1.232	–0.126	0.016	3.882	<90%	6.947	–0.038	–0.006	0.000	3.913	<90%
Total PDI	82.720	0.259	0.041	0.002	56.217	<90%	79.952	–25.681	–0.183	0.033	55.314	<90%	81.206	–17.850	–0.181	0.033	55.335	<90%
HISPDI	30.868	0.021	0.009	0.000	20.370	<90%	30.206	–8.008	–0.158	0.025	20.117	<90%	30.562	–6.564	–0.184	0.034	20.024	<90%
<NSD>	4.980	0.011	0.076	0.006	1.354	<90%	4.871	–0.950	–0.280	0.078	1.306	>95%*	4.913	–0.754	–0.316	0.100	1.291	>98%**
LISNSD	11.959	0.059	0.140	0.020	3.740	<90%	11.680	–1.067	–0.113	0.013	3.753	<90%	11.713	–1.304	–0.197	0.039	3.703	<90%
Total NSD	58.130	0.004	0.001	0.000	32.747	<90%	56.072	–27.726	–0.339	0.115	30.803	>98%**	57.203	–25.537	–0.445	0.198	29.326	>99.9%**
Total NHD	24.199	0.147	0.089	0.008	14.702	<90%	23.101	–8.175	–0.222	0.049	14.391	<90%	23.502	–5.654	–0.219	0.048	14.402	<90%
Total NMHD	5.677	0.030	0.046	0.002	5.886	<90%	5.437	–1.858	–0.126	0.016	5.846	<90%	5.536	–1.071	–0.104	0.011	5.861	<90%
NTCA	110.633	0.305	0.045	0.002	61.186	<90%	106.689	–39.526	–0.259	0.067	59.160	>90%	108.467	–31.741	–0.296	0.087	58.507	>95%*

*Inferred correlation is statistically significant at *cl* > 95%.
**Inferred correlation is statistically significant at *cl* > 98%.

Table 3. Summary of tropical cyclone statistics against climate factors (single-variate fits), 1960–2013 (Continued).

	<ASAT>						<GLOTI>						<MLCO2>					
Parameter	***a***	***b***	***r***	r^2	***se***	***cl***	***a***	***b***	***r***	r^2	***se***	***cl***	***a***	***b***	***r***	r^2	***se***	***cl***
FSD	281.414	–10.713	–0.174	0.030	33.077	<90%	183.324	–14.362	–0.107	0.011	33.404	<90	287.671	–0.308	–0.221	0.049	32.636	<90%
LSD	223.568	9.225	0.210	0.044	23.482	<90%	304.156	27.607	0.287	0.083	22.980	>95%*	209.712	0.289	0.291	0.085	24.149	>95%*
LOS	–56.846	19.939	0.256	0.065	41.268	>90%	121.832	41.968	0.245	0.060	41.387	>90%	–76.959	0.598	0.338	0.114	39.956	>98%**
NTC	–22.591	3.578	0.429	0.184	4.119	>99.8%**	8.815	10.107	0.553	0.306	3.803	>99.9%**	–25.399	0.105	0.555	0.308	3.770	>99.9%**
NH	–2.676	0.931	0.182	0.033	2.760	<90%	5.215	3.738	0.333	0.111	2.646	>98%	–4.478	0.030	0.261	0.068	2.859	>90%
NMH	–5.958	0.885	0.258	0.066	1.812	>90%	1.983	1.810	0.241	0.058	1.823	>90%	–2.980	0.015	0.199	0.040	1.953	<90%
NUSLFH	–1.614	0.322	0.117	0.014	1.492	<90%	1.447	–0.010	–0.002	0.000	1.502	<90%	0.616	0.002	0.038	0.001	1.564	<90%
<LAT>	32.251	–1.023	–0.167	0.028	3.307	<90%	23.702	–4.566	–0.341	0.116	3.139	>98%**	38.425	–0.045	–0.327	0.107	2.708	>99%**
<LONG>	77.213	–1.448	–0.136	0.019	5.756	<90%	65.133	–6.575	–0.282	0.080	5.584	>95%*	85.754	–0.064	–0.264	0.070	6.372	>90%
PWS	84.665	4.169	0.104	0.011	21.881	<90%	122.866	5.471	0.062	0.004	21.959	<90%	138.463	–0.041	–0.044	0.002	22.465	<90%
<PWS>	88.026	–1.589	–0.100	0.010	8.650	<90%	74.734	–7.078	–0.203	0.041	8.525	<90%	109.771	–0.105	–0.291	0.085	8.169	>95%*
LP	1,033.173	–10.109	–0.249	0.062	21.561	>90%	942.603	–21.350	–0.240	0.058	21.544	>90%	981.652	–0.127	–0.138	0.019	22.642	<90%
<LP>	989.712	–0.943	–0.067	0.004	7.843	<90%	980.053	2.766	0.089	0.008	7.728	<90%	962.171	0.053	0.165	0.027	8.225	<90%
<ACE>	6.323	0.240	0.035	0.001	3.732	<90%	9.219	–2.417	–0.162	0.026	3.684	<90%	20.601	–0.034	–0.221	0.049	3.541	<90%
Total ACE	–223.135	34.073	0.312	0.097	56.749	>95%*	84.033	64.567	0.270	0.073	57.513	>95%*	–85.405	0.530	0.214	0.046	58.438	<90%
HISACE	–15.568	4.892	0.165	0.027	16.034	<90%	30.294	2.342	0.036	0.001	16.249	<90%	32.379	–0.004	–0.006	0.000	16.172	<90%
<PDI>	3.275	0.387	0.054	0.003	3.905	<90%	7.498	–2.159	–0.138	0.019	3.876	<90%	18.702	–0.034	–0.207	0.043	3.979	<90%
Total PDI	–206.843	30.395	0.295	0.087	53.769	>95%*	68.335	53.054	0.235	0.055	54.683	>90%	–53.696	0.387	0.166	0.027	55.401	<90%
HISPDI	–22.487	5.610	0.151	0.023	20.141	<90%	29.481	5.164	0.063	0.004	20.331	<90%	31.348	–0.002	–0.002	0.000	20.488	<90%
<NSD>	5.627	–0.072	–0.029	0.001	1.356	<90%	4.818	0.485	0.089	0.008	1.354	<90%	3.706	0.004	0.062	0.004	0.993	<90%
LISNSD	–1.586	1.405	0.204	0.041	3.701	<90%	11.451	1.212	0.080	0.006	3.765	<90%	5.564	0.018	0.113	0.013	3.562	<90%
Total NSD	–80.718	14.618	0.244	0.060	31.756	>90%	42.629	60.822	0.464	0.215	29.013	>99.9%**	–154.552	0.607	0.447	0.200	29.193	>99.9%**
Total NHD	–30.148	5.670	0.210	0.044	14.431	<90%	21.963	6.836	0.116	0.013	14.660	<90%	11.831	0.034	0.055	0.003	14.699	<90%
Total NMHD	–21.322	2.832	0.263	0.069	5.686	>90%	4.532	4.092	0.173	0.030	5.804	<90%	–2.574	0.023	0.095	0.009	5.909	<90%
NTCA	–204.500	33.072	0.295	0.087	58.516	>95%*	89.455	79.122	0.323	0.104	57.973	>98%**	–127.784	0.677	0.267	0.071	59.110	>95%*

*Inferred correlation is statistically significant at *cl* > 95%.
**Inferred correlation is statistically significant at *cl* > 98%.

2.8.1 Inferred Correlations Against <AMO>

Figure 19 shows the scatterplot for NTC versus <AMO>, identifying the years of extreme values. The inferred regression is given approximately as $y = 11.7 + 12.9x$, having $r = 0.55$, $r^2 = 0.31$, $se = 3.8$, and $cl > 99.9\%$. Fisher's exact test for 2×2 contingency tables suggests that the probability of obtaining the observed result, or one more suggestive of a departure from independence, is $P = 0.6\%$. Hence, there is reason to believe, based on the expected value for <AMO> in the year 2014 (i.e., being of positive value), that NTC will lie in the upper-right quadrant of the scatterplot (i.e., NTC ≥ 11). The mean value for <AMO> during the more recent interval 1995–2013 measures 0.163. Using this value for <AMO> for the year 2014, one infers NTC = 13.8 ± 3.8 (the ±1 *se* prediction interval), or NTC ≥ 10.

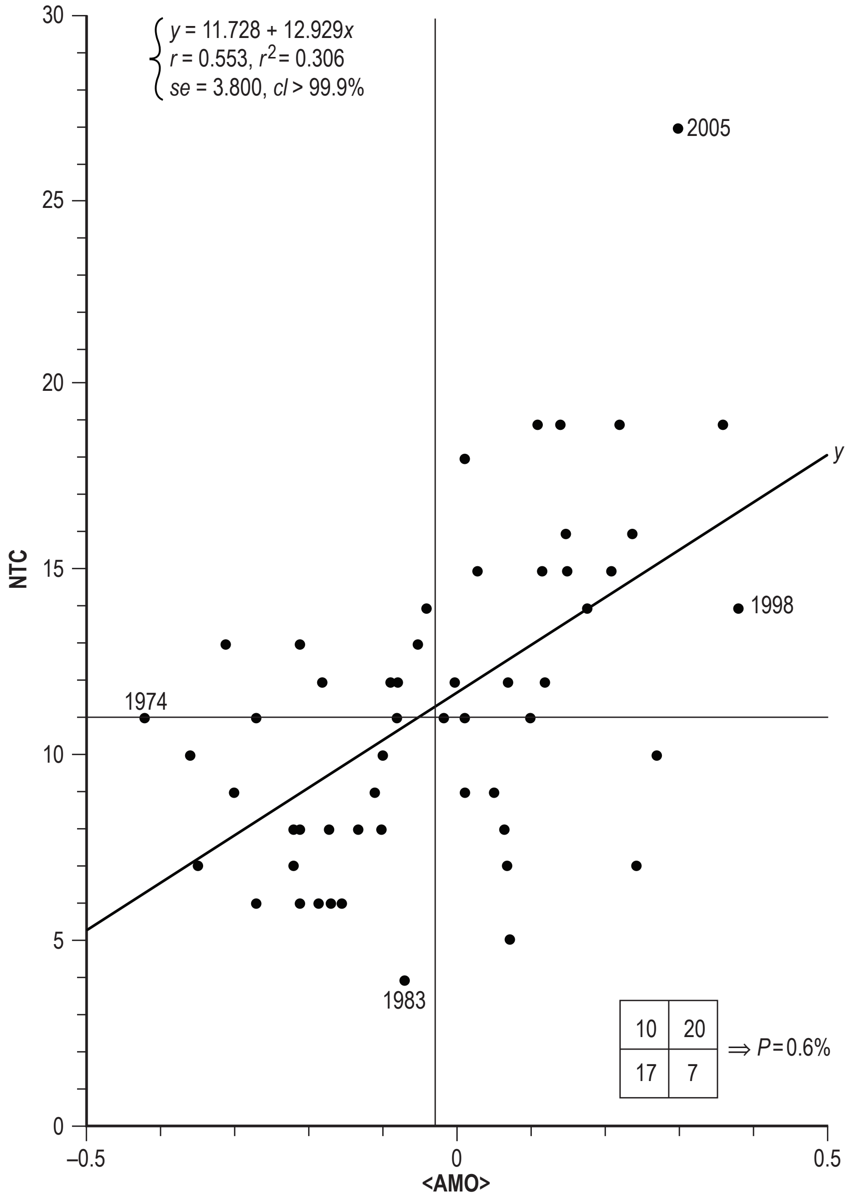

Figure 19. Scatterplot of NTC versus <AMO>.

Figure 20 depicts the scatterplot for NH versus <AMO>, identifying the years of extreme values. The inferred regression is given approximately as $y = 6.4 + 7.1x$, having $r = 0.49$, $r^2 = 0.24$, $se = 2.4$, and $cl > 99.9\%$. Fisher's exact test for 2×2 contingency tables suggests that the probability of obtaining the observed result, or one more suggestive of a departure from independence, is $P = 5.0\%$. Hence, based on the expected value for <AMO> in the year 2014 (i.e., being of positive value), NH is expected to lie in the upper-right quadrant of the scatterplot (i.e., NH $\geq$ 6). The mean value for <AMO> during the more recent interval 1995–2013 measures 0.163. Using this value for <AMO> for the year 2014, one infers NH = 7.6 ± 2.4, or NH $\geq$ 5 (rounded to the nearest whole number).

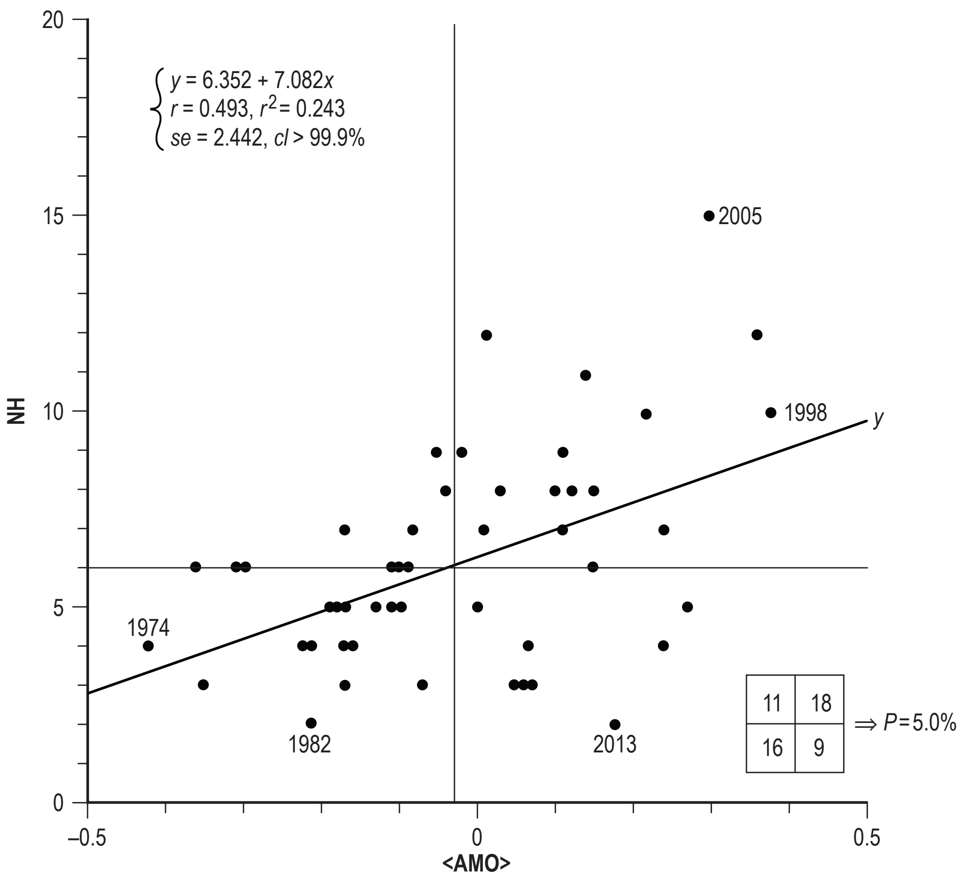

Figure 20. Scatterplot of NH versus <AMO>.

Figure 21 displays the scatterplot for NMH versus <AMO>, identifying the years of extreme values. The inferred regression is given approximately as $y = 2.6 + 4.4x$, having $r = 0.46$, $r^2 = 0.21$, $se = 1.7$, and $cl > 99.9\%$. Fisher's exact test for 2×2 contingency tables suggests that the probability of obtaining the observed result, or one more suggestive of a departure from independence, is $P = 0.5\%$. Hence, based on the expected value for <AMO> in the year 2014 (i.e., being of positive value), NMH is expected to lie in the upper-right quadrant of the scatterplot (i.e., NMH ≥ 2). The mean value for <AMO> during the more recent interval 1995–2013 measures 0.163. Using this value for <AMO> for the year 2014, one infers NMH = 3.3 ± 1.7, or NMH ≥ 2 (rounded to the nearest whole number).

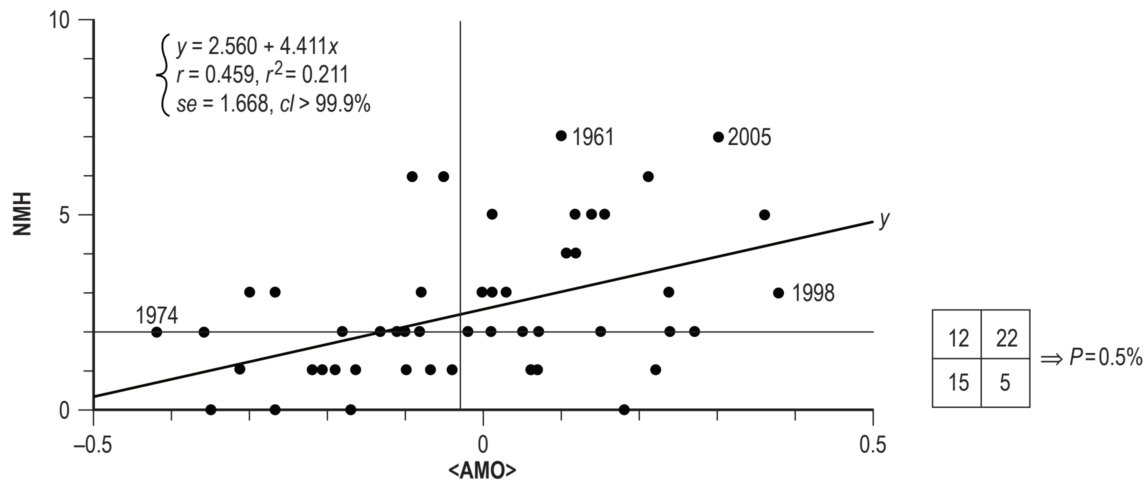

Figure 21. Scatterplot of NMH versus <AMO>.

Figure 22 shows the scatterplot for <LAT> versus <AMO>, identifying the years of extreme values. The inferred regression is given approximately as $y = 22.3 - 9.2x$, having $r = -0.54$, $r^2 = 0.29$, $se = 2.8$, and $cl > 99.9\%$. Fisher's exact test for 2×2 contingency tables suggests that the probability of obtaining the observed result, or one more suggestive of a departure from independence, is $P = 0.7\%$. Hence, based on the expected value for <AMO> in the year 2014 (i.e., being of positive value), <LAT> is expected to lie in the lower-right quadrant of the scatterplot (i.e., <LAT> < 22° N.). The mean value for <AMO> during the more recent interval 1995–2013 measures 0.163. Using this value for <AMO> for the year 2014, one infers <LAT> = 20.8 ± 2.8° N., or <LAT> < 23.6° N.

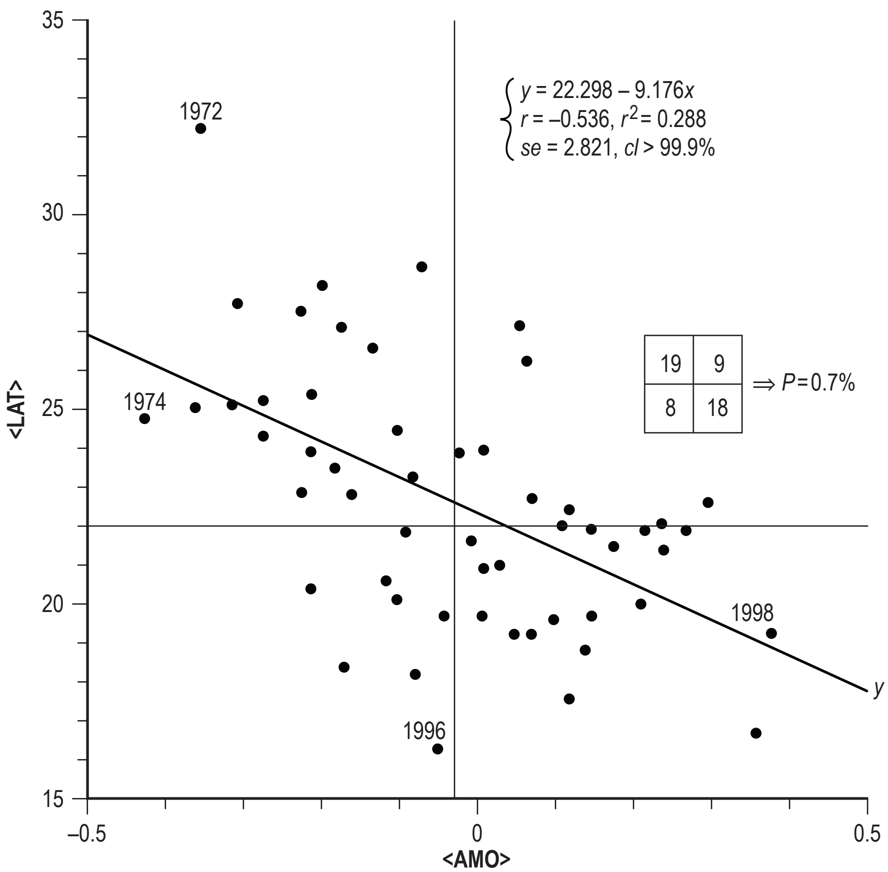

Figure 22. Scatterplot of <LAT> versus <AMO>.

Figure 23 depicts the scatterplot for <LONG> versus <AMO>, identifying the years of extreme values. The inferred regression is given approximately as $y = 63.2 - 10.5x$, having $r = -0.35$, $r^2 = 0.12$, $se = 5.4$, and $cl > 99\%$. Fisher's exact test for 2×2 contingency tables suggests that the probability of obtaining the observed result, or one more suggestive of a departure from independence, is $P = 29.3\%$. The mean value for <AMO> during the more recent interval 1995–2013 measures 0.163. Using this value for <AMO> for the year 2014, one infers <LONG> = 61.5 ± 5.4° W., or <LONG> < 67° W.

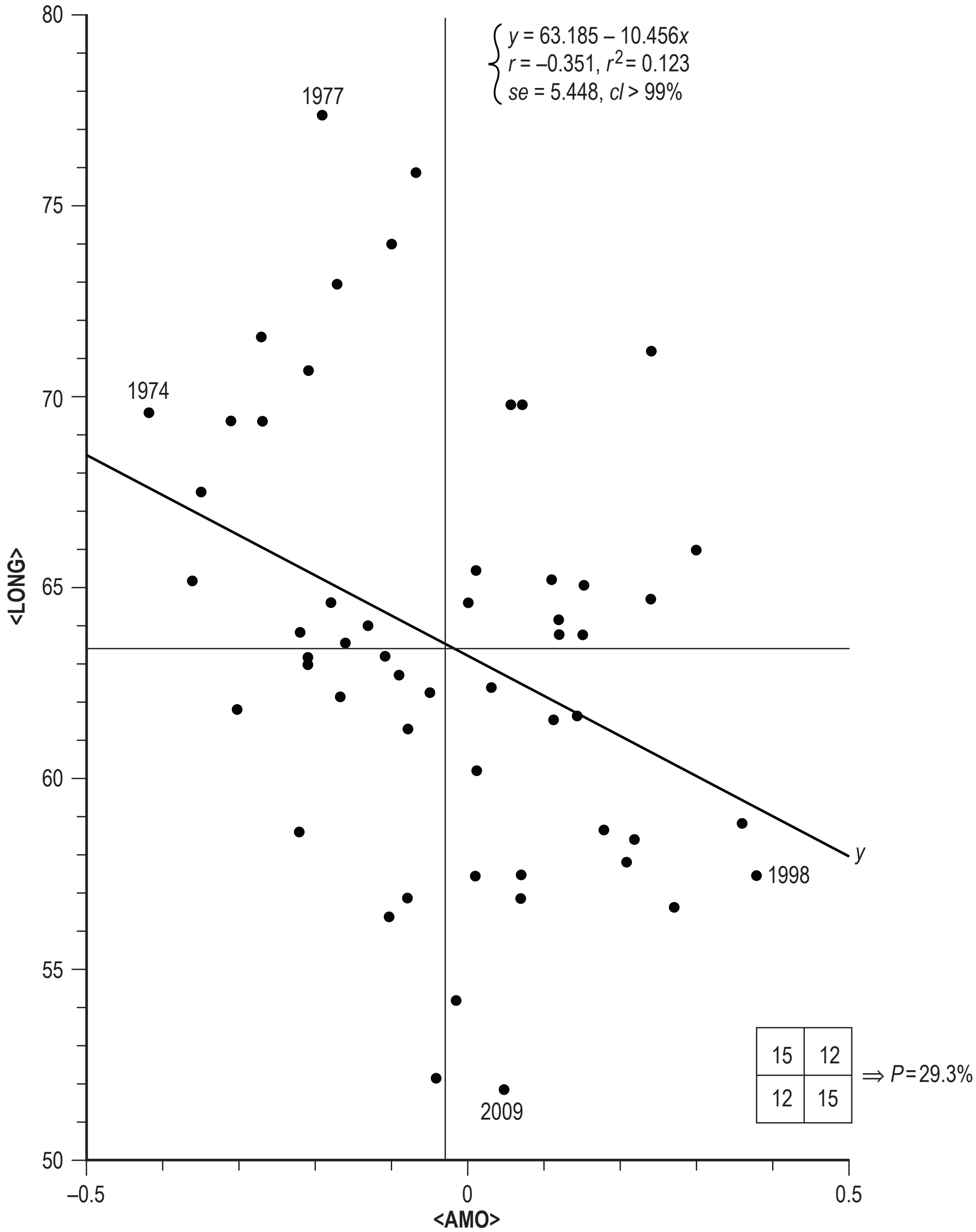

Figure 23. Scatterplot of <LONG> versus <AMO>.

Figure 24 displays the scatterplot for LP versus <AMO>, identifying the years of extreme values. The inferred regression is given approximately as $y = 936.0 - 44.8x$, having $r = -0.39$, $r^2 = 0.16$, $se = 20.4$, and $cl > 99.5\%$. Fisher's exact test for 2×2 contingency tables suggests that the probability of obtaining the observed result, or one more suggestive of a departure from independence, is $P = 2.8\%$. The mean value for <AMO> during the more recent interval 1995–2013 measures 0.163. Using this value for <AMO> for the year 2014, one infers LP = 928.7 ± 20.4 mb, or LP < 949.1 mb.

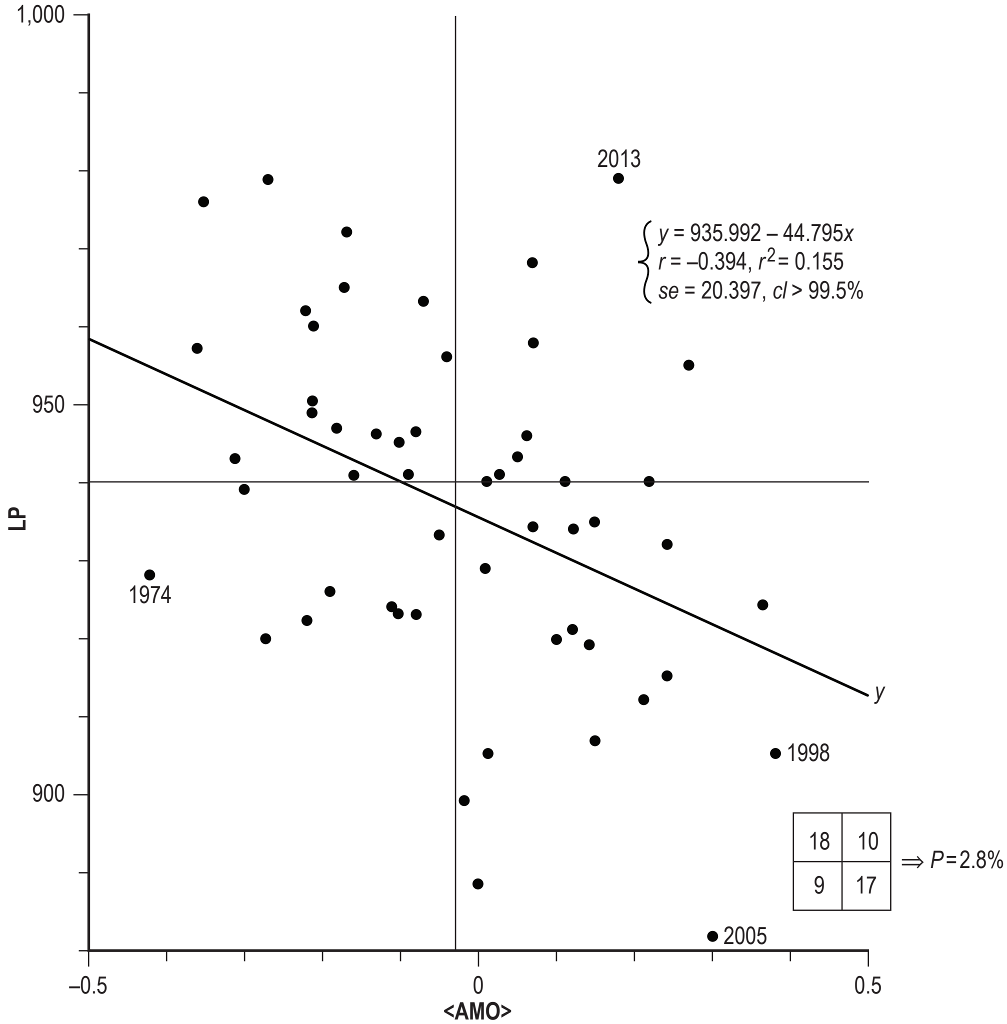

Figure 24. Scatterplot of LP versus <AMO>.

Figure 25 shows the scatterplot for total ACE versus <AMO>, identifying the years of extreme values. The inferred regression is given approximately as $y = 104.8 + 165.7x$, having $r = 0.54$, $r^2 = 0.29$, $se = 50.2$, and $cl > 99.9\%$. Fisher's exact test for 2×2 contingency tables suggests that the probability of obtaining the observed result, or one more suggestive of a departure from independence, is $P = 0.7\%$. The mean value for <AMO> during the more recent interval 1995–2013 measures 0.163. Using this value for <AMO> for the year 2014, one infers total ACE = 131.8 ± 50.2, or total ACE ≥ 81.6 (units are 10^4 kt^2).

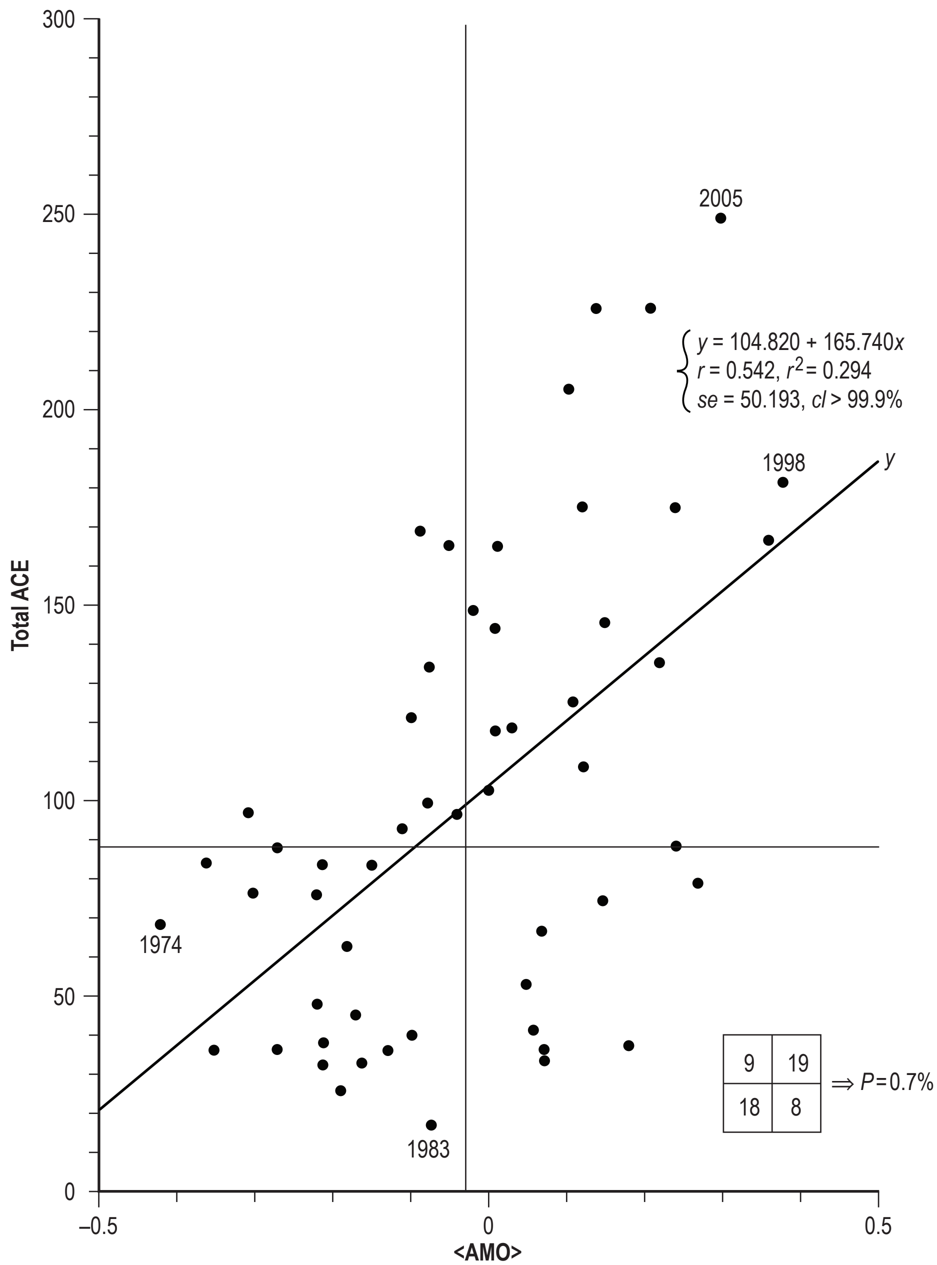

Figure 25. Scatterplot of total ACE versus <AMO>.

Figure 26 depicts the scatterplot for HISACE versus <AMO>, identifying the years of extreme values. The inferred regression is given approximately as $y = 31.8 + 32.9x$, having $r = 0.40$, $r^2 = 0.16$, $se = 14.9$, and $cl > 99.5\%$. Fisher's exact test for 2×2 contingency tables suggests that the probability of obtaining the observed result, or one more suggestive of a departure from independence, is $P = 1.4\%$. The mean value for <AMO> during the more recent interval 1995–2013 measures 0.163. Using this value for <AMO> for the year 2014, one infers HISACE = 37.1 ± 14.9, or HISACE ≥ 22.2 (units are 10^4 kt^2).

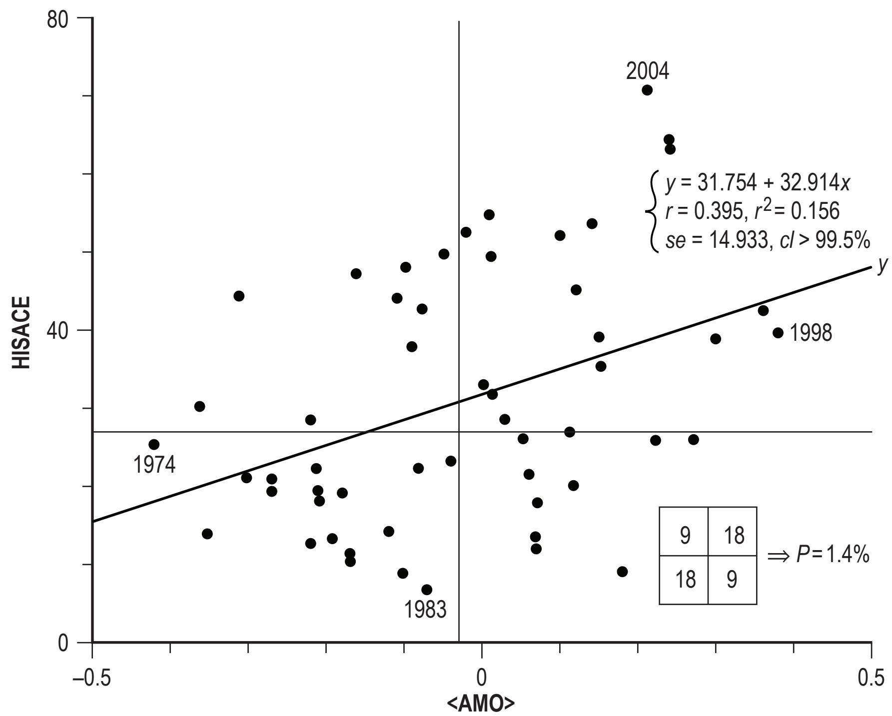

Figure 26. Scatterplot of HISACE versus <AMO>.

Figure 27 displays the scatterplot for total PDI versus <AMO>, identifying the years of extreme values. The inferred regression is given approximately as $y = 85.9 + 154.6x$, having $r = 0.54$, $r^2 = 0.29$, $se = 47.5$, and $cl > 99.9\%$. Fisher's exact test for 2×2 contingency tables suggests that the probability of obtaining the observed result, or one more suggestive of a departure from independence, is $P = 0.045\%$. The mean value for <AMO> during the more recent interval 1995–2013 measures 0.163. Using this value for <AMO> for the year 2014, one infers total PDI = 111.1 ± 47.5, or total PDI ≥ 63.6 (units are 10^6 kt^3).

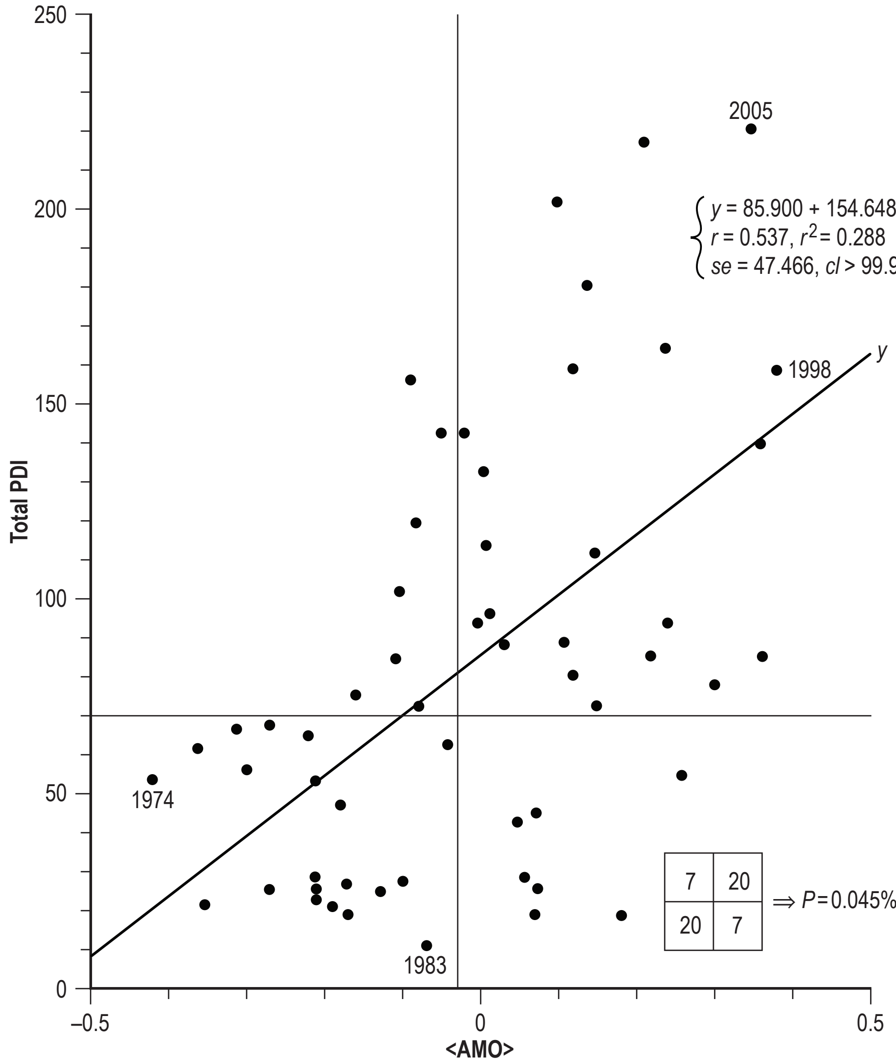

Figure 27. Scatterplot of total PDI versus <AMO>.

Figure 28 shows the scatterplot for HISPDI versus <AMO>, identifying the years of extreme values. The inferred regression is given approximately as $y = 31.9 + 42.9x$, having $r = 0.41$, $r^2 = 0.17$, $se = 18.6$, and $cl > 99.8\%$. Fisher's exact test for 2×2 contingency tables suggests that the probability of obtaining the observed result, or one more suggestive of a departure from independence, is $P = 1.4\%$. The mean value for <AMO> during the more recent interval 1995–2013 measures 0.163. Using this value for <AMO> for the year 2014, one infers HISPDI = 38.9 ± 18.6, or HISPDI ≥ 20.3 (units are 10^6 kt^3).

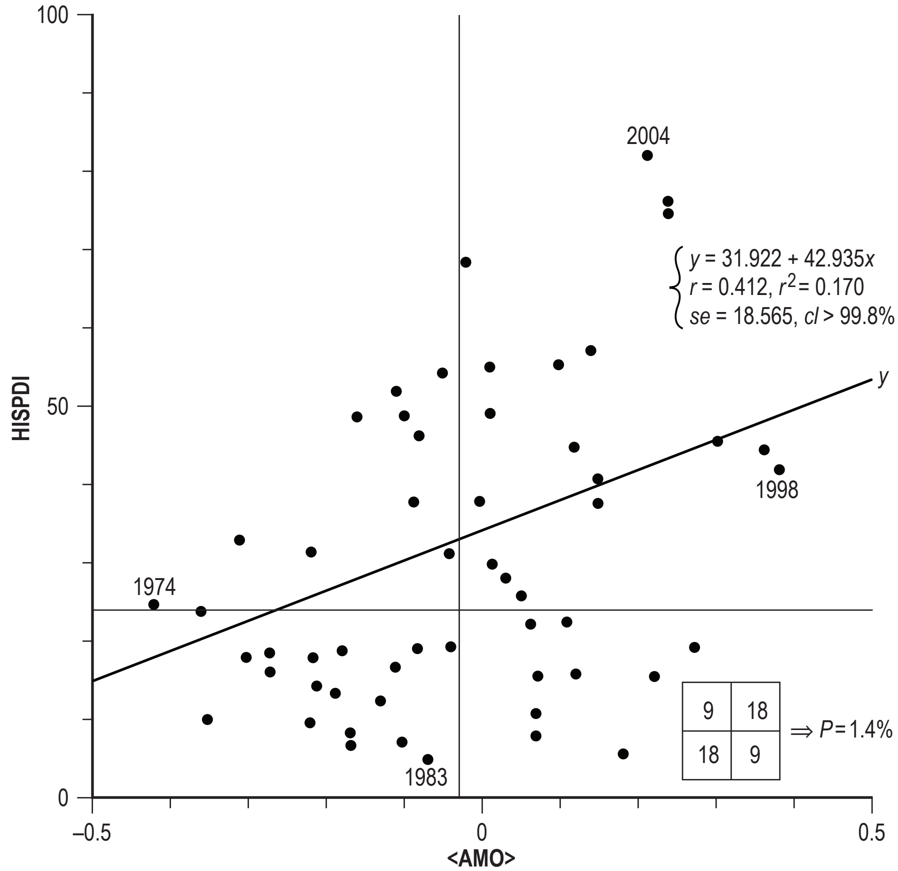

Figure 28. Scatterplot of HISPDI versus <AMO>.

Figure 29 depicts the scatterplot for <NSD> versus <AMO>, identifying the years of extreme values. The inferred regression is given approximately as $y = 5.0 + 2.5x$, having $r = 0.36$, $r^2 = 0.13$, $se = 1.3$, and $cl > 99\%$. Fisher's exact test for 2×2 contingency tables suggests that the probability of obtaining the observed result, or one more suggestive of a departure from independence, is $P = 29.3\%$. The mean value for <AMO> during the more recent interval 1995–2013 measures 0.163. Using this value for <AMO> for the year 2014, one infers <NSD> = 5.4 ± 1.3 days, or <NSD> ≥ 4.1 days.

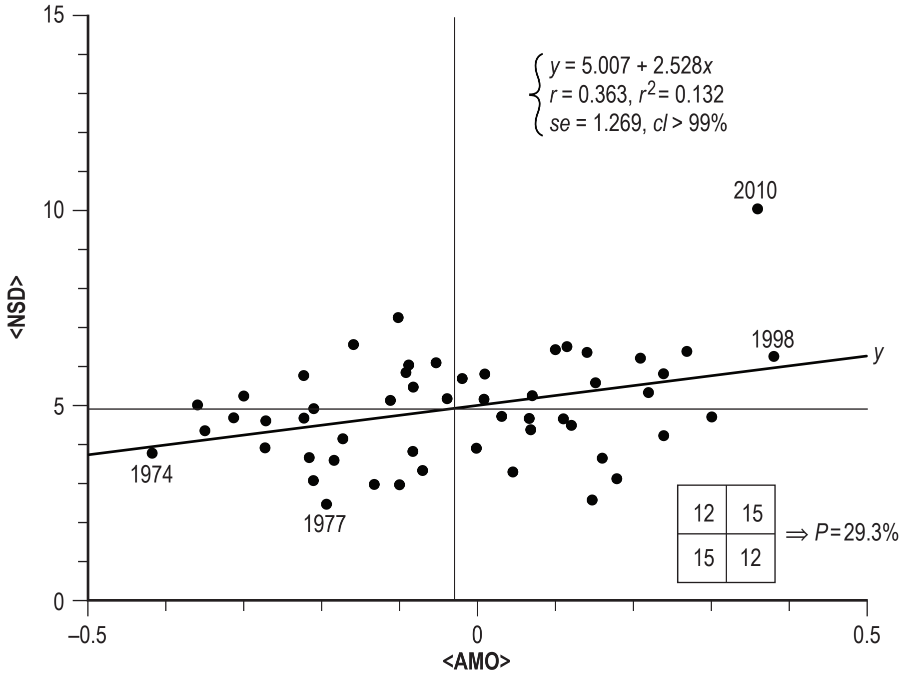

Figure 29. Scatterplot of <NSD> versus <AMO>.

Figure 30 displays the scatterplot for total NSD versus <AMO>, identifying the years of extreme values. The inferred regression is given approximately as $y = 60.7 + 98.6x$, having $r = 0.59$, $r^2 = 0.35$, $se = 26.5$, and $cl > 99.9\%$. Fisher's exact test for 2×2 contingency tables suggests that the probability of obtaining the observed result, or one more suggestive of a departure from independence, is $P = 0.3\%$. The mean value for <AMO> during the more recent interval 1995–2013 measures 0.163. Using this value for <AMO> for the year 2014, one infers total NSD = 76.8 ± 26.5 days, or total NSD ≥ 50.3 days.

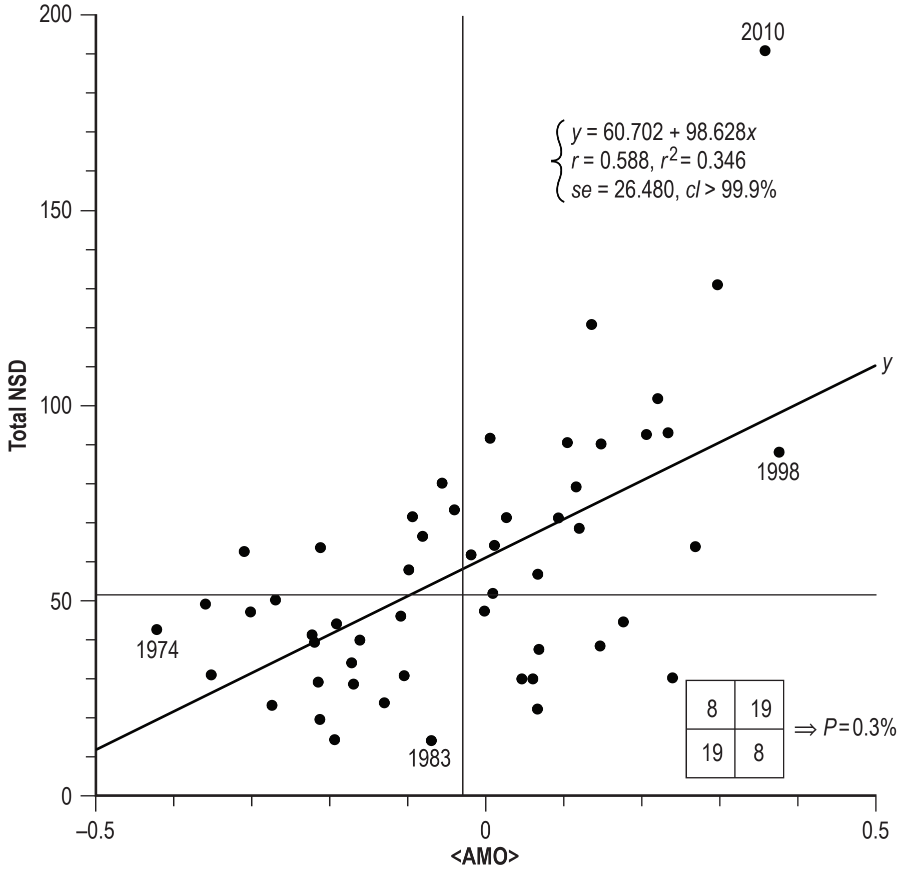

Figure 30. Scatterplot of total NSD versus <AMO>.

Figure 31 shows the scatterplot for total NHD versus <AMO>, identifying the years of extreme values. The inferred regression is given approximately as $y = 24.6 + 32.4x$, having $r = 0.43$, $r^2 = 0.18$, $se = 13.3$, and $cl > 99.8\%$. Fisher's exact test for 2×2 contingency tables suggests that the probability of obtaining the observed result, or one more suggestive of a departure from independence, is $P = 5.1\%$. The mean value for <AMO> during the more recent interval 1995–2013 measures 0.163. Using this value for <AMO> for the year 2014, one infers total NHD = 29.8 ± 13.3 days, or total NHD ≥ 16.5 days.

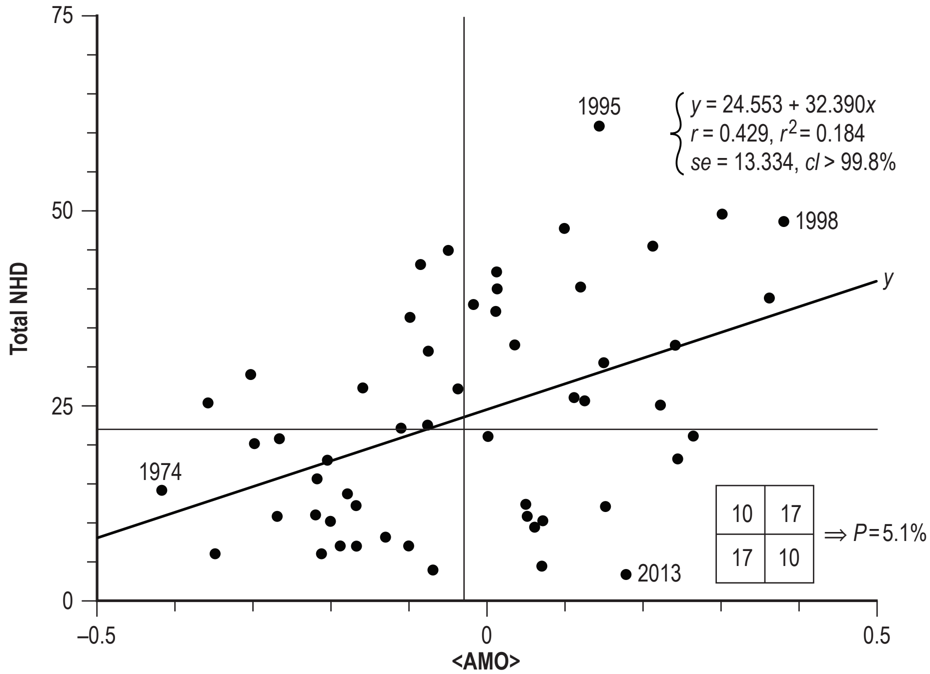

Figure 31. Scatterplot of total NHD versus <AMO>.

Figure 32 depicts the scatterplot for total NMHD versus <AMO>, identifying the years of extreme values. The inferred regression is given approximately as $y = 6.0 + 14.9x$, having $r = 0.49$, $r^2 = 0.24$, $se = 5.1$, and $cl > 99.9\%$. Fisher's exact test for 2×2 contingency tables suggests that the probability of obtaining the observed result, or one more suggestive of a departure from independence, is $P = 0.3\%$. The mean value for <AMO> during the more recent interval 1995–2013 measures 0.163. Using this value for <AMO> for the year 2014, one infers total NMHD = 8.4 ± 5.1 days, or total NMHD ≥ 3.3 days.

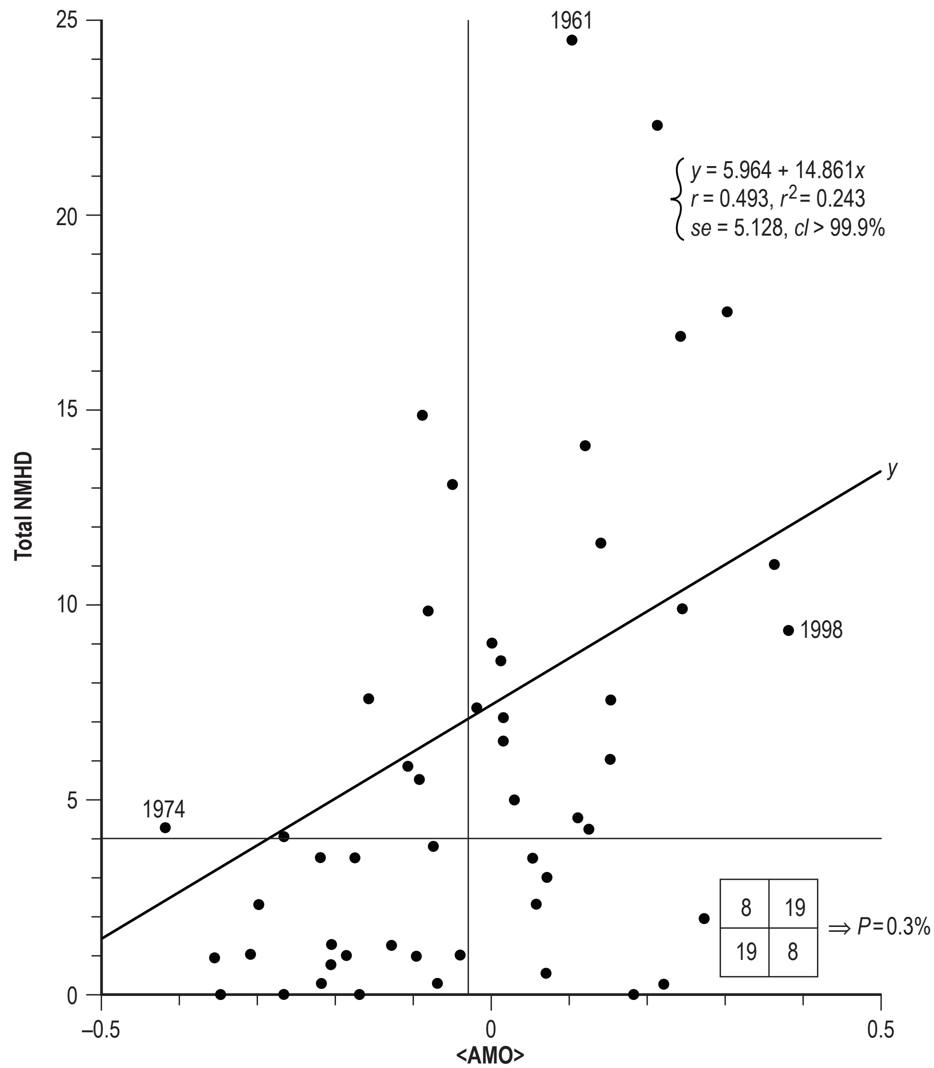

Figure 32. Scatterplot of total NMHD versus <AMO>.

Figure 33 displays the scatterplot for NTCA versus <AMO>, identifying the years of extreme values. The inferred regression is given approximately as $y = 114.3 + 178.1x$, having $r = 0.57$, $r^2 = 0.32$, $se = 50.4$, and $cl > 99.9\%$. Fisher's exact test for 2×2 contingency tables suggests that the probability of obtaining the observed result, or one more suggestive of a departure from independence, is $P = 0.3\%$. The mean value for <AMO> during the more recent interval 1995–2013 measures 0.163. Using this value for <AMO> for the year 2014, one infers NTCA = 143.3 ± 50.4 days, or NTCA ≥ 92.9%.

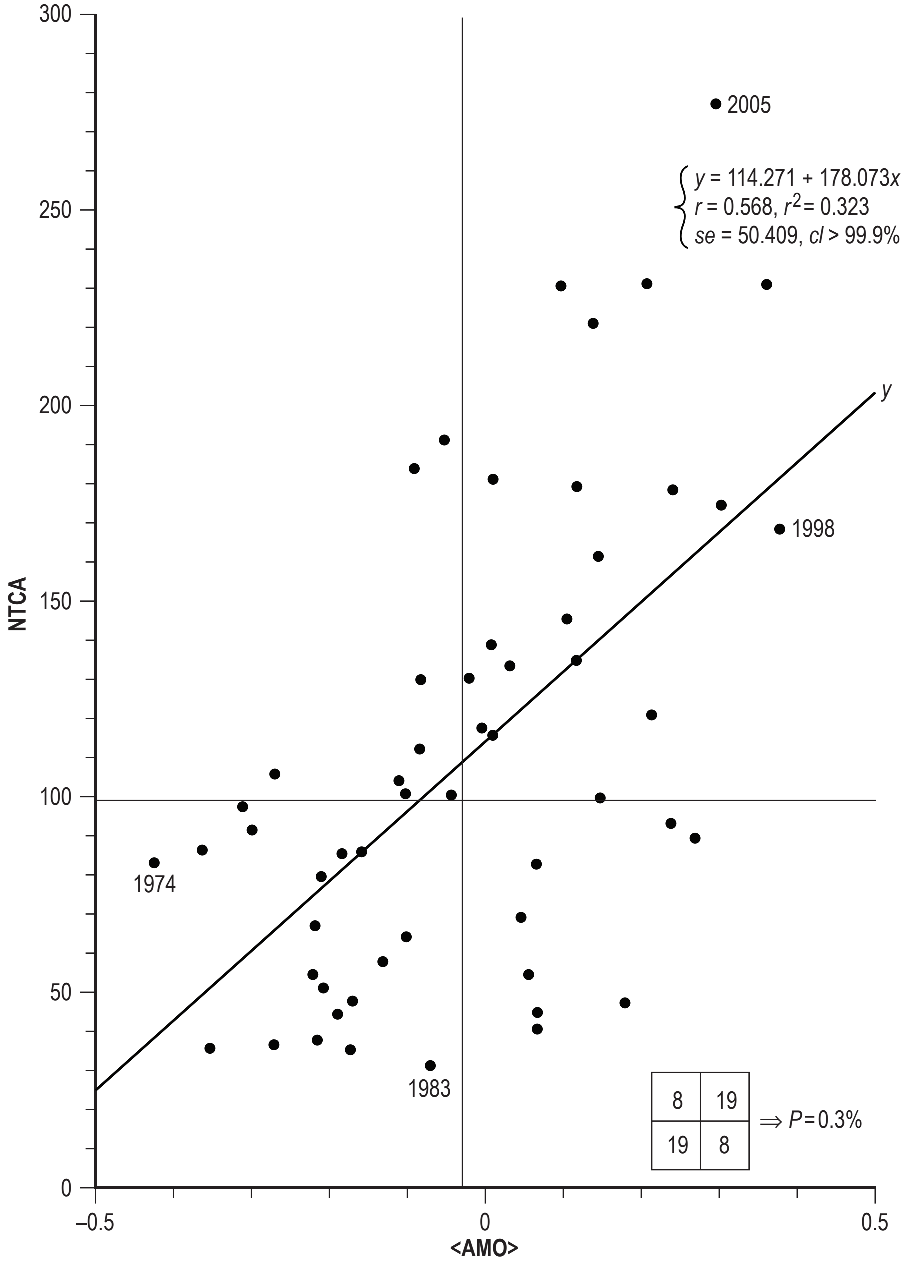

Figure 33. Scatterplot of NTCA versus <AMO>.

2.8.2 Inferred Correlations Against <SOI>

Figure 34 shows the scatterplots of (a) NTC, (b) NMH, and (c) <LP> versus <SOI>, identifying the years of extreme values in each panel. Concerning NTC versus <SOI>, the inferred regression is given approximately as $y = 11.4 + 0.2x$, having $r = 0.35$, $r^2 = 0.12$, $se = 4.3$, and $cl > 99\%$. Fisher's exact test for 2×2 contingency tables suggests that the probability of obtaining the observed result, or one more suggestive of a departure from independence, is $P = 8.5\%$. The mean value for <SOI> during the more recent interval 1995–2013 measures 2.1. Using this value for <SOI> for the year 2014, one infers NTC $= 11.9 \pm 4.3$, or NTC ≥ 8 (rounded to the nearest whole number).

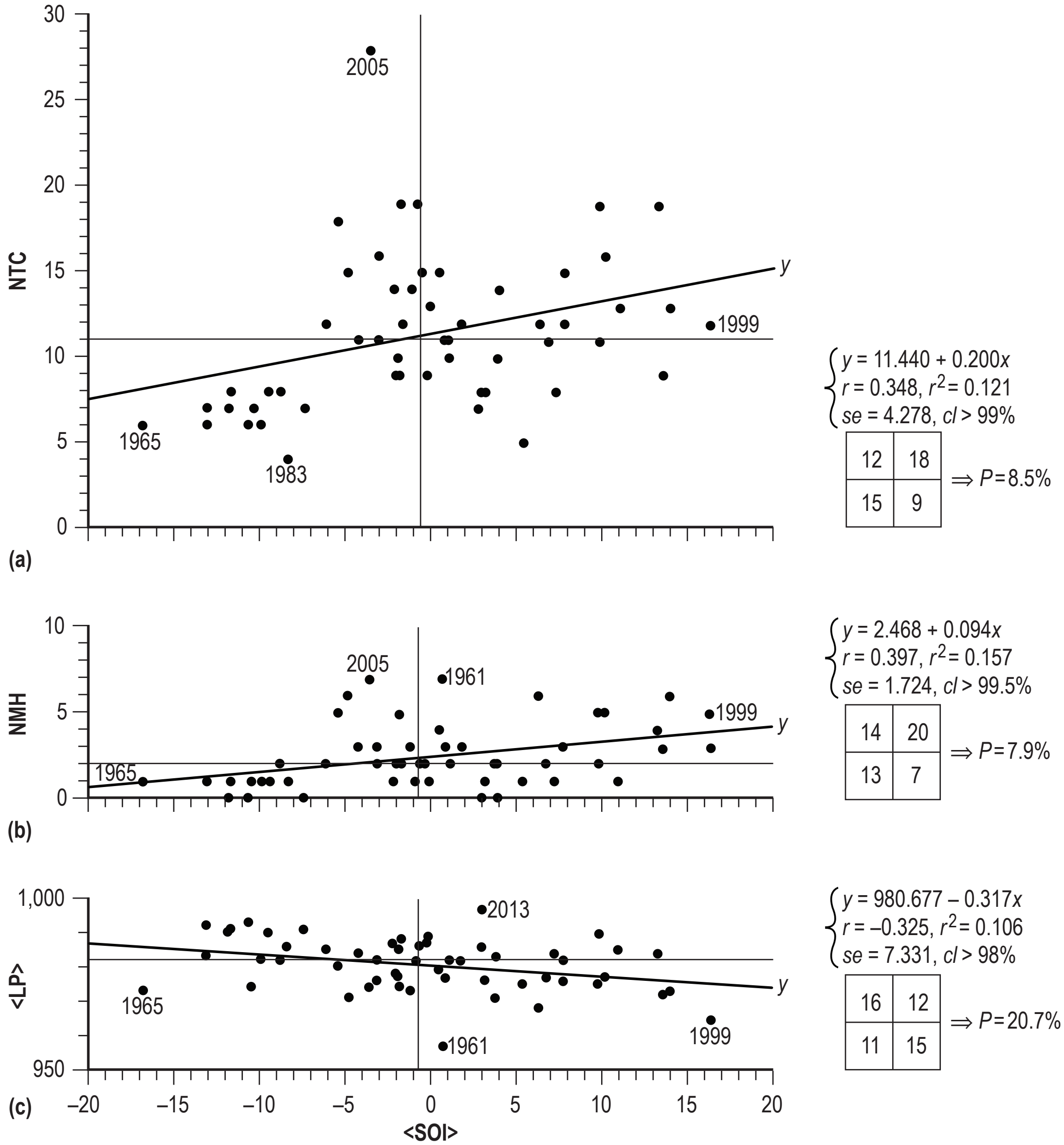

Figure 34. Scatterplots of (a) NTC, (b) NMH, and (c) <LP> versus <SOI>.

Concerning NMH versus <SOI>, the inferred regression is given approximately as $y = 2.5 + 0.1x$, having $r = 0.40$, $r^2 = 0.16$, $se = 1.7$, and $cl > 99.5\%$. Fisher's exact test for 2×2 contingency tables suggests that the probability of obtaining the observed result, or one more suggestive of a departure from independence, is $P = 7.9\%$. The mean value for <SOI> during the more recent interval 1995–2013 measures 2.1. Using this value for <SOI> for the year 2014, one infers NMH = 2.7 ± 1.7, or NMH ≥ 1.

Concerning <LP> versus <SOI>, the inferred regression is given approximately as $y = 980.7 - 0.3x$, having $r = -0.33$, $r^2 = 0.11$, $se = 7.3$, and $cl > 98\%$. Fisher's exact test for 2×2 contingency tables suggests that the probability of obtaining the observed result, or one more suggestive of a departure from independence, is $P = 20.7\%$. The mean value for <SOI> during the more recent interval 1995–2013 measures 2.1. Using this value for <SOI> for the year 2014, one infers <LP> = 980.0 ± 7.3 mb, or <LP> < 987.3 mb.

Figure 35 depicts the scatterplots of (a) total ACE and (b) LISNSD versus <SOI>, identifying the years of extreme values in each panel. Concerning total ACE versus <SOI>, the inferred regression is given approximately as $y = 101.1 + 2.4x$, having $r = 0.32$, $r^2 = 0.10$, $se = 56.6$, and $cl > 98\%$. Fisher's exact test for 2×2 contingency tables suggests that the probability of obtaining the observed result, or one more suggestive of a departure from independence, is $P = 20.7\%$. The mean value for <SOI> during the more recent interval 1995–2013 measures 2.1. Using this value for <SOI> for the year 2014, one infers total ACE = 106.2 ± 56.6, or total ACE ≥ 49.6 (units in 10^4 kt^2).

Concerning LISNSD versus <SOI>, the inferred regression is given approximately as $y = 11.8 + 0.1x$, having $r = 0.22$, $r^2 = 0.05$, $se = 3.6$, and $cl > 99.8\%$. Fisher's exact test for 2×2 contingency tables suggests that the probability of obtaining the observed result, or one more suggestive of a departure from independence, is $P = 39.2\%$. The mean value for <SOI> during the more recent interval 1995–2013 measures 2.1. Using this value for <SOI> for the year 2014, one infers LISNSD = 12.0 ± 3.6 days, or LISNSD ≥ 8.4 days.

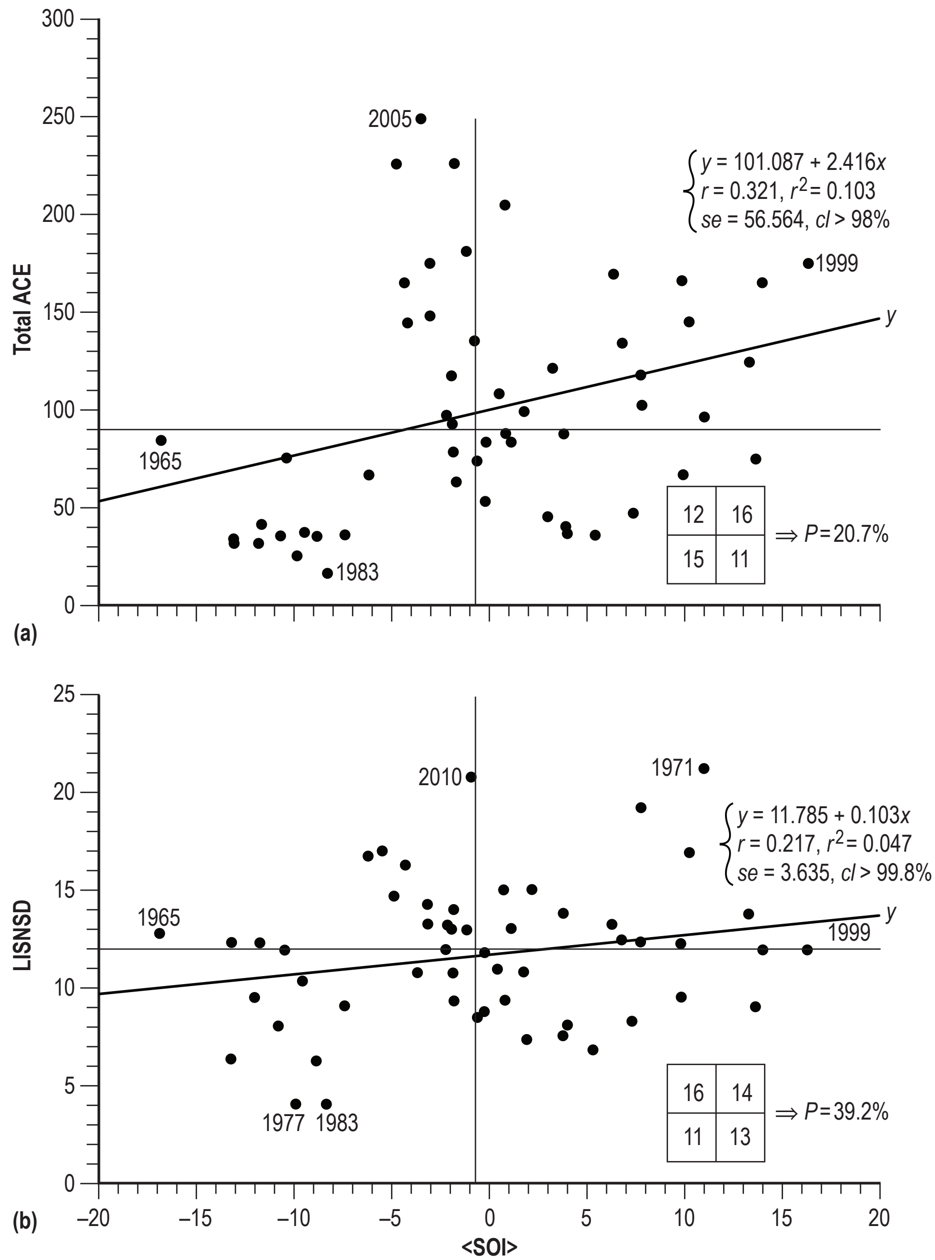

Figure 35. Scatterplots of (a) total ACE and (b) LISNSD versus <SOI>.

Figure 36 displays the scatterplots of (a) total NSD, (b) total NHD, and (c) NTCA versus <SOI>, identifying the years of extreme values in each panel. Concerning total NSD versus <SOI>, the inferred regression is given approximately as $y = 58.5 + 1.5x$, having $r = 0.36$, $r^2 = 0.13$, $se = 30.5$, and $cl > 99\%$. Fisher's exact test for 2×2 contingency tables suggests that the probability of obtaining the observed result, or one more suggestive of a departure from independence, is $P = 50.0\%$. The mean value for <SOI> during the more recent interval 1995–2013 measures 2.1. Using this value for <SOI> for the year 2014, one infers total NSD = 61.6 ± 30.5 days, or total NSD ≥ 31.1 days.

Concerning total NHD versus <SOI>, the inferred regression is given approximately as $y = 23.9 + 0.6x$, having $r = 0.32$, $r^2 = 0.10$, $se = 14.0$, and $cl > 98\%$. Fisher's exact test for 2×2 contingency tables suggests that the probability of obtaining the observed result, or one more suggestive of a departure from independence, is $P = 50.0\%$. The mean value for <SOI> during the more recent interval 1995–2013 measures 2.1. Using this value for <SOI> for the year 2014, one infers total NHD = 25.1 ± 14.0 days, or total NHD ≥ 11.1 days.

Concerning NTCA versus <SOI>, the inferred regression is given approximately as $y = 110.3 + 2.8x$, having $r = 0.36$, $r^2 = 0.13$, $se = 57.1$, and $cl > 99\%$. Fisher's exact test for 2×2 contingency tables suggests that the probability of obtaining the observed result, or one more suggestive of a departure from independence, is $P = 29.3\%$. The mean value for <SOI> during the more recent interval 1995–2013 measures 2.1. Using this value for <SOI> for the year 2014, one infers NTCA = 116.2 ± 57.1%, or NTCA ≥ 59.1%.

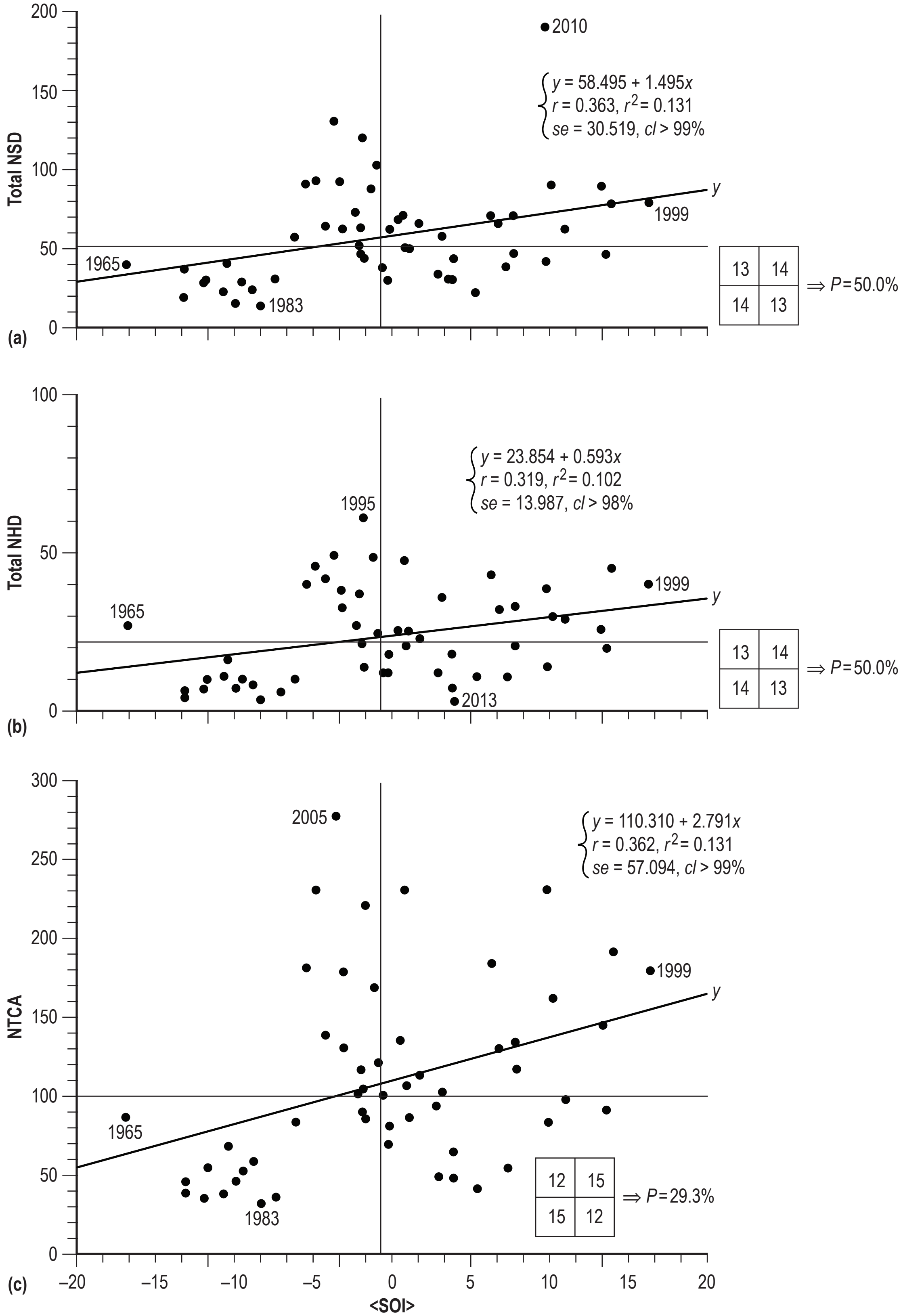

Figure 36. Scatterplots of (a) total NSD, (b) total NHD, and (c) NTCA versus <SOI>.

2.8.3 Inferred Correlations Against <MLCO2>

Figure 37 shows the scatterplot of LOS versus <MLCO2>, identifying the years of extreme values. The inferred regression is given approximately as $y = -77.0 + 0.60x$, having $r = 0.34$, $r^2 = 0.11$, $se = 40.0$, and $cl > 98\%$. Fisher's exact test for 2×2 contingency tables suggests that the probability of obtaining the observed result, or one more suggestive of a departure from independence, is $P = 13.8\%$. Because the atmospheric concentration of CO_2 increases each year, it makes no sense to apply the mean of <MLCO2> for the more recent interval (377.86 ppm). Instead, it is better to use the average rate of increase during the more recent interval for determining the likely level of <MLCO2> for the year 2014. Hence, for the year 2014, one expects <MLCO2> to measure about $396.48 + 1.98 \pm 0.48$ ppm, or about 398.46 ± 0.48 ppm. Using the value <MLCO2> = 398.46 ppm for the year 2014, one infers LOS = 161.3 ± 40.0 days, or LOS ≥ 121 days (rounded to the nearest whole day).

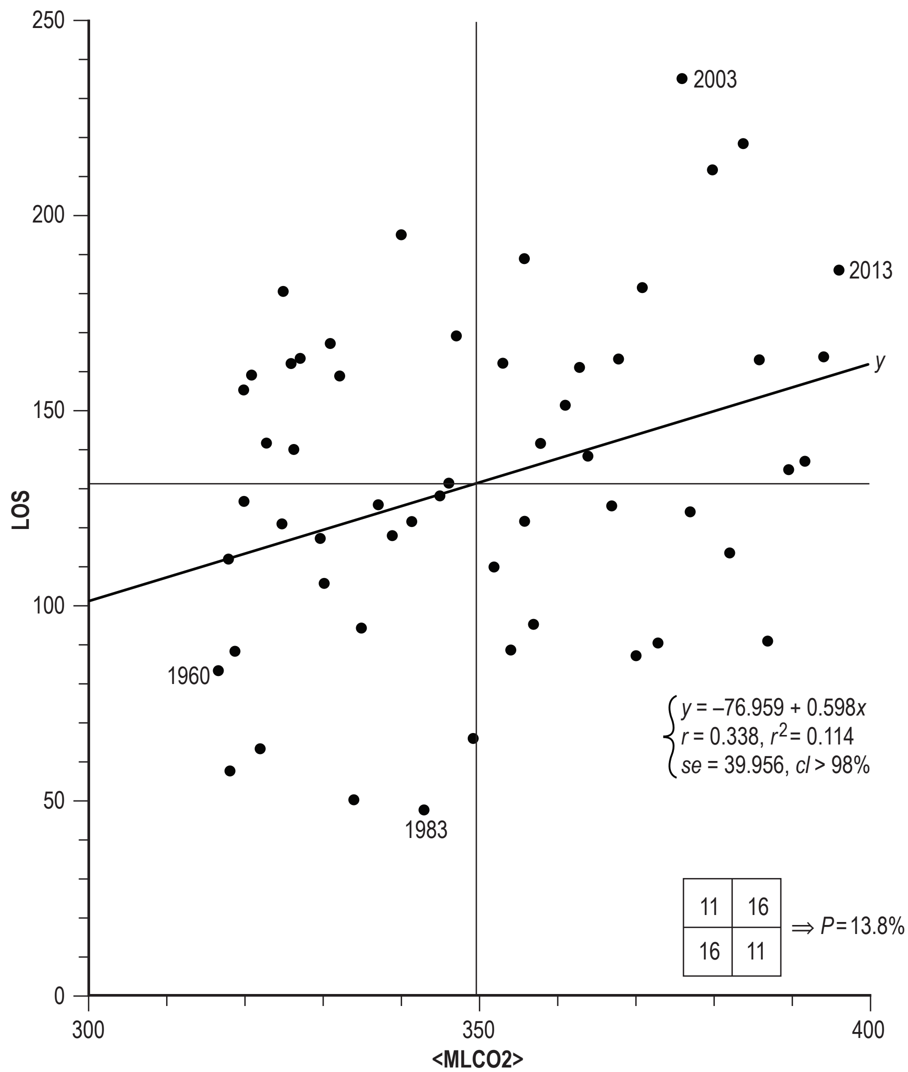

Figure 37. Scatterplot of LOS versus <MLCO2>.

Figure 38 depicts the scatterplot of NTC versus <MLCO2>, identifying the years of extreme values. The inferred regression is given approximately as $y = -25.4 + 0.11x$, having $r = 0.56$, $r^2 = 0.31$, $se = 3.8$, and $cl > 99.9\%$. Fisher's exact test for 2×2 contingency tables suggests that the probability of obtaining the observed result, or one more suggestive of a departure from independence, is $P = 5.0\%$. Using the value of <MLCO2> = 398.46 ppm for the year 2014, one infers NTC = 16.4 ± 3.8, or NTC ≥ 13 (rounded to the nearest whole number).

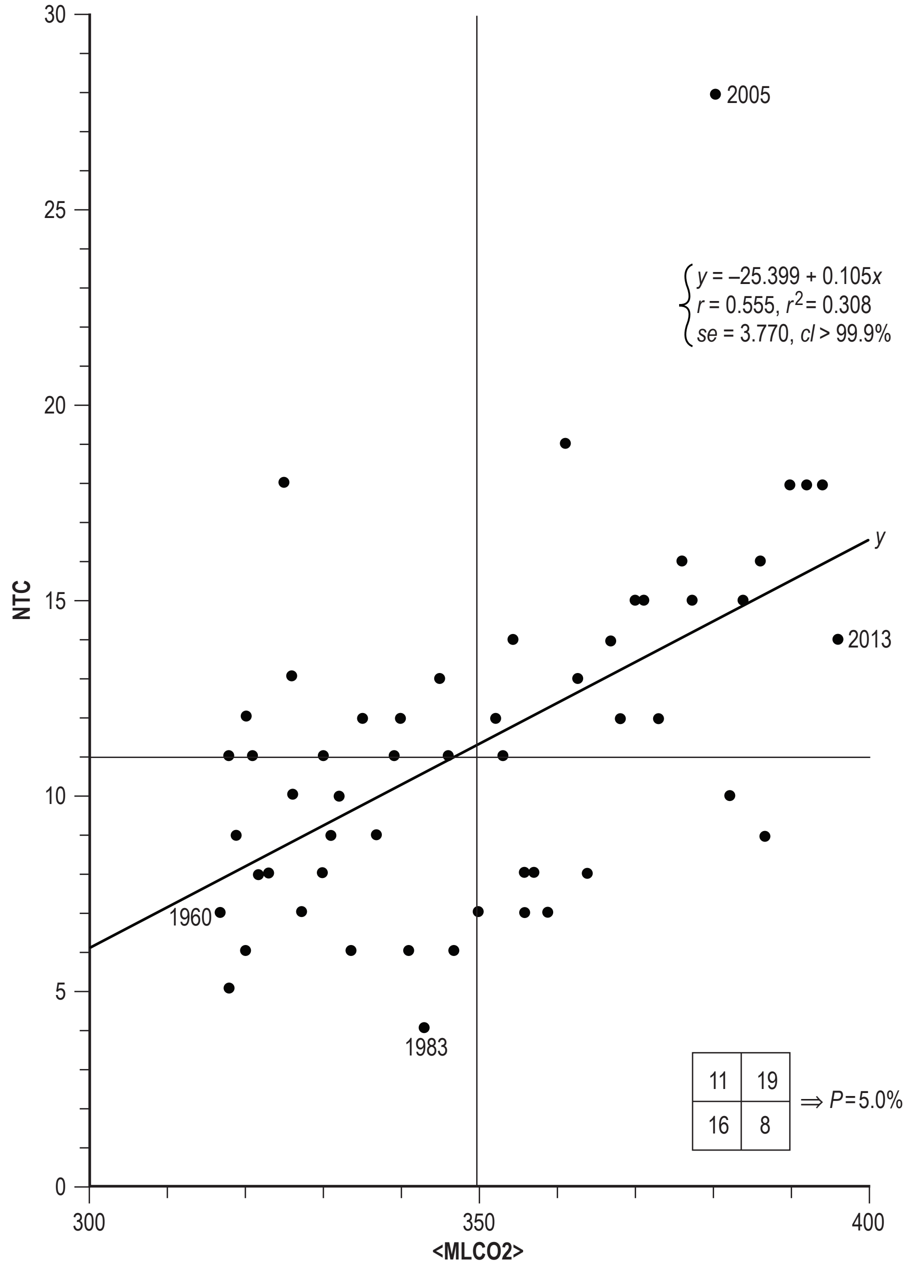

Figure 38. Scatterplot of NTC versus <MLCO2>.

Figure 39 displays the scatterplot of <LAT> versus <MLCO2>, identifying the years of extreme values. The inferred regression is given approximately as $y = 38.4 - 0.05x$, having $r = -0.33$, $r^2 = 0.11$, $se = 2.7$, and $cl > 99\%$. Fisher's exact test for 2×2 contingency tables suggests that the probability of obtaining the observed result, or one more suggestive of a departure from independence, is $P = 0.1\%$. Using the value of <MLCO2> = 398.46 ppm for the year 2014, one infers <LAT> = 20.5 ± 2.7° N., or <LAT> < 23.2° N.

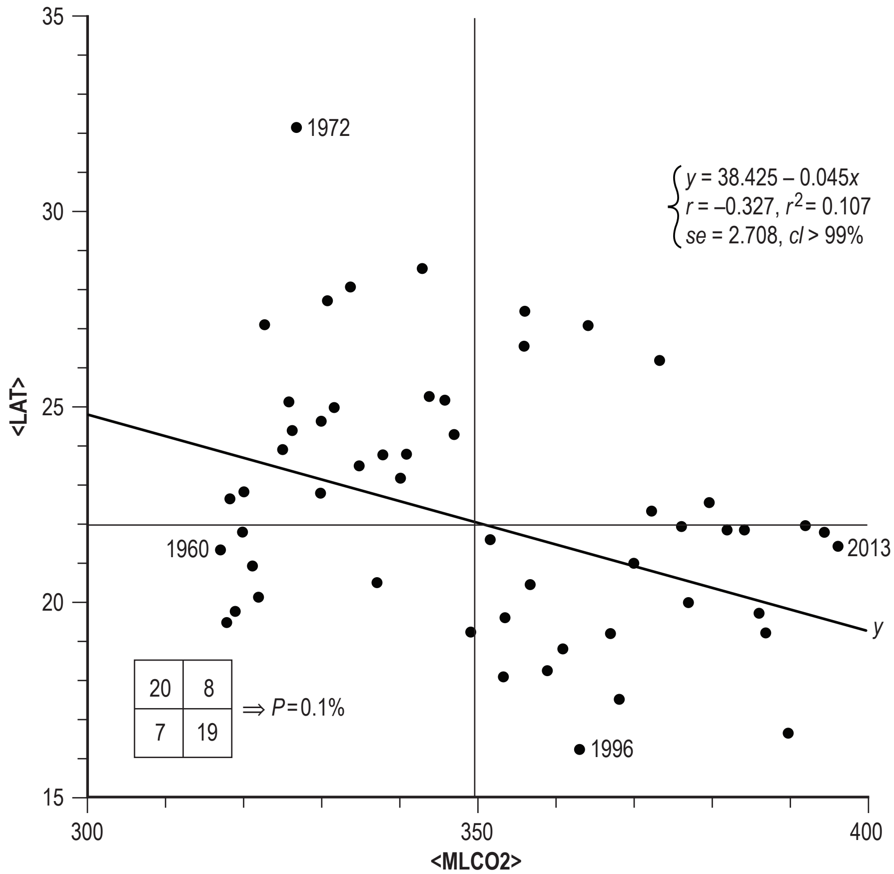

Figure 39. Scatterplot of <LAT> versus <MLCO2>.

Figure 40 shows the scatterplot of total NSD versus <MLCO2>, identifying the years of extreme values. The inferred regression is given approximately as $y = -154.6 + 0.61x$, having $r = 0.45$, $r^2 = 0.20$, $se = 29.2$, and $cl > 99.9\%$. Fisher's exact test for 2×2 contingency tables suggests that the probability of obtaining the observed result, or one more suggestive of a departure from independence, is $P = 5.1\%$. Using the value of <MLCO2> = 398.46 ppm for the year 2014, one infers total NSD = 87.3 ± 29.2 days, or total NSD ≥ 58 days (rounded to the nearest whole day).

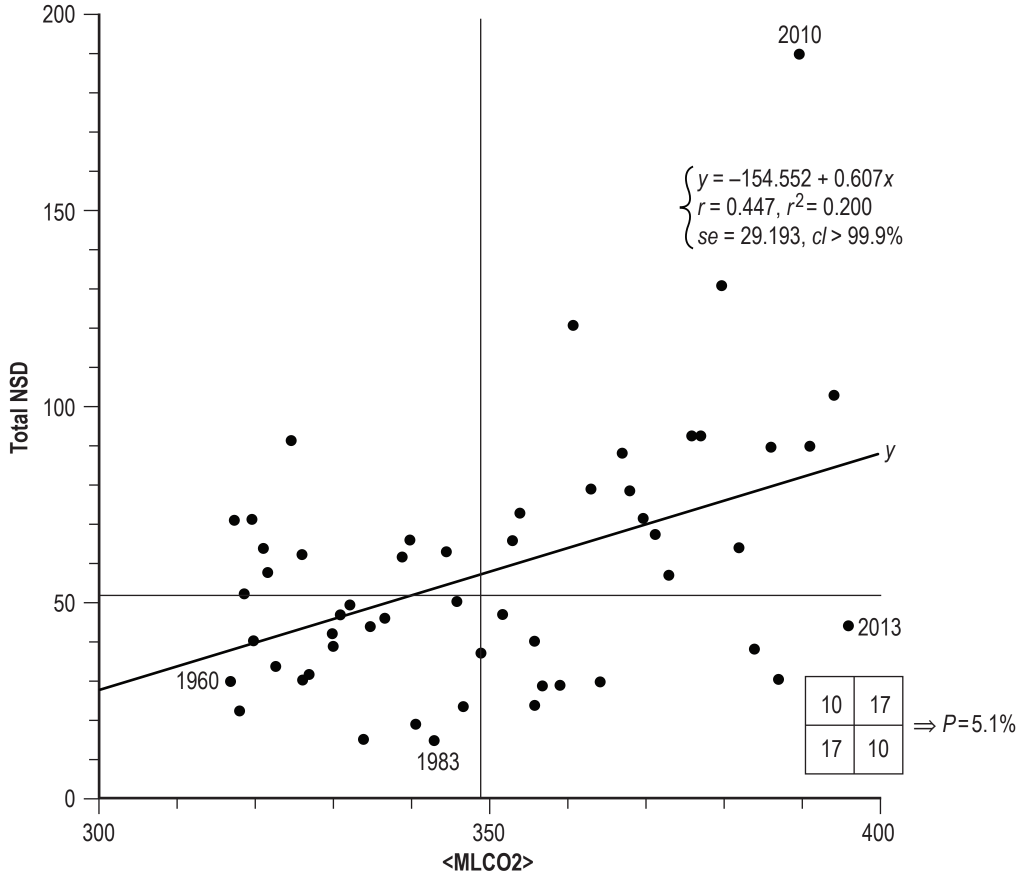

Figure 40. Scatterplot of total NSD versus <MLCO2>.

2.8.4 Inferred Correlations Against <GLOTI>

Figure 41 depicts the scatterplots of (a) total NSD and (b) NTCA versus <GLOTI>, identifying the years of extreme values. Concerning total NSD versus <GLOTI>, the inferred regression is given approximately as $y = 42.6 + 60.8x$, having $r = 0.46$, $r^2 = 0.22$, $se = 29.0$, and $cl > 99.9\%$. Fisher's exact test for 2×2 contingency tables suggests that the probability of obtaining the observed result, or one more suggestive of a departure from independence, is $P = 1.4\%$. Using the value of <GLOTI> = 0.54 °C for the year 2014 (i.e., the mean value for the more recent interval 1995–2013), one infers total NSD = 75.5 ± 29.0 days, or total NSD ≥ 46 days (rounded to the nearest whole day).

Concerning NTCA versus <GLOTI>, the inferred regression is given approximately as $y = 89.5 + 79.1x$, having $r = 0.32$, $r^2 = 0.10$, $se = 58.0$, and $cl > 98\%$. Fisher's exact test for 2×2 contingency tables suggests that the probability of obtaining the observed result, or one more suggestive of a departure from independence, is $P = 1.4\%$. Using the value of <GLOTI> = 0.54 °C for the year 2014, one infers NTCA = 132.2 ± 58.0%, or NTCA ≥ 74.2%.

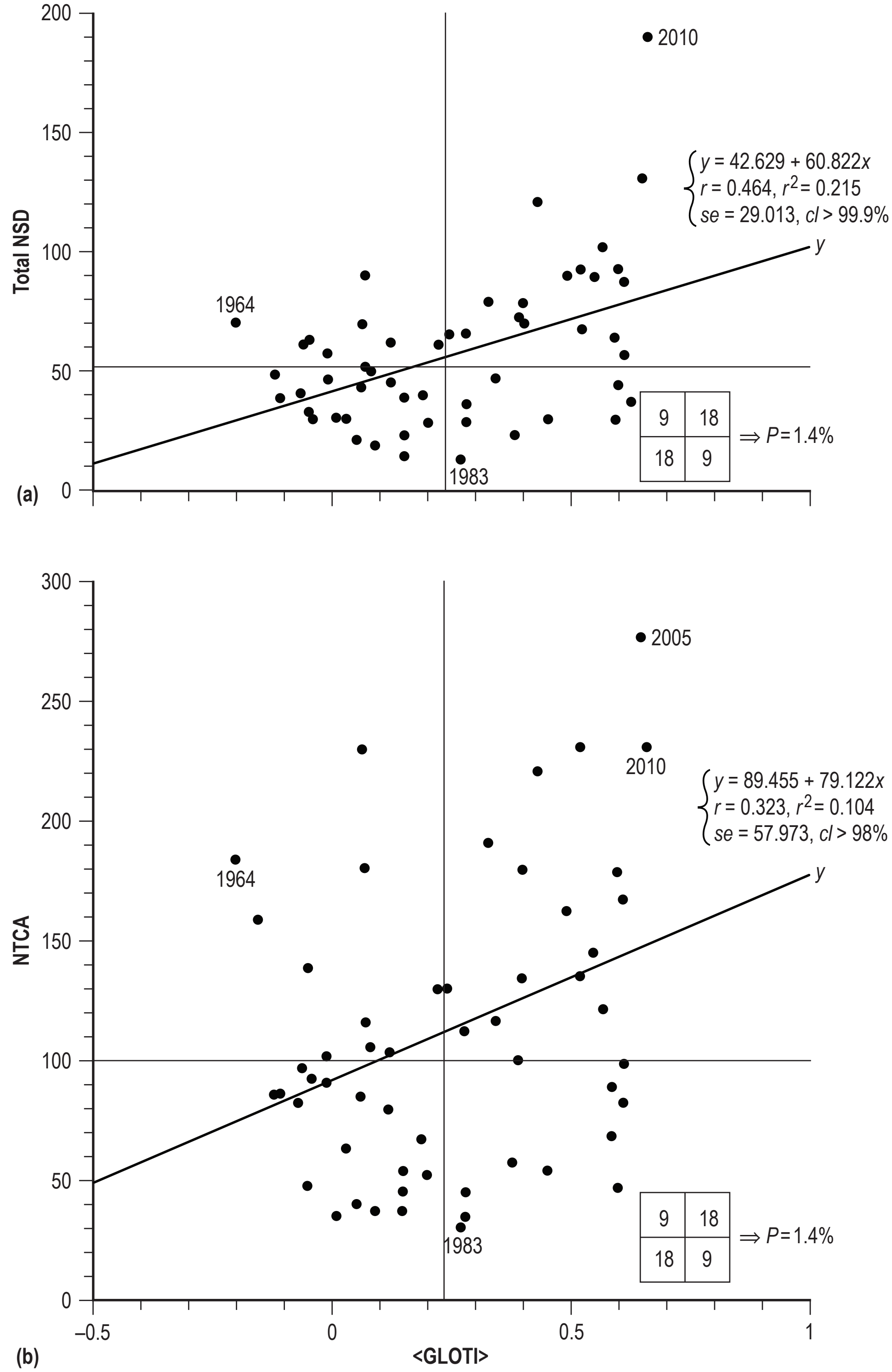

Figure 41. Scatterplots of (a) total NSD and (b) NTCA versus <GLOTI>.

2.8.5 Inferred Correlations Against <ONI>

Figure 42 displays the scatterplots of (a) LSD and (b) NTC versus <ONI>, identifying the years of extreme values. Concerning LSD versus <ONI>, the inferred regression is given approximately as $y = 311.2 - 14.8x$, having $r = -0.37$, $r^2 = 0.13$, $se = 22.3$, and $cl > 99\%$. Fisher's exact test for 2×2 contingency tables suggests that the probability of obtaining the observed result, or one more suggestive of a departure from independence, is $P = 5.1\%$. Using the value of <ONI> = –0.12 °C for the year 2014 (i.e., the mean value for the more recent interval 1995–2013), one infers LSD = 312.0 ± 22.3 (day of year (DOY)), or LSD ≥ 291 (DOY = on or after about October 18, 2014).

Concerning NTC versus <ONI>, the inferred regression is given approximately as $y = 11.4 - 2.6x$, having $r = -0.33$, $r^2 = 0.11$, $se = 4.3$, and $cl > 98\%$. Fisher's exact test for 2×2 contingency tables suggests that the probability of obtaining the observed result, or one more suggestive of a departure from independence, is $P = 0.1\%$. Using the value of <ONI> = –0.12 °C for the year 2014, one infers NTC = 11.7 ± 4.3, or NTC ≥ 7 (rounded to the nearest whole number). (For the overall interval 1960–2013, there were 14 years classified as ENY. The mean NTC during these years equals 8.7, having $sd = 3.8$ and extremes of 4 to 18.)

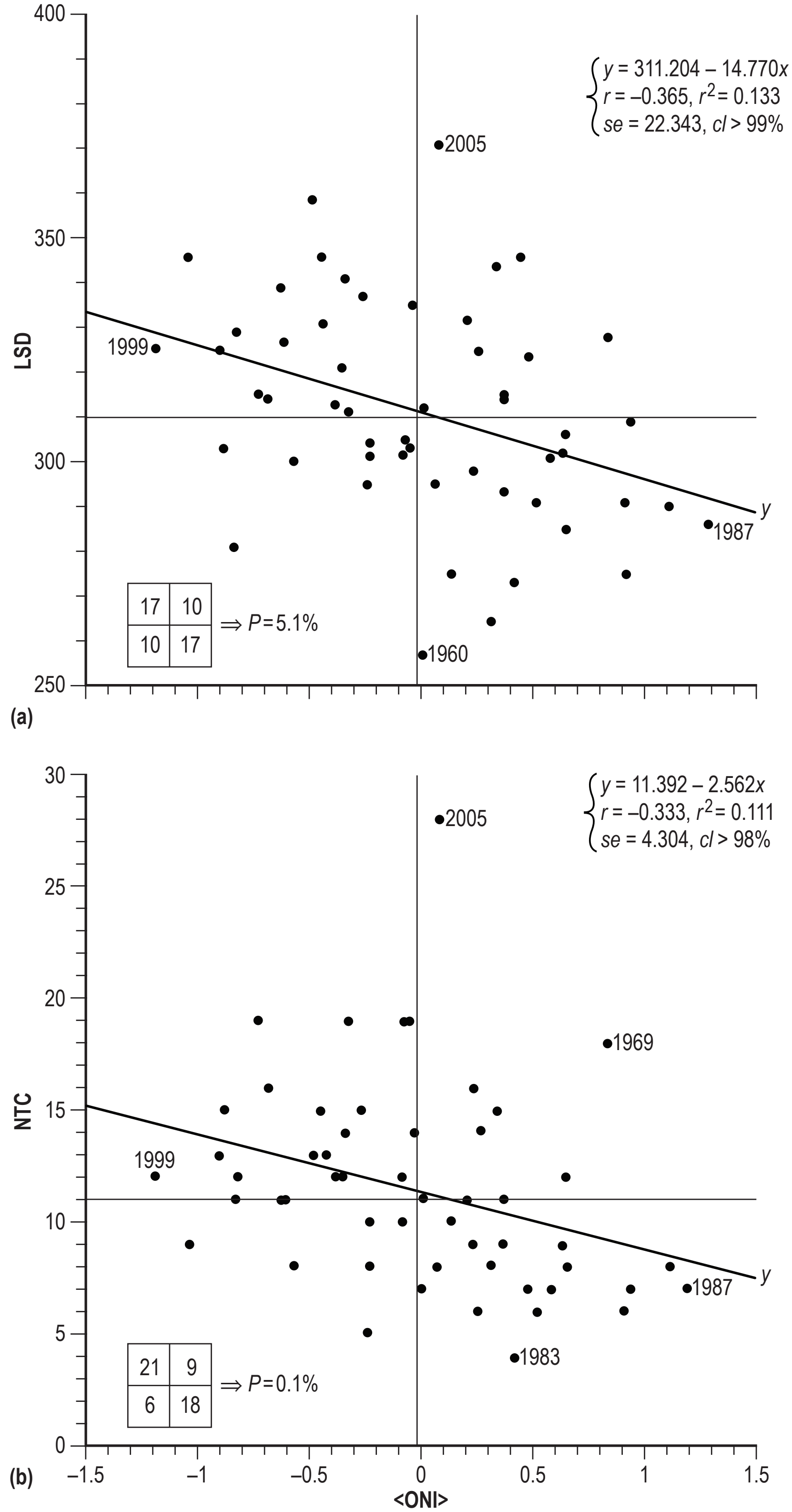

Figure 42. Scatterplots of (a) LSD and (b) NTC versus <ONI>.

2.8.6 Inferred Correlations Against <NAO> CRU

Figure 43 shows the scatterplots of (a) NH, (b) <NSD>, and (c) total NSD versus <NAO> CRU, identifying the years of extreme values in each subpanel. Concerning NH versus <NAO> CRU, the inferred regression is given approximately as $y = 6.1 - 1.9x$, having $r = -0.38$, $r^2 = 0.15$, $se = 2.6$, and $cl > 99.5\%$. Fisher's exact test for 2×2 contingency tables suggests that the probability of obtaining the observed result, or one more suggestive of a departure from independence, is $P = 29.3\%$. Using the value of <NAO> CRU = –0.30 for the year 2014, one infers NH = 6.7 ± 2.6, or NH < 9.

Concerning <NSD> versus <NAO> CRU, the inferred regression is given approximately as $y = 4.9 - 0.8x$, having $r = -0.32$, $r^2 = 0.10$, $se = 1.3$, and $cl > 98\%$. Fisher's exact test for 2×2 contingency tables suggests that the probability of obtaining the observed result, or one more suggestive of a departure from independence, is $P = 50.0\%$. Using the value of <NAO> CRU = –0.30 for the year 2014, one infers <NSD> = 5.1 ± 1.3, or <NSD> < 6 days (rounded to the nearest whole day).

Concerning total NSD versus <NAO> CRU, the inferred regression is given approximately as $y = 57.2 - 25.5x$, having $r = -0.45$, $r^2 = 0.20$, $se = 29.3$, and $cl > 99.9\%$. Fisher's exact test for 2×2 contingency tables suggests that the probability of obtaining the observed result, or one more suggestive of a departure from independence, is $P = 29.3\%$. Using the value of <NAO> CRU = –0.30 for the year 2014, one infers total NSD = 64.9 ± 29.3, or total NSD < 94 days (rounded to the nearest whole day).

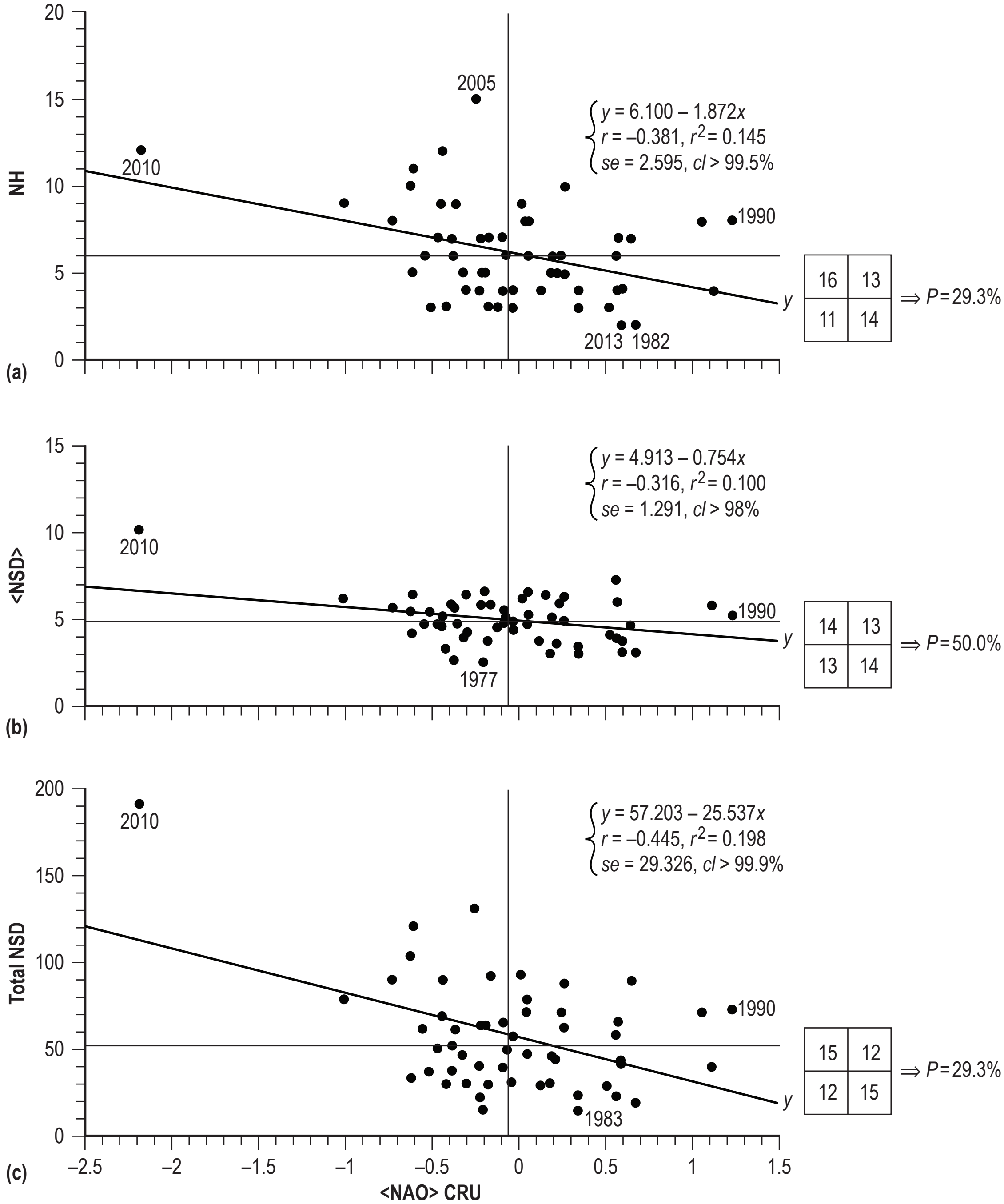

Figure 43. Scatterplots of (a) NH, (b) <NSD>, and (c) total NSD versus <NAO> CRU.

2.8.7 Inferred Correlations Against <NAO> CPC

Figure 44 depicts the scatterplots of (a) NH and (b) total NSD versus <NAO> CPC. Concerning NH versus <NAO> CPC, the inferred regression is given approximately as $y = 6.0 - 2.4x$, having $r = -0.34$, $r^2 = 0.12$, $se = 2.6$, and $cl > 98\%$. Fisher's exact test for 2×2 contingency tables suggests that the probability of obtaining the observed result, or one more suggestive of a departure from independence, is $P = 29.3\%$. Using the value of <NAO> CPC = –0.18 for the year 2014, one infers NH = 6.4 ± 2.6, or NH < 9.

Concerning total NSD versus <NAO> CPC, the inferred regression is given approximately as $y = 56.1 - 27.7x$, having $r = -0.34$, $r^2 = 0.12$, $se = 30.8$, and $cl > 98\%$. Fisher's exact test for 2×2 contingency tables suggests that the probability of obtaining the observed result, or one more suggestive of a departure from independence, is $P = 29.3\%$. Using the value of <NAO> CPC = –0.18 for the year 2014, one infers total NSD = 61.1 ± 30.8, or total NSD < 92 days (rounded to the nearest whole day).

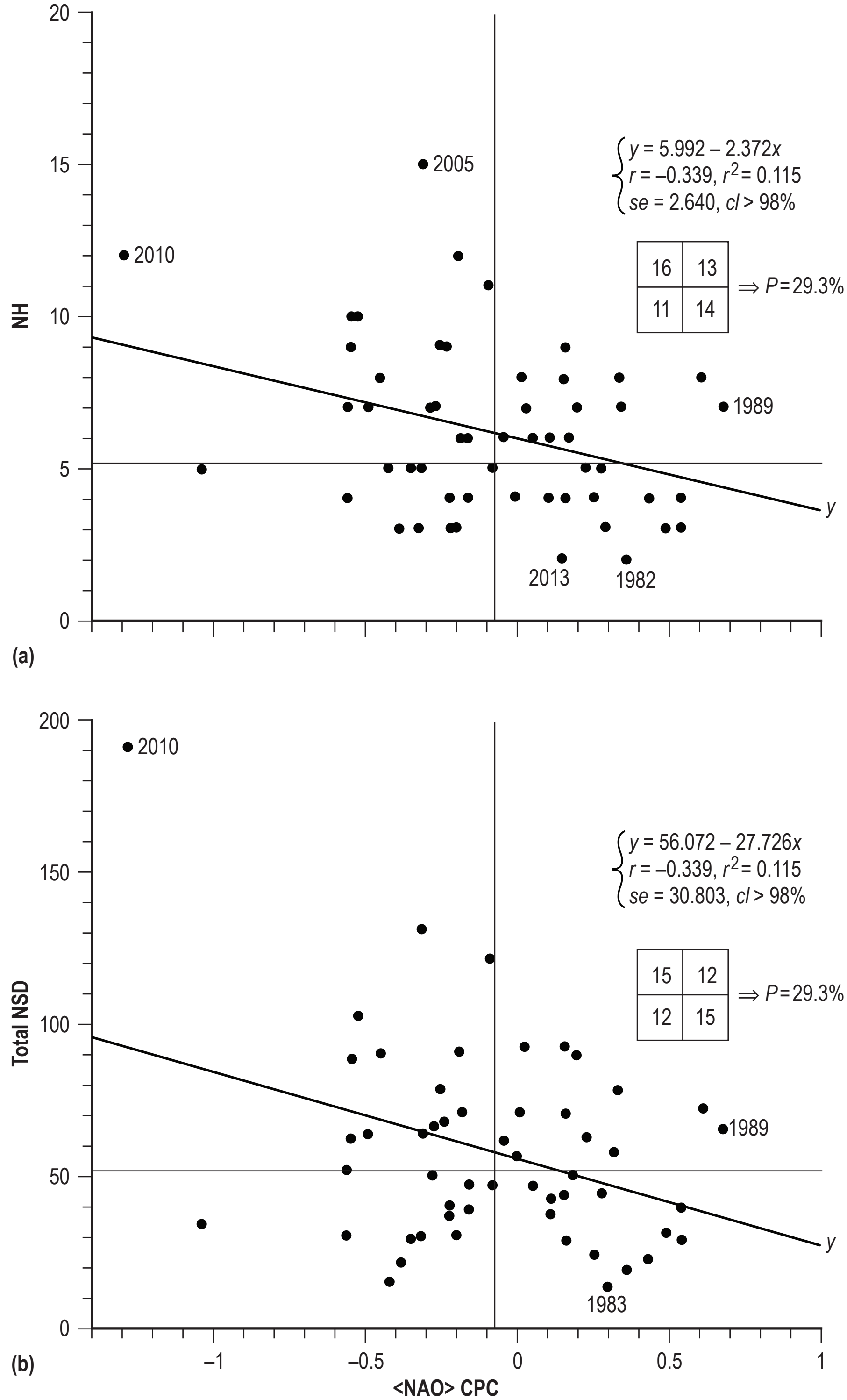

Figure 44. Scatterplots of (a) NH and (b) total NSD versus <NAO> CPC.

2.8.8 Inferred Correlation Against <ASAT>

Figure 45 displays the scatterplot of NTC versus <ASAT>. The inferred correlation is given approximately as $y = -22.6 + 3.6x$, having $r = 0.43$, $r^2 = 0.18$, $se = 4.1$, and $cl > 99.8\%$. Fisher's exact test for 2×2 contingency tables suggests that the probability of obtaining the observed result, or one more suggestive of a departure from independence, is $P = 0.6\%$. Using the value of <ASAT> = 9.97 °C for the year 2014, one infers NTC = 13.1 ± 4.1, or NTC ≥ 9.

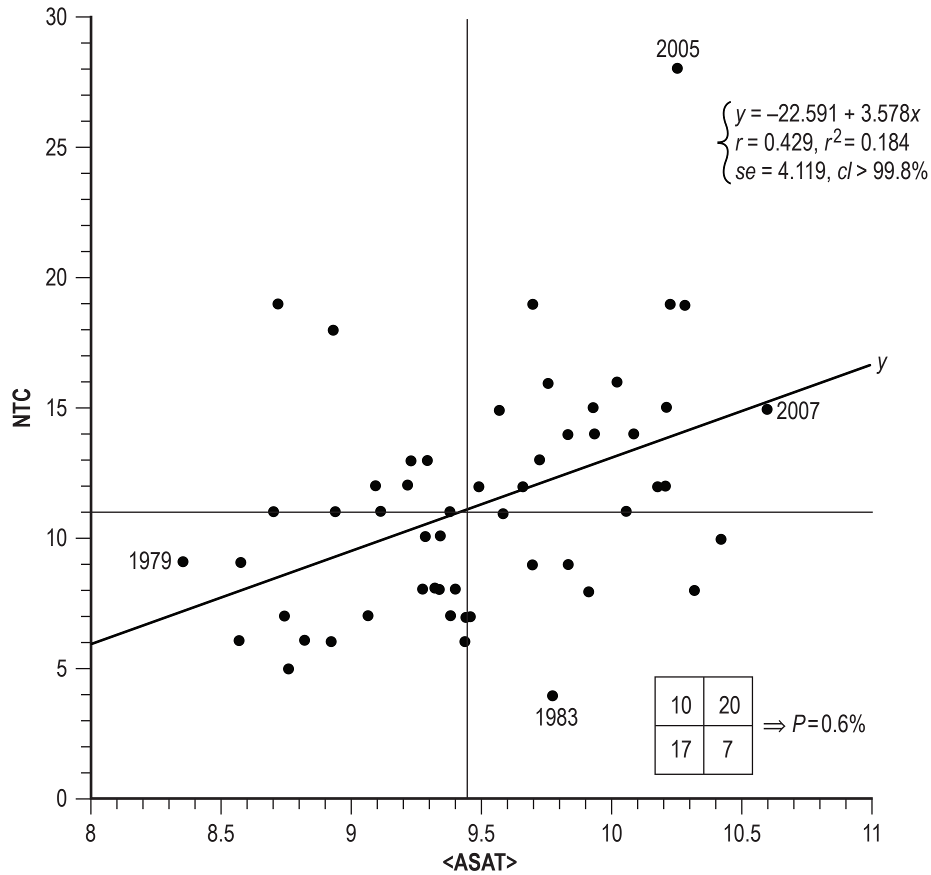

Figure 45. Scatterplot of NTC versus <ASAT>.

2.8.9 Inferred Correlations for NTC Using Single-Variate, Bivariate, and Trivariate Fits Based on Selected Climate-Related Factors

Table 4 provides a comparison of the observed yearly NTC with those based on selected inferred single-variate fits (<AMO>, <SOI>, and <MLCO2>), bivariate fits (<AMO> and <SOI>, and <AMO> and <MLCO2>), and on a specific trivariate fit (<AMO>, <SOI>, and <MLCO2>). From the table, one finds that estimates made using <AMO> or <MLCO2>, both having $r = 0.55$ and $se = 3.8$, appear to be slightly more reliable than the estimates using <SOI> ($r = 0.35$ and $se = 4.3$). Some improvement is found when using the bivariate fits ($R_{y12} = 0.62$ and $S_{y12} = 3.6$), with the trivariate fit providing the best improvement ($R_{y12} = 0.65$ and $S_{y12} = 3.5$). For the single-variate fits, the fit having the best ±1 difference between estimated and observed NTC, surprisingly, appears to be the one using <MLCO2> (having an estimate of ±1 for 20 of the 54 years, or about 37% success). Accepting a broader error range (±3), one finds that <AMO> is the better estimator for NTC (39 of 54 years, or 72%). For the bivariate fits, the one using <AMO> and <SOI> appears to be the slightly better estimator of NTC, having ±1 for 22 of 54 years (41%) and ±3 for 41 of 54 years (76%). The trivariate fit has a ±1 error range for 23 of 54 years (43%) and a ±3 error range for 43 of 54 years (80%). Based on <AMO>, the estimates for NTC were poor (≥ ±5) for 11 of the 54 years, including the years 1960, 1962, 1969, 1971, 1974, 1983, 1987, 1995, 2005, 2006, and 2011. Based on the bivariate fit using <AMO> and <SOI>, the estimates for NTC were poor for 9 of the 54 years, including the years 1960, 1962, 1969, 1973,1983, 1995, 2005, 2006, and 2012. Based on the trivariate fit using <AMO>, <SOI>, and <MLCO2>, the estimates for NTC were poor for 9 of the 54 years, including the years 1960, 1962, 1969, 1973, 1983, 1995, 2005, 2006, and 2009. (Only NTC was examined using bivariate and trivariate fits as a test case simply to determine the amount of improvement one might expect by incorporating more than one variable for estimating a tropical cyclone parameter.)

Table 4. Comparison of observed and predicted NTC values based on selected fits.

Year	Observed	*P*(<AMO>)	*P*(<SOI>)	*P*(<MLCO2>)	*P*(<AMO>,<SOI>)	*P*(<AMO>, <MLCO2>)	*P*(<AMO>,<SOI>, <MLCO2>)
1960	7	15	12	8	15	11	11
1961	11	13	12	8	13	10	10
1962	5	13	13	8	14	10	11
1963	9	12	11	8	11	10	9
1964	12	11	13	8	12	9	10
1965	6	10	8	8	7	8	7
1966	11	12	11	8	11	10	9
1967	8	10	12	8	11	9	9
1968	8	10	12	9	10	8	9
1969	18	12	10	9	11	10	9
1970	10	10	12	9	14	9	11
1971	13	8	14	9	10	7	9
1972	7	7	10	9	6	7	6
1973	8	9	13	9	16	8	13
1974	11	6	13	9	8	7	8
1975	9	8	14	9	8	8	8
1976	10	7	12	9	7	7	7
1977	6	9	9	10	8	9	8
1978	12	9	11	10	9	9	9
1979	9	10	11	10	10	10	10
1980	11	11	11	10	11	11	10
1981	12	11	12	10	11	10	10
1982	6	9	9	10	7	9	8
1983	4	11	10	11	10	11	10
1984	13	9	11	11	9	10	9
1985	11	8	12	11	9	10	10
1986	6	8	9	11	7	9	8
1987	7	13	9	11	10	12	10
1988	12	12	13	12	13	12	12
1989	11	11	13	12	12	11	11
1990	14	11	11	12	11	12	11
1991	8	10	10	12	9	11	10
1992	7	9	9	12	7	10	9
1993	8	9	10	12	8	10	10
1994	7	9	9	12	8	11	10
1995	19	14	11	12	13	13	13
1996	13	11	14	13	13	12	13
1997	8	12	9	13	10	13	11
1998	14	17	11	13	16	16	15
1999	12	13	15	13	16	14	15
2000	15	12	13	13	13	13	14

Table 4. Comparison of observed and predicted NTC values based on selected fits (Continued).

Year	Observed	*P*(<AMO>)	*P*(<SOI>)	*P*(<MLCO2>)	*P*(<AMO>,<SOI>)	*P*(<AMO>, <MLCO2>)	*P*(<AMO>,<SOI>, <MLCO2>)
2001	15	13	12	14	13	14	14
2002	12	13	10	14	12	14	13
2003	16	15	11	14	14	15	15
2004	15	14	10	14	14	15	15
2005	28	16	11	14	15	16	16
2006	10	15	11	15	15	16	16
2007	15	14	11	15	13	15	15
2008	16	14	13	15	15	15	16
2009	9	12	11	15	12	14	14
2010	19	16	13	16	18	17	18
2011	19	13	14	16	15	15	16
2012	19	15	11	16	14	16	16
2013	14	14	12	16	15	16	17
±1		17	12	20	22	19	23
±2		28	28	31	33	30	32
±3		39	38	36	41	40	43
Range	4–28	6–17	8–15	8–16	6–18	7–17	6–17

P(<AMO>) = 11.728 + 12.929 <AMO>, *r* = 0.553, *se* = 3.8.
P(<SOI>) = 11.440 + 0.200 <SOI>, *r* = 0.348, *se* = 4.3.
P(<MLCO2>) = –25.399 + 0.105 <MLCO2>, *r* = 0.555, *se* = 3.8.
P(<AMO>, <SOI>) = 11.750 + 12.225 <AMO> + 0.168 <SOI>, R_{y12} = 0.625, S_{y12} = 3.6.
P(<AMO>, <MLCO2>) = –11.535 + 8.098 <AMO> + 0.066 <MLCO2>, R_{y12} = 0.620, S_{y12} = 3.6.
P(<AMO>, <SOI>, <MLCO2>) = –20.025 + 0.600 *P*(<AMO>, <SOI>) + 0.070 <MLCO2>, R_{y12} = 0.653, S_{y12} = 3.5.

3. SUMMARY

This is the second part of a two-part study of the 615 tropical cyclones that occurred in the North Atlantic basin during the weather satellite era, 1960–2013. Part 1 investigated the statistics of some 25 parameters associated with the tropical cyclones (e.g., NTC, NSD, PWS, ACE, etc.). Part 2 has examined the statistics of 9 specific climate-related parameters, both in relation to each other and in relation to the aforementioned 25 parameters discussed in part 1.

Regarding the intercorrelational behavior of the climate-related factors, perhaps surprisingly, one finds that <ONI> and <SOI>, factors associated with the determination of the phasing for the El Niño Southern Oscillation phenomenon, are found to correlate strongly ($r = -0.896$ and $cl > 99.9\%$) only against each other and not against any of the other climate-related factors. On the other hand, <NAO>, <ASAT>, and <GLOTI> are all found to correlate strongly against <AMO>, while <QBO> is found not to correlate strongly against any of the other climate-related factors ($|r| < 0.21$ and $cl < 90\%$). Also, <AMO>, <ASAT>, and <GLOTI> are found to correlate strongly against <MLCO2>, especially <GLOTI> ($r = 0.932$ and $cl > 99.9\%$).

Regarding the correlational behavior of the 25 tropical cyclone parameters against the 9 climate-related factors, one finds that more of the tropical cyclone parameters correlate strongly against <AMO> than any other factor, with 15 of the 25 tropical cyclone parameters correlating very strongly against <AMO> having $cl > 98\%$ and an additional 5 tropical cyclone parameters correlating strongly against <AMO> having $cl > 95\%$. Only FSD, LSD, LOS, NUSLFH, and <PWS> fail to correlate strongly against <AMO>. The second best climate-related factor is <SOI>, with 8 tropical cyclone parameters correlating very strongly against <SOI> having $cl > 98\%$ and an additional 5 parameters correlating strongly against <SOI> having $cl > 95\%$.

Interestingly, none of the climate-related factors appear to correlate with the FSD. Hence, there appears to be no way for accurately predicting ahead of time using any of the 9 climate-related factors as to when to expect the FSD of a hurricane season. On the other hand, the LSD does appear to be related to <ONI>, <SOI>, <GLOTI>, and <MLCO2>, but in contrasting ways. For example, a positive (negative) <ONI> associated with a negative (positive) <SOI> suggests that the LSD will occur sooner (later) rather than later (sooner) in the hurricane season, while increased global warming (positive <GLOTI>) and increased atmospheric concentration of CO_2 (<MLCO2>) suggests that the LSD will occur later rather than earlier during the hurricane season, with the correlation against <ONI> being the slightly stronger correlation ($cl > 99\%$). Regarding the LOS, it has been established that once the FSD is known, an estimate can be made for the LOS. Of the 9 climate-related factors, only <MLCO2> appears to correlate strongly with the LOS ($cl > 98\%$). Hence, given the increasing atmospheric concentration of CO_2, one expects the LOS to slowly increase in length over time.

For estimating the NTC, the climate-related factors <AMO>, <ASAT>, <GLOTI>, and <MLCO2> all provide some degree of being able to reliably estimate it. Since all of these climate-related factors are now of positive value, this would seem to indicate a strong preference for the NTC to be of average to higher-than-average number for the current hurricane season. (The long-term average is about 11 tropical cyclones per season during the overall interval 1960–2013, although since 1995, the average has been higher, about 15 tropical cyclones per season with the fewest number over the past 19 years being 8 in 1997.)

Regarding the NH and NMH, they are found to correlate more strongly against <AMO> than the other climate-related factors. Hence, as with NTC, because the <AMO> is presently in its warm (positive value) phase and is expected to remain so for another decade or so, one expects the NH and NMH probably to be of average to higher-than-average number during the current hurricane season (the long-term average of NH and NMH is 6 and 2, respectively, while being 8 and 3, respectively, over the past 19 years.)

Regarding the mean seasonal NUSLFH (<NUSLFH>), none of the climate-related factors provide any indication as to how many will occur. The <NUSLFH> appears random, ranging in number from 0 to 6 per yearly season.

Regarding the total NSD, total NHD, and total NMHD, again, because the <AMO> is in its warm (positive values) phase, one expects values for these tropical cyclone parameters during the current hurricane season to probably be average to higher-than-average number (the long-term averages for these parameters are about 58, 24, and 6 days, respectively, and about 82, 30, and 8 days, respectively, for the past 19 years). For the NTCA (which is based on NTC, NH, NMH, total NSD, total NHD, and total NMHD), one expects activity to be average to higher than average. (The long-term average of NTCA for the overall interval 1960–2013 is about 110%, while the average over the past 19 years has been about 148%.)

Recall that table 3 provides the inferred linear regressions for the 25 tropical cyclone parameters against the 9 specific climate-related factors. Below is table 5, which gives a summary of the estimates for the tropical cyclone parameters on the basis of averages for the interval 1995–2013 using <AMO> and <SOI> as the climate forcing agents and on the basis of the projected value of <MLCO2> for the year 2014. Likewise, table 6 is included, which gives a summary of the estimates for the tropical cyclone parameters on the basis of whether the year 2014 will be classified as either an ENY or a NENY.

Table 5. Summary of estimates for the North Atlantic basin tropical cyclone parameters (rounded to nearest whole number) for the 2014 hurricane season based on the means for the interval 1995–2013 for <AMO> and the projected value of <MLCO2> for 2014.

Parameter	1960–2013 Average	1995–2013 Average	*P*(<AMO>)	*P*(<SOI>)	*P*(<MLCO2>)
FSD	180(33)	170(31)	179(34)	180(34)	165(33)
LSD	311(24)	320(24)	315(24)	313(24)	325(24)
LOS	133(42)	152(43)	137(42)	134(42)	161(40)
NTC	11(5)	15(5)	14(4)	12(4)	16(4)
NH	6(3)	8(3)	8(2)	6(3)	7(3)
NMH	2(2)	3(2)	3(2)	3(2)	3(2)
NUSLFH	1(1)	2(2)	2(1)	1(1)	1(2)
<LAT>	22.5(3.3)	20.9(2.8)	21(3)	22(3)	20(3)
<LONG>	63.5(5.8)	62.0(4.6)	61(5)	63(6)	60(6)
PWS	124(22)	127(20)	130(21)	125(22)	122(22)
<PWS>	72.9(8.6)	71.9(9.6)	74(8)	74(8)	68(8)
LP	937(22)	930(21)	929(20)	936(22)	931(23)
<LP>	980.8(7.7)	980.1(7.7)	979(7)	980(7)	983(8)
<ACE>	8.6(3.7)	8.8(3.5)	10(4)	9(4)	7(4)
Total ACE	100.5(59.2)	134.6(64.8)	132(50)	106(57)	126(58)
HISACE	30.9(16.1)	35.9(15.7)	37(15)	32(16)	31(16)
<PDI>	6.9(3.9)	7.2(3.5)	8(4)	7(4)	5(4)
Total PDI	81.8(55.7)	110.8(61.9)	111(48)	87(54)	101(55)
HISPDI	30.8(20.2)	36.6(21.0)	39(19)	32(20)	31(20)
<NSD>	4.94(1.35)	5.31(1.66)	5(1)	5(1)	5(1)
LISNSD	11.76(3.74)	13.09(3.45)	13(4)	12(4)	13(4)
Total NSD	58.12(32.44)	82.05(38.60)	77(26)	62(31)	87(29)
Total NHD	23.70(14.62)	29.87(16.13)	30(13)	25(14)	25(15)
Total NMHD	5.57(5.84)	8.08(6.37)	8(5)	6(6)	7(6)
NTCA	109.6(60.7)	148.3(65.6)	143(50)	116(57)	142(59)

Table 6. Summary of estimates for the North Atlantic basin tropical cyclone parameters based on whether the year 2014 is classified as ENY or NENY (rounded to nearest whole number).

Parameter	ENY(14)	NENY(40)	*t*
FSD	190(38)	176(31)	1.4
LSD	299(18)	315(24)	–2.3
LOS	110(41)	140(40)	–2.4
NTC	9(4)	12(4)	–2.4
NH	5(3)	7(3)	–2.1
NMH	2(2)	3(2)	–1.6
NUSLFH	1(1)	2(2)	–1.8
<LAT>	25(4)	22(3)	2.0
<LONG>	65(7)	63(5)	1.2
PWS	125(21)	124(22)	0.1
<PWS>	71(9)	73(9)	–0.7
LP	940(19)	936(23)	0.6
<LP>	983(7)	980(8)	1.2
<ACE>	8(4)	9(4)	–0.8
Total ACE	72(60)	110(56)	–2.1
HISACE	27(18)	32(15)	–1.0
<PDI>	6(4)	7(4)	–0.8
Total PDI	59(57)	90(54)	–1.8
HISPDI	26(22)	32(20)	–0.9
<NSD>	4(1)	5(1)	–3.2
LISNSD	11(4)	12(3)	–1.0
Total NSD	41(25)	64(33)	–2.4
Total NHD	16(15)	26(14)	–2.3
Total NMHD	4(6)	6(6)	–1.1
NTCA	81(59)	120(59)	–2.1

Concerning table 6, one observes that an ENY, on average, tends to have a later-occurring FSD, a sooner-occurring LSD, and a shorter LOS than a NENY, with the differences in means being statistically important ($cl > 95\%$) for LSD and LOS. Likewise, an ENY, on average, tends to have fewer NTC and NH than a NENY. Other statistically important differences include a higher <LAT>, lower total ACE, fewer <NSD>, fewer total NSD, fewer total NHD, and smaller NTCA than a NENY.

According to the June 5, 2014, diagnostic discussion, the CPC and the International Research Institute for Climate and Society have reported that there is a 70% chance of an El Niño developing during the Northern Hemisphere summer during the year 2014, increasing to an 80% chance during the fall and winter. As to whether or not the year will be classified as ENY or not, it is dependent simply upon how soon ENL conditions manifest themselves and how strong the event becomes. Through the first four months of the year, the ONI has been of negative value, with its values indicative of El Niño-neutral conditions. Should neutral conditions continue through July, then the year 2014 would, by the definition of ENY employed in this TP, necessarily have to be classified as a NENY, even if an El Niño event should actually develop during the latter portion of the year. During the 54 years spanning 1960–2013, there have been 14 years that had ENL conditions persisting at least 6 months within the year, or about one ENY every 4 years. The longest span between ENYs during the weather satellite era has been 5 years. Since the last ENY occurred in 2009, clearly one anticipates the year 2014 to be an ENY.

REFERENCES

1. Wilson, R.M.: "Statistical Aspects of North Atlantic Basin Tropical Cyclones During the Weather Satellite Era, 1960–2013: Part 1," NASA/TP—2014–218196, NASA Marshall Space Flight Center, Huntsville, AL, 82 pp., July 2014.

2. Climate Prediction Center, "Historical El Niño/La Niña episodes (1950–present)," <http://www.cpc.ncep.noaa.gov/products/analysis_monitoring/ensostuff/ensoyears.shtml>, June 5, 2014.

3. Climate Prediction Center, "Niño 3.4 Daten, <www.cpc.ncep.noaa.gov/products/analysis_monitoring/ensostuff/detrend.nino34.ascii.txt>, June 2014.

4. Australia Bureau of Meteorology, "Southern Oscillation Index," <www.bom.gov.au/climate/glossary/soi.shtml>, February 2012.

5. Australia Bureau of Meteorology, "S.O.I. (Southern Oscillation Index) Archives–1876 to present," <www.bom.gov.au/climate/current/soihtm1.shtml>, June 2014.

6. Schlesinger, M.E.; and Ramankutty, N.: "An oscillation in the global climate system of period 65–70 years," *Nature*, Vol. 367, No. 6465, pp. 723–726, doi:10.1038/367723a0, February 1994.

7. Dijkstra, H.A.; te Raa, L.; Schmeits, M.; and Gerrits, J.: "On the physics of the Atlantic Multidecadal Oscillation," *Ocean Dyn.*, Vol. 56, No. 1, pp. 36–50, doi:10.1007/s10236-005-0043-0, May 2006.

8. Grossmann, I.; and Klotzbach, P.J.: "A Review of North Atlantic Modes of Natural Variability and Their Driving Mechanisms," *J. Geophys. Res.*, Vol. 114, No. D24, 14 pp., doi:10.1029/2009JD012728, December 2009.

9. Broecker, W.S.: "The Great Ocean Conveyor," *Oceanography*, Vol. 4, No. 2, p. 79, doi:10.1063/1.41925, 1991.

10. NOAA Earth System Research Laboratory, "AMO data," <www.esrl.noaa.gov/psd/data/correlation/amon.us.long.data>, July 2014.

11. Saundry, P.: "Atlantic meridional overturning circulation," <www.eoearth.org/view/article/150290/>, March 2010.

12. Maruyama, T.: "The Quasi-Biennial Oscillation (QBO) and Equatorial Waves–A Historical Review," *Papers in Meteorology and Geophysics*, Vol. 48, No. 1, pp. 1–17, doi:10.2467/mripapers.48.1, September 1997.

13. Hamilton, K.: "Observations of Tropical Stratospheric Winds before World War II," *Bull. Am. Meteor. Soc.,* Vol. 79, No. 7, p. 1367, doi:10.1175/1520-0477(1998)079<1367:OOTSWB> 2.0.CO;2, July 1998.

14. Baldwin, M.P.; Gray, L.J.; Dunkerton, T.J.; et al.: "The Quasi-Biennial Oscillation," *Rev. Geophys.*, Vol. 39, No. 2, pp. 179–229, doi:10.1029/1999RG000073, May 2001.

15. Mazzarella, A.; and Giuliacci, A.: "On the Dominance of 28-Month Harmonic in the Equatorial-Stratospheric-Wind Quasi Biennial Oscillation," *The Open Atmospheric Science Journal*, Vol. 4, No. 1, pp. 53–56, doi:10.2174/1874282301004010053, 2010.

16. Mazzarella, A.; Giuliacci, A.; and Liritzis, I.: "QBO of the Equatorial-Stratospheric Winds Revisited: New methods to verify the dominance of 28-month cycle," *International Journal of Ocean and Climate Systems*, Vol. 2, No. 1, pp. 19–26, doi:10.1260/1759-3131.2.1.19, March 2011.

17. NOAA Earth System Research Laboratory, "QBO data," <www.esrl.noaa.gov/psd/data/correlation/qbo.data>, June 2014.

18. Hurrell, J.W.; Kushnir, Y.; and Visbeck, M.: "The North Atlantic Oscillation," *Science*, Vol. 291, No. 5504, pp. 603–605, doi:10.1126/science.1058761, January 2001.

19. Visbeck, M.H.; Hurrell, J.W.; Polvani, L.; and Cullen, H.M.: "The North Atlantic Oscillation: Past, Present, and Future," *PNAS*, Vol. 98, No. 23, pp. 12,876–12,877, doi:10.1073/pnas.231391598, November 2001.

20. NOAA Earth System Research Laboratory, "NOA data," <www.esrl.noaa.gov/psd/data/correlation/nao.data>, June 2014.

21. Osborn, T.: "North Atlantic Oscillation index data," <http://www.cru.uea.ac.uk/~timo/datapages/naoi.htm>, June 2014.

22. Butler, C.J.; and Johnston, D.J.: "A provisional long mean air temperature series for Armagh observatory," *J. Atmos. Terr. Phys.*, Vol. 58, No. 14, pp. 1657–1672, doi:10.1016/0021-9169(95)00148-4, November 1996.

23. Wilson, R.M.: "Evidence for solar-cycle forcing and secular variation in the Armagh Observatory temperature record (1844–1992)," *J. Geophys. Res.*, Vol. 103, No. D10, pp. 11,159–11,171, doi:10.1029/98JD00531, May 1998.

24. Butler, C.J.; García Suárez, A.M.; Coughlin, A.D.S.; and Morrell, C.: "Air Temperatures at Armagh Observatory, Northern Ireland, from 1796 to 2002," *Int. J. Climatol.*, Vol. 25, No. 8, pp. 1055–1079, doi:10.1002/joc.1148, June 2005.

25. Wilson, R.M.; and Hathaway, D.H.: “Examination of the Armagh Observatory Annual Mean Temperature Record, 1844–2004,” NASA/TP—2006–214434, NASA Marshall Space Flight Center, Huntsville, AL, 28 pp., July 2006.

26. Wilson, R.M.: “Solar Cycle and Anthropogenic Forcing of Surface-Air Temperature at Armagh Observatory, Northern Ireland,” NASA/TP—2010–216375, NASA Marshall Space Flight Center, Huntsville, AL, 28 pp., March 2010.

27. Wilson, R.M.: “Estimating the Mean Surface Air Temperature at Armagh Observatory, Northern Ireland, and the Global Land-Ocean Temperature Index for Sunspot Cycle 24, the Current Ongoing Sunspot Cycle,” NASA/TP—2013–217484, NASA Marshall Space Flight Center, Huntsville, AL, 60 pp., July 2013.

28. Wilson, R.M.: “On the Trend of the Annual Mean, Maximum, and Minimum Temperature and the Diurnal Temperature Range in the Armagh Observatory, Northern Ireland, Dataset, 1844–2012,” NASA/TP—2013–217494, NASA Marshall Space Flight Center, Huntsville, AL, 62 pp., November 2013.

29. Armagh Observatory Meteorology Data Bank, “Calibrated Data,” <http://climate.arm.ac.uk/calibrated.html>, November 2012.

30. Armagh Observatory Meteorology Data Bank, “Monthly Records,” <http://climate.arm.ac.uk/scan.html>, January 2008.

31. Wilson, R.M.: “The Global Land-Ocean Temperature Index in Relation to Sunspot Number, the Atlantic Multidecadal Oscillation Index, the Mauna Loa Atmospheric Concentration of CO_2, and Anthropogenic Carbon Emissions,” NASA/TP—2013–217485, NASA Marshall Space Flight Center, Huntsville, AL, 32 pp., July 2013.

32. Wilson, R.M.: “On the Relationship Between Global Land-Ocean Temperature and Various Descriptors of Solar-Geomagnetic Activity and Climate,” NASA/TP—2014–218193, NASA Marshall Space Flight Center, Huntsville, AL 62 pp., April 2014.

33. Goddard Institute for Space Studies, “GISS Surface Temperature Analysis (GISTEMP),” <http://data.giss.nasa.gov/gistemp/>, February 2014.

34. Goddard Institute for Space Studies, “Global-mean monthly, seasonal, and annual means,” <http://data.giss.nasa.gov/gistemp/tabledata_v3/GLB.Ts+dSST.txt>, February 2014.

35. Keeling, C.D.: “The Concentration and Isotopic Abundances of Carbon Dioxide in the Atmosphere,” *Tellus*, Vol. 12, No. 2, pp. 200–203, doi:10.1111/j.2153-3490.1960.tb01300.x, May 1960.

36. Bolin, B.; and Keeling, C.D.: “Large-scale atmospheric mixing as deduced from seasonal and meridional variations of carbon dioxide,” *J. Geophys. Res.*, Vol. 68, No. 13, pp. 3899–3920, doi:10.1029/JZ068i013p03899, July 1963.

37. Pales, J.C.; and Keeling, C.D.: "The concentration of atmospheric carbon dioxide in Hawaii," *J. Geophys. Res.*, Vol. 70, No. 24, pp. 6053–6076, doi:10.1029/JZ070i024p06053, December 1965.

38. Bolin, B.; and Bischof, W.: "Variations of the carbon dioxide content of the atmosphere in the northern hemisphere," *Tellus*, Vol. 22, No. 4, pp. 431–442, doi:10.1111/j.2153-3490.1970.tb00508.x, August 1970.

39. Bacastow, R.B.; Keeling, C.D.; and Whorf, T.P.: "Seasonal amplitude increase in atmospheric CO_2 concentration at Mauna Loa, Hawaii, 1959–1982" *J. Geophys. Res.-Atmos.*, Vol. 90, No. D6, pp. 10,529–10,540, doi:10.1029/JD090iD06p10529, October 1985.

40. Thoning, K.W.; Tans, P.P.; and Komhyr, W.D.: "Atmospheric carbon dioxide at Mauna Loa Observatory: 2. Analysis of the NOAA GMCC data, 1974–1985," *J. Geophys. Res.-Atmos.*, Vol. 94, No. D6, pp. 8549–8565, doi:10.1029/JD094iD06p08549, June 1989.

41. NOAA Earth System Research Laboratory, "Mauna Loa CO_2 annual mean data," <ftp://aftp.cmdl.noaa.gov/products/trends/co2/co2_annmean_mlo.txt>, February 2014.

42. CO_2 Now, "Earth's CO_2 Home Page," <http://co2now.org/>, June 2014.

REPORT DOCUMENTATION PAGE						Form Approved OMB No. 0704-0188

The public reporting burden for this collection of information is estimated to average 1 hour per response, including the time for reviewing instructions, searching existing data sources, gathering and maintaining the data needed, and completing and reviewing the collection of information. Send comments regarding this burden estimate or any other aspect of this collection of information, including suggestions for reducing this burden, to Department of Defense, Washington Headquarters Services, Directorate for Information Operation and Reports (0704-0188), 1215 Jefferson Davis Highway, Suite 1204, Arlington, VA 22202-4302. Respondents should be aware that notwithstanding any other provision of law, no person shall be subject to any penalty for failing to comply with a collection of information if it does not display a currently valid OMB control number.
PLEASE DO NOT RETURN YOUR FORM TO THE ABOVE ADDRESS.

1. REPORT DATE *(DD-MM-YYYY)*	2. REPORT TYPE	3. DATES COVERED *(From - To)*
01–07–2014	Technical Publication	

4. TITLE AND SUBTITLE	5a. CONTRACT NUMBER
Statistical Aspects of North Atlantic Basin Tropical Cyclones During the Weather Satellite Era, 1960–2013: Part 2	5b. GRANT NUMBER
	5c. PROGRAM ELEMENT NUMBER
6. AUTHOR(S)	5d. PROJECT NUMBER
Robert M. Wilson	5e. TASK NUMBER
	5f. WORK UNIT NUMBER
7. PERFORMING ORGANIZATION NAME(S) AND ADDRESS(ES) George C. Marshall Space Flight Center Huntsville, AL 35812	8. PERFORMING ORGANIZATION REPORT NUMBER M–1387
9. SPONSORING/MONITORING AGENCY NAME(S) AND ADDRESS(ES) National Aeronautics and Space Administration Washington, DC 20546–0001	10. SPONSORING/MONITOR'S ACRONYM(S) NASA
	11. SPONSORING/MONITORING REPORT NUMBER NASA/TP—2014–218198

12. DISTRIBUTION/AVAILABILITY STATEMENT
Unclassified-Unlimited
Subject Category 47
Availability: NASA STI Information Desk (757–864–9658)

13. SUPPLEMENTARY NOTES
Prepared by the Science and Research Office, Science and Technology Office

14. ABSTRACT
Weather satellites have been viewing the Earth's weather systems almost continuously since the launch of TIROS-1 in April 1960. During the weather satellite era (1960–2013), some 615 tropical cyclones have formed in the North Atlantic basin, varying in yearly number between 4 in 1983 and 28 in 2005 and averaging about 11 tropical cyclones per year. A comparison of the subintervals 1960–1994 and 1995–2013 clearly shows, however, that the number of tropical cyclones that formed in the North Atlantic basin substantially increased, from about 9 per year in the earlier interval to about 15 per year during the more recent interval, with the fewest number (8) during the more recent interval occurring in 1997. Examined in this Technical Publication, part 2 of a two-part study, are the inferred statistical relationships between a number of tropical cyclone parameters (25) and specific climate-related factors (9).

15. SUBJECT TERMS
tropical cyclones, North Atlantic basin, the 2014 tropical cyclone season, climate

16. SECURITY CLASSIFICATION OF:			17. LIMITATION OF ABSTRACT	18. NUMBER OF PAGES	19a. NAME OF RESPONSIBLE PERSON
a. REPORT	b. ABSTRACT	c. THIS PAGE			STI Help Desk at email: help@sti.nasa.gov
U	U	U	UU	90	19b. TELEPHONE NUMBER *(Include area code)* STI Help Desk at: 757–864–9658

Standard Form 298 (Rev. 8-98)
Prescribed by ANSI Std. Z39-18

National Aeronautics and
Space Administration
IS20
George C. Marshall Space Flight Center
Huntsville, Alabama 35812